PRECISE VARIATIONAL CALCULATIONS OF S^e, P^e, AND D^e STATES OF FEW-ELECTRON ATOMS

by

Toreniyaz Shomenov

A Thesis Submitted to the Faculty of the

DEPARTMENT OF PHYSICS

In Partial Fulfillment of the Requirements
For the Degree of

DOCTOR OF PHILOSOPHY IN PHYSICS

In the School of Sciences and Humanities

NAZARBAYEV UNIVERSITY

2024

NAZARBAYEV UNIVERSITY, SCHOOL OF SCIENCES AND HUMANITIES

As members of the thesis committee, we certify that we have read the thesis prepared by Toreniyaz Shomenov entitled

PRECISE VARIATIONAL CALCULATIONS OF S^e, P^e, AND D^e STATES OF FEW-ELECTRON ATOMS

and recommend that it be accepted as fulfilling the thesis requirement for the degree of Doctor of Philosophy in Physics.

_____ Date: May 5, 2024

Prof. Sergiy Bubin, Lead Supervisor

Department of Physics, Nazarbayev University, Kazakhstan

_____ Date: May 5, 2024

Prof. Kálmán Varga, External Co-Supervisor

Department of Physics and Astronomy, Vanderbilt University, USA

_____ Date: May 5, 2024

Prof. Haiyan Fan-Hagenstein, Internal Examiner

Department of Chemistry, Nazarbayev University, Kazakhstan

_____ Date: May 5, 2024

Prof. Shant Shabhazian, External Examiner

Department of Physics, Shahid Beheshti University, Iran

Final approval and acceptance of this thesis is contingent upon the candidate's submission of the final copies of the thesis to the Department of Physics.

I hereby certify that I have read this thesis prepared under my direction and recommend that it be accepted as fulfilling the thesis requirement.

_____ Date: May 5, 2024

Thesis Director: Sergiy Bubin

Table of contents

ABSTRACT

This dissertation explores the products of Explicitly Correlated Gaussians(ECGs) and bipolar harmonics within the framework of the Rayleigh-Ritz variational method. These functions can accurately describe arbitrary quantum systems in the S, P, and D states of even parity, with dominant configurations where two particles have orbital angular momenta $l_i = 1$ (which may couple to $L = 0, 1, 2$) or a single particle with $l_i = 2 (L = 2)$, while other particles carry zero angular momentum ($l_i = 0$). The key developement in this dissertation lies in an elegant mathematical representation of the basis functions in the form $[\boldsymbol{v}_k'\boldsymbol{r}][\boldsymbol{w}_k'\boldsymbol{r}] \exp[-\boldsymbol{r}'\boldsymbol{A}_k\boldsymbol{r}]$. This representation significantly simplifies differentiation of the matrix elements of the Hamiltonian, overlap, and other important operators compared to the previously employed form, $\boldsymbol{r}'\boldsymbol{W}_k\boldsymbol{r} \exp[-\boldsymbol{r}'\boldsymbol{A}_k\boldsymbol{r}]$, where $\boldsymbol{W}_k$ is a sparse $3n \times 3n$ symmetric matrix. It is demonstrated that the former scheme significantly enhances the efficiency of numerical calculations by 1-2 orders of magnitude, opening new avenues for conducting high-precision calculations of few-particle quantum systems (including few-electron atoms, molecules, and positronic complexes) with spectroscopic accuracy. Moreover, with the new representation of the basis functions this work will present detailed derivations and compact expressions for the matrix elements of overlap, Hamiltonian, and the matrix elements necessary for computing the analytic gradient of energy with respect to Gaussian nonlinear parameters, making their implementation into computer code considerably more straightforward. Matrix elements required for computing leading relativistic corrections and other operators will also be derived and provided in a compact form. The dissertation discusses and presents results from various tests conducted using formulas implemented into a large computer program for variational calculations. Together, these findings have the potential for applications in precision-measurement physics and theoretical spectroscopy computations.

Acknowledgment

I express my gratitude for the invaluable support and resources provided during the course of my Ph.D. journey. The Shabyt high-performance computer cluster at Nazarbayev University played a pivotal role, serving as the primary platform for the extensive numerical calculations presented in this dissertation. Furthermore, I would like to extend my gratitude to the University of Arizona Research Computing. I am thankful to Professors Ludwik Adamowicz and Sergiy Bubin for their assistance in obtaining access to the computer clusters. The use of HPC facilities in Arizona was critical for performing calculations reported in this dissertation.

Special thanks are owed to my thesis advisor, Professor Sergiy Bubin, whose guidance and constructive criticism were instrumental throughout my Ph.D. journey. His unwavering support played a crucial role in the completion of my Ph.D. projects and the finalization of this dissertation.

I would also like to express my sincere gratitude to Professor Ludwik Adamowicz for his support during the internship at the University of Arizona. The internship, initiated by Professor Sergiy Bubin, provided me with invaluable experiences in the field, contributing to my professional growth.

Lastly, I appreciate the contributions of postdoctoral scholars Saeed Nasiri and Dmitry Tumakov, as well as graduate student Pavel Rzhevskii. Our insightful conversations proved instrumental in overcoming challenges encountered during the development of my thesis projects.

To all those mentioned and countless others who have supported and influenced my academic journey, I extend my heartfelt thanks.

1 Introduction

Thanks to the advancements in modern computer technology, it is now possible to compute the spectrum of small atoms and molecules with a degree of precision that is comparable with that of high-resolution spectroscopic experiments. Theoretical formulations, derived directly from the fundamental principles of quantum mechanics, have been developed and implemented on high-performance computer (HPC) clusters for conducting large-scale quantum mechanical calculations. These computational codes, including those and the formalism summarized in this dissertation, are primarily used to enhance, predict, and validate the total energies corresponding to an angular momentum state of specific systems.

1.1 High-accuracy calculations

High accuracy calculations that aim to determine the energies and wave functions of small atoms and molecules have always played a crucial role in physics and chemistry [1–10]. These calculations, often reaching near-exact results, are important for exploring properties such as electron correlations [11], relativistic effects [12–15], molecular bonds [16–18], and the quantum dynamics of nuclei [19–21]. Such research works have not only validated theoretical foundations but have also enhanced our comprehension of the electronic structures of atoms and molecules, shedding light on their behavior without the distortions introduced by rough approximations [22, 23]. With the continual advancement of experimental techniques performing highly precise measurements, adjustments in theoretical models become important to adequately describe neglected effects and interactions, or those previously treated more approximately.

Theoretical high-accuracy measurements of small atoms and molecules hold promise not only for advancing the validation of theoretical models and assessing their limitations but also for progressing precision measurement science by accurately determining fundamental constants, nuclear radii, nuclear quadrupole moments, and more. For instance, evaluating the proton/electron mass ratio [24], finding the nuclear charge radii [25–29] serve as examples in this regard.

Furthermore, high-precision calculations play a crucial role as a model for establishing

benchmark results against which other, less precise methods can be evaluated. This rigorous comparison enables the refinement and improvement of computationally cheaper theoretical approaches. The computation of the total nonrelativistic energy of quantum systems is a pivotal example in this regard. Even with highly accurate experimental data on ionization potentials, electron affinities, dissociation energies, or transition frequencies, determining the total nonrelativistic energy precisely remains challenging. Specifically, achieving energy convergence to a relative accuracy of 10^{-6} to 10^{-9} or higher in theoretical calculations presents a formidable challenge. This difficulty arises due to the necessity of knowing the binding energies of all subsystems and, notably, the precise contributions of correlation effects, as well as relativistic, quantum electrodynamics (QED), and finite-size effects of nuclei [30–38]. Relativistic effects, of course, cannot be measured directly in experiments. While these properties of small systems have been calculated very accurately, the current difficulty involves expanding these calculations to encompass atoms containing more than 5 electrons and small molecular systems with three or more nuclei.

The ongoing advancements in experimental techniques have significantly enhanced the accuracy of measurements related to spectroscopy of few-particle systems. Consequently, the demand for high precision in computational methods has grown in parallel. For instance, recent achievements in laser spectroscopy have allowed the determination of the fundamental ground tone vibrations of H_2, HD, and D_2 with an accuracy of $10^{-4}\ cm^{-1}$ [39], imposing a stringent test on quantum electrodynamics within chemically bound systems.

1.2 Computational techniques to the Schrödinger equation

It is evident that, unlike simpler cases, the solutions to the Schrödinger equation, even for few-particle systems, cannot be solved in analytical form. To overcome this challenge, computational scientists employ sophisticated numerical techniques and advanced computational methods, leveraging computers to compute the properties of quantum systems with high precision. There are numerous methods that have been devised for the numerical solution of the Schrödinger equation with high precision. These methods include Quantum Monte Carlo (QMC) methods [40, 41], the method of configuration-interaction (CI) expansion of the wave function [42], the method of coupled-cluster (CC) expansions

[43], the use of hyperspherical harmonics (HH) in the wave function approximation [44], many-body perturbation theory (MBPT) approaches [45, 46], multi-component Hartree-Fock (MCHF) strategies [47], among others.

The method of hypersphrical harmonics

The method of hyperspherical harmonics (HH) employs various well-established mathematical tools, such as Fourier series theory, orthogonal polynomials, and solutions for systems of ordinary differential equations. Therefore, the method of Hyperspherical Harmonics mainly consists of closed analytical expressions for many quantities, including the potential matrix elements in HH basis [44]. Consequently, while it may seem that the analytical approach loses its importance in light of advanced computing technology, it can aid in the separation of numerical approximations in separate steps, making the calculations more straightforward.

The main idea of hyperspherical harmonics is to transform the N-body center-of-mass Schrödinger equation containing $3N-3$ variables into a system of coupled differential equations containing only one variable. These equations are then solved using the mathematical tools mentioned above. The transformation of the Schrödinger equation is achieved by expanding the N-body exact state of the system as:

$$\Psi(\rho,\theta) = \sum_K \phi_K(\rho)\mathcal{Y}_K(\theta), \tag{1}$$

where $\mathcal{Y}_K(\theta)$ represents the HH functions, and ρ is the hyperradius. The angle θ represents $3N-4$ angular variables, while K contains $3N-5$ angular operators that commute with the Hamiltonian of the system and with each other. Additionally, K includes a quantum number k, which represents the grand total angular momentum [44].

Quantum Monte Carlo

Quantum Monte Carlo methods constitute a large class of numerical techniques used to study quantum systems, employing the Monte Carlo technique to approximate multi-dimensional integrals. The concept of the Monte Carlo method is straightforward to understand, yet it is incredibly powerful. All it requires is the generation of random

numbers and checking them against specific criteria.

Consider a classic example of Monte Carlo methods for estimating π using Python code. For this purpose, envision a square board with a circle inside. To simulate the value of π, throw darts onto the board, keeping track of the number of darts that land inside the circle and the total number of darts thrown. Using the ratio of π to the areas of the circle and square, denoted as $A_{cirle} = \pi r^2$ and $A_{square} = 4r^2$, respectively, we can directly estimate the value of π. It is evident that as the number of darts thrown or the number of iterations grows, the result becomes more accurate.

Below, you can find the Python code that performs this estimation, providing output for 10 identical experiments. Through this simple example, we can understand how randomness and selectivity can be employed to obtain real results.

```
import random as rn
for i in range(10):
   n=20000000
   iter = 0
   for k in range(n):
      x = rn.uniform(0, 1)
      y = rn.uniform(0, 1)
      if (x**2 + y**2) <= 1:
         iter=iter+1
      Pi = 4 * iter/n
   print("Pi is: ",Pi,  " in ", i+1, " simulation.")
```

The following output is generated

```
Pi is:  3.142048  in  1  simulation.
Pi is:  3.141446  in  2  simulation.
 ..............................
Pi is:  3.1414142  in  10  simulation.
```

Quantum Monte Carlo methods come in various forms, such as Variational Monte Carlo (VMC), Diffusion Monte Carlo, Gaussian Quantum Monte Carlo, Time-dependent

Quantum Monte Carlo, and more. Among these forms, Variational Monte Carlo is the closest to the formalism described in this dissertation, as it is based on the minimization of the expectation value of the Hamiltonian (13). However, this method is employed to approximate the ground state energy of the system, similar to other variational methods, with the exception of numerically evaluating multi-dimensional integrals. For a detailed introduction to this technique, please refer to the work by Toulouse et al. [48].

Configuration Interaction

Configuration Interaction (CI) is the linear variational method for solving the time-independent electronic Schrödinger equation within the Born-Oppenheimer approximation. The exact electronic wave function $|\Psi\rangle$ is expanded as a linear combination of n-electron basis functions (where n is the number of electrons):

$$|\Psi\rangle = \sum_i c_i |\Phi_i\rangle. \tag{2}$$

Here the linear coefficients c_i are called the CI coefficients in expanding the basis set. Substituting the wave function into the Schrodinger equation results in a matrix form of eigenvalue equation that is convenient for its numerical solution (similar to 3.1). In practice, the symmetry properties of the system under consideration are included in the linear expansion functions $|\Phi\rangle$ in accordance with the antisymmetrization principle. To satisfy this principle, a wavefunction describing a system of fermions must be antisymmetric with respect to the permutations of spatial and spin coordinates for any pair of fermionic particles. This can be done by using the Slater determinants as linear expansion functions. Slater determinant is written as follows:

$$\Phi = \frac{1}{\sqrt{N!}} \begin{vmatrix} \phi_i & \phi_j & \phi_k & \dots & \phi_l \\ \phi_i & \phi_j & \phi_k & \dots & \phi_l \\ \phi_i & \phi_j & \phi_k & \dots & \phi_l \\ \vdots & \vdots & \vdots & & \vdots \\ \phi_i & \phi_j & \phi_k & \dots & \phi_l. \end{vmatrix} \tag{3}$$

This matrix expression for the Slater determinant can also be written in abbreviated form as $|\phi_i\phi_j \dots \phi_l\rangle$ or $|ij \dots l\rangle$. It is easy to confirm that the given determinant is uniquely specified by the arrow of occupied orbitals and permuting the coordinates of pair of electrons transform the determinant into its swapped rows, which basicly changes the sign. Therefore, the Slater determinant directly satisfies the antisymmetrization principle.

When the linear expansion in Eq.(2) includes the basis functions out of all the possible Slater determinants from a complete set of one-electron basis functions $[\phi]$, then the electronic wave function $|\Psi\rangle$ is considered to be exact solution to the electronic Schrodinger equation and is called Full Configuration Interaction method [42]. However, it is impossible to perform a complete full CI technique as the complete set of orbitals is infinite. Therefore, in practice, the wave functions is formed as a linear combination of limited number of Slater determinants. In this procedure, the resulting eigenstates and the eigenvalue are exact only within the space spanned by the one-electron basis set. As vary large number of Slater determinants are used in the expansion procedure, full CI method is very expensive to perform calculations and can be used for testing less accurate approaches.

To restrict the size of the basis set to decease the computational time, one can neglect the N-electron functions in the CI wave function (2) that do not contribute to the expansion. This can be done by constructing the configuration state functions (CSFs), which are linear combinations of Slater determinants chosen to be eigenstates of square of the total spin operator of the system, S^2. This is because, if the exact wave function $|\Psi\rangle$ is an eigenstate of some Hermitian operator, then the expansion functions $|\Phi_i\rangle$ are also eigenstates of this operators with different eigenvalues. Therefore, these expansion functions can be safely neglected in the linear expansion of the exact wave function $|\Psi\rangle$ [42].

Coupled Cluster approach

The Coupled Cluster (CC) method begins with a Hartree-Fock reference wave function [49, 50], which is the description of the quantum many-body system in a stationary state. Hartry Fock wave function basicly is the solution to a set of N-coupled equations resulting from approximating the N-body wave function of the quantum system as a single Slater determinant for N spin orbitals. Coming back to the CC approaches, the key idea is to

express the exact wave function $|\Psi\rangle$ as an exponential of a cluster operator acting on the Hartree-Fock reference wave function $|\Phi_0\rangle$

$$|\Psi\rangle = e^T |\Phi_0\rangle. \tag{4}$$

Here T is the cluster operator, which by acting on the reference wave function $|\Phi_0\rangle$ produces a linear combinations of excited determinants from the reference state. It is important to mention that it is also possible to use Configuration Interaction wave function and other self consistent field functions as a reference. Namely, the cluster operator T contains excitations of electrons from occupied to virtual orbitals. The general form of the cluster operator is given by:

$$T = T_1 + T_2 + \cdots + T_n, \tag{5}$$

where T_1 represents single excitations, T_2 represents double excitations, and so on. The number of terms depends on the level of approximation, with CCSD including only single double excitations, and CCSDT adding a perturbative corrections for triple excitations [43, 51, 52]. In addition to these, CCSDTQ is considered to be more complicated coupled cluster method, and used for high-accuracy calculations of small molecules [51].

In the framework of the second quantization theory, in which the exact states of the system are considered as field operators, the coupled cluster operators in (5) are written as follows:

$$T_1 = \sum_i \sum_a t_a^i \hat{a}^a \hat{a}_i, \tag{6}$$

$$T_2 = \frac{1}{4} \sum_{i,j} \sum_{a,b} t_{ab}^{ij} \hat{a}^a \hat{a}^b \hat{a}_j \hat{a}_i, \tag{7}$$

$$\cdots \tag{8}$$

$$T_n = \frac{1}{(n!)^2} \sum_{i_1,i_2,\ldots,i_n} \sum_{a_1,a_2,\ldots,a_n} t_{a_1,a_2,\ldots a_n}^{i_1,i_2,\ldots,i_n} \hat{a}^{a_1} \hat{a}^{a_2} \ldots \hat{a}^{a_n} \hat{a}_{i_1} \hat{a}_{i_2} \ldots \hat{a}_{i_n}. \tag{9}$$

Here, $\hat{a}^a$ and $\hat{a}_i$ are the creation and annihilation operators, respectively, written in canonical form. While the superscript and subscript indices i, j represent the occupied holes, the indices a, b represent the unoccupied orbitals or states. If we apply the one particle and two-particle cluster operators T_1 and T_2 to the reference wave function $|\Phi_0\rangle$, without acting it with the exponential as in Eq. (4), then we can obtain the linear combination of

the singly and doubly excited Slater determinants, respectively. This procedure is then becomes similar to the Configuration Interaction expansion of the wave function, where we solve for the unknown coefficients t_a^i and t_{ab}^{ij} to approximate the exact state of the system, $|\Psi\rangle$.

In order to act with the exponential of the cluster operator T, one needs to use the Taylor series. For example, if we consider the one -particle and two-particle operators T_1 and T_2, respectively, then

$$e^T = 1 + T_1 + T_2 + \frac{1}{2}T_1^2 + \frac{1}{2}T_2^2 + \frac{1}{2}T_1T_2 + \frac{1}{2}T_2T_1 + \dots \tag{10}$$

While in reality, this sequence is limited due to the finite number of occupied molecular orbitals and excitations, the size remains considerable. Even with advanced massively parallel computers in present, the computational demands are overwhelming, except for scenarios involving a few electrons and minimal basis sets. This is particularly true when accounting for all contributions to the cluster operator, not just T_1 and T_2. Frequently, for computational feasibility, the cluster operator is restricted to singles and doubles (CCSD) only. Although this approach is more affordable, it generally gives not very accurate calculations [53].

At the heart of these methods lie basis functions, essential for approximating the wave functions of quantum systems. The most commonly employed technique is the Rayleigh-Ritz variational method, which is discussed in section 3. This method approximates the wave function by representing it as a linear combination of certain basis functions. When provided with a suitable basis set capable of effectively representing the wave function, one can achieve remarkably precise solutions to the Schrödinger equation for atomic and molecular systems. For example, several benchmark variational computations of three-particle quantum systems, employing Hylleraas-type basis functions and it is later variants, have yielded impressive results. These calculations have achieved energy eigenvalues with estimated accuracies surpassing 20 or even 40 decimal figures [5, 54, 55]. Variants of variational approach include the Hartree-Fock method, configuration-interaction expansion, the use of hyperspherical harmonics basis, and the variational quantum Monte Carlo, all of which are specific instances of the broader variational method

1.3 Variational methods with the use of ECGs

Employing correlated basis functions that explicitly depend on the distances between particles provides a robust method for performing large-scale variational calculations on small atoms, molecules, and other bound quantum systems. Among these basis functions, explicitly correlated Gaussians (ECGs) [56, 57] stand out as the most promising choice. What makes ECGs particularly appealing is their unique property—they allow for the analytical evaluation of all necessary matrix elements, regardless of the number of particles involved. This analytical tractability sets ECGs apart, as other types of basis functions often encounter significant challenges, and sometimes impossibilities, when extending calculations beyond three or four electrons. For instance, while calculating two- and three-electron atomic systems with high accuracy is achievable using Hylleraas-type functions [58, 59] or Slater type basis functions [60], extending these functional approaches beyond three electrons proves to be cumbersome due to the difficulties of analytically calculating their matrix elements [61]. While ECGs do not satisfy the Kato cusp conditions [62] (at short interparticle distances) and rapidly decay at long distances, they have already demonstrated great flexibility and performance in many applications involving quantum few-body systems of various natures. These applications range from electronic structure of small atoms and molecules to the nuclear structure and excitonic complexes [22, 23, 63–66].

The S-states of few-particle quantum systems ($L = 0$) require the use of spherically symmetric basis functions, such as simple all-particle ECGs [67]. To investigate states with non-zero angular momenta, these ECGs need to be multiplied by specific angular factors, which can conveniently be expressed in Cartesian coordinates [68–70]. Further discussions and detailed analysis of the types of ECG basis functions are presented in Section 4. For now, let us briefly mention the specific types of ECG basis functions that are relevant to the present work. Specifically, this dissertation focuses on ECGs with prefactors suitable for describing states with the following dominant particle configurations:

a) Two particles occupy p-states ($l_i = 1$, where l_i represent individual orbital angular momenta), whereas the remaining particles occupy s-states ($l_i = 0$). This configuration gives rise to multiparticle states with S, P, or D symmetries of the even parity, shortly

denoted as S^e, P^e, or D^e states.

b) One particle occupies a d-state, while the others live in s-states, resulting in multiparticle D states of the even symmetry (D^e states).

ECGs of this kind have been previously applied in computations for few-particle quantum systems[71–77]. These studies include benchmark data on leading relativistic corrections for singlet D states of the Be atom [75] and doublet D states of the Li atom [76]. Additionally, excited state energies, including those of highly excited Rydberg spectra, were reported in previous articles [72–74].

However, the usage of existing algorithms has primarily been restricted to lithium and beryllium atoms. The calculations on the nonrelativistic energies of the ground and first exited triplet P symmetry of the carbon atom [23] on current computer hardware proved challenging, necessitating excessively long computations. The substantial computational difficulty of the analytical expressions for Hamiltonian and overlap matrix elements posed a significant bottleneck in the calculations. It is noteworthy that precise calculations in quantum few-body systems using Explicitly Correlated Gaussians (ECGs) demand optimizing its nonlinear parameters very extensively and generating very large basis sets. Hence, there is a critical need to develop novel approaches that can largely accelerate the calculation of matrix elements and enhance the optimization of nonlinear parameters for practical applications.

This dissertation discusses a highly efficient scheme for computing matrix elements and provides detailed derivations for all the necessary matrix elements with ECG basis functions for the dominant particle configurations mentioned earlier. It then presents the final results in a compact matrix format for easy and efficient implementation of the derived formulas in the computer code for high-accuracy calculations of quantum few-body systems. These matrix elements are derived for the expectation values of various operators encompassing the Hamiltonian and overlap, as well as Dirac delta functions, and consequently, various operators derivable from the Dirac delta function. We will also present matrix elements necessary for computing the Mass-Velocity and Orbit-Orbit corrections encountered in relativistic corrections [23].

Moreover, in Section 3, we introduce the formalism, and in Section 2, the notation scheme used in the dissertation. The operators representing leading relativistic corrections

will be briefly described in Section 8, while their matrix elements with symmetry-adapted ECG basis functions, described in Section 4, will be derived and presented in Sections 9 and 10. In addition to these, the results of calculations for various systems based on the formulas provided in this dissertation will be presented and discussed in Section 12. The method used in generating the basis functions and their optimizations will be discussed in Section 11.

2 Notations

This dissertation includes numerous analytical expressions presented in a general matrix format, derived through the framework of matrix differential calculus [78]. Within this matrix approach, in this work we will encounter various types of vectors and matrices, whose dimensions depend on various factors such as the number of particles, degrees of freedom per particle, choice of coordinates, and the length of the variational basis. To eliminate any potential confusion stemming from these vector and matrix dimensions, this section introduces a notation scheme adopted from our recent article [79].

To begin, specific integer constants are defined here to establish these dimensions, and particular symbols are reserved to represent them:

- ν - Represents the number of degrees of freedom per particle. Since this thesis focuses on particles moving in 3D, ν is 3.
- N - Stands for the total number of particles in the system of interest. $\nu N = 3N$ indicates the total number of degrees of freedom.
- $n = N - 1$ - Represents the number of (pseudo)particles. In this dissertation, $\nu n = 3n$ is the number of degrees of freedom associated with the internal or the relative movement of the particles (Section 3.3).
- $\mathcal{N}$ - Represents the number of ECG basis functions employed in expanding the wave function.

To differentiate between various categories of vectors and matrices, we will employ notations involving distinct alphabets, cases, and font types. This approach is intended to clarify the specific type of matrix, vector, or scalar represented by each character. Additionally, we will adopt specific symbols to represent common operations on scalars, matrices, and vectors. While there are a few exceptions to the rules outlined below (such as the symbols N, n, and $\mathcal{N}$ that have been reserved previously), these exceptions are straightforward and should not lead to any confusion.

- α, β, γ, etc. – Scalars are represented using lowercase Greek letters.

- $\boldsymbol{\alpha}$, $\boldsymbol{\beta}$, $\boldsymbol{\gamma}$, etc. – 3-component vectors are written using lowercase Greek letters represented in bold font.

- a, b, c, etc. – n-component vectors are represented using lowercase Latin letters. Here n is the number of pseudo-particles.

- $\boldsymbol{a}$, $\boldsymbol{b}$, $\boldsymbol{c}$, etc. – $3n$-component vectors are represented using lowercase Latin letters in bold font.

- a, b, c, etc. – N-component vectors are represented using lower case Latin letters in serif font. Here N is the number of particles.

- $\mathbf{a}$, $\mathbf{b}$, $\mathbf{c}$, etc. – $3N$-component vectors are represented using lower case Latin letters in bold serif font.

- $\boldsymbol{\Lambda}$, $\boldsymbol{\Xi}$, $\boldsymbol{\Omega}$, etc. – 3×3 matrices are represented using upper-case bold Greek letters.

- A, B, C, etc. – $n \times n$ matrices are represented using uppercase Latin letters.

- $\boldsymbol{A}$, $\boldsymbol{B}$, $\boldsymbol{C}$, etc. – $3n\times3n$ matrices are represented using uppercase Latin letters in bold font.

- $\mathtt{a}$, $\mathtt{b}$, $\mathtt{c}$, etc. – $\mathcal{N}$-component vectors in the Hilbert space of basis functions are represented using lowercase Latin letters in typewriter font.

- $\mathtt{A}$, $\mathtt{B}$, $\mathtt{C}$, etc. – $\mathcal{N}\times\mathcal{N}$ matrices are represented using uppercase Latin letters in typewriter font.

- $\mathcal{A}$, $\mathcal{B}$, $\mathcal{C}$, etc. – operators are represented using calligraphic font.

- $\mathbf{I}$, I, $\boldsymbol{I}$, $\mathtt{I}$ – These are identity matrices with different dimensions: $\mathbf{I}$ is the 3×3 identity matrix, I is the $n\times n$ identity matrix, $\boldsymbol{I}$ is the $3n\times3n$ identity matrix, and $\mathtt{I}$ is the $\mathcal{N}\times\mathcal{N}$ identity matrix.

- $\mathrm{tr}\, A$, $\mathrm{tr}\, \boldsymbol{A}$, etc. – tr is used to denote the trace of a matrix.

- $|\boldsymbol{\Lambda}|$, $|A|$, $|\boldsymbol{A}|$, etc. – The vertical bars indicate the determinant of a matrix. Nevertheless, if what is enclosed within the vertical bars is a vector (such as $|\boldsymbol{\alpha}|$, $|a|$), or a scalar, then the bars represent the magnitude of the vector or scalar, respectively.

- $\boldsymbol{\Lambda}^{-1}$, A^{-1}, $\boldsymbol{A}^{-1}$, etc. – the superscipt -1 of matrices is used to denote the inverse operation.
- $\boldsymbol{\alpha}'$, a', A', $\boldsymbol{A}'$, etc. – The superscript prime symbol of matrices or vectors is used to denote the transpose operation.
- $a \otimes \boldsymbol{\alpha}$, $A \otimes B$, $\boldsymbol{A} \otimes \boldsymbol{B}$, etc. – denotes the Kronecker product of matrices or vectors.

3 Formalism

3.1 The variational principle

The variational principle, based on the Ritz theorem [80], asserts that the expectation value of Hamiltonian, computed with a normalized trial wave function $\psi(\boldsymbol{r})$ (where $\langle\psi(\boldsymbol{r})|\psi(\boldsymbol{r})\rangle = 1$), provides an upper limit to the ground state energy of the system, as it is expressed below:

$$\varepsilon = \langle\psi(\boldsymbol{r})|\mathtt{H}|\psi(\boldsymbol{r})\rangle \geq \varepsilon_0. \tag{11}$$

Adjusting the trial wave function $\psi(\boldsymbol{r})$ allows for a precise approximation of the exact wave function of the system, limited only by computational capabilities. In practice, $\psi(\boldsymbol{r})$ is expanded in terms of some suitable basis functions

$$\psi(\boldsymbol{r}) = \sum_{k=1}^{\mathcal{N}} \mathtt{c}_k \left|\phi_k\left(\{\alpha\}_k\right)\right\rangle, \tag{12}$$

where the basis functions $\phi_k\left(\{\alpha\}_k\right)$ may contain adjustable parameters $\{\alpha_k\}$. Coefficients $\mathtt{c}_k$ and parameters α_k in the trial wave function are optimized to minimize the expectation value of the Hamiltonian. The minimization with respect to the linear coefficients $\mathtt{c}_k$ leads to a generalized eigenvalue problem expressed as:

$$\mathtt{Hc} = \varepsilon\mathtt{Sc}, \tag{13}$$

where $\mathtt{c}$ represents a column vector comprising coefficients c_k, and $\mathtt{H}$ and $\mathtt{S}$ are $\mathcal{N}\times\mathcal{N}$ Hamiltonian and overlap matrices, respectively, with matrix elements defined as:

$$H_{kl} = \langle\phi_k|\mathtt{H}|\phi_l\rangle, \quad S_{kl} = \langle\psi_k|\psi_l\rangle. \tag{14}$$

Minimizing the energy concerning the parameters α_k gives rise to a nonlinear optimization problem. Solving the generalized eigenvalue problem (13), which involves hermitian (or symmetric, in the case of real basis functions) matrices $\mathtt{H}$ and $\mathtt{S}$, provides $\mathcal{N}$ solutions—comprising eigenvalues $\varepsilon^{(i)}$ and their corresponding eigenvectors $\mathbf{c}^{(i)}$. Following the principles of the mini-max theorem, organizing the eigenvalues $\varepsilon^{(i)}$ in ascending order establishes the first eigenvalue $\varepsilon^{(1)}$ as an upper bound for the exact ground state energy. Similarly, the second eigenvalue $\varepsilon^{(2)}$ establishes an upper bound for the energy of the first excited state, and so forth [81].

3.2 The nonrelativistic Hamiltonian

In this dissertation, we consider a general quantum system of N particles with Coulomb interaction between them. Let $\mathsf{r}_i, \mathsf{m}_i$ and q_i represent the position vector, mass and charge of the i-th particle in the laboratory Cartesian coordinate frame. The nonrelativistic Hamiltonian of the system in atomic units can be expressed in the following form:

$$\mathcal{H} = -\sum_{i=1}^{N} \frac{1}{2\mathsf{m}_i} \boldsymbol{\nabla}^2_{\mathbf{r}_i} + \sum_{i=1}^{N} \sum_{j>i}^{N} \frac{\mathsf{q}_i \mathsf{q}_j}{\mathsf{r}_{ij}}. \tag{15}$$

In this expression $\mathsf{r}_{ij} = |\mathbf{r}_j - \mathbf{r}_i|$ is the distance between i-th and j-th particles, and $\boldsymbol{\nabla}_{\mathbf{r}_i}$ is the gradient with respect to the position vector of the i-th particle.

3.3 Separating the center of mass motion

In the computation for bound states of quantum systems, it is crucial to seperate the center of mass motion from the laboratory frame Hamiltonian (15). This method involves positioning one particle, typically the heaviest, at the origin of the internal reference frame. Subsequently, the coordinates of the remaining particles are defined in relation to this reference particle. Without loss of generality, we can designate this reference particle as particle 1. The relation between the internal and laboratory coordinates is then expressed as

$$\boldsymbol{r}_i = \mathbf{r}_{i+1} - \mathbf{r}_1, \qquad i = 1 \ldots n. \tag{16}$$

The total mass of the system is $\mathsf{m}_{\text{tot}} = \sum_{i=1}^{N} \mathsf{m}_i$ and the coordinate of the center of mass is defined as follows:

$$\boldsymbol{r}_N = \mathbf{r}_{\text{cm}} = \sum_{i=1}^{N} \frac{\mathsf{m}_i \mathbf{r}_i}{\mathsf{m}_{\text{tot}}}. \tag{17}$$

Using these relations, it is possible to transform the laboratory Cartesian coordinate with N particles to the new internal coordinate system with $n = N - 1$ pseudo-particles, with masses $m_i = \mathsf{m}_{i+1}$ and charges $q_i = \mathsf{q}_{i+1}$, where $i = 0 \ldots n$. In this notation, m_0 represents the mass, and q_0 represents the charge of the reference particle (particle 1).

In order to transform to this new coordinates $\{\boldsymbol{r}, \boldsymbol{r}_N\}$ it is necessary to write the gradient $\boldsymbol{\nabla}^2_{\mathbf{r}_i}$ in equation (15) in terms of the internal coordinates $\boldsymbol{r}_i$ and define the reduced

masses as $\mu_i = m_0 m_i / (m_0 + m_i)$. With $\mathbf{r}_i = \mathbf{r}_i(\mathsf{x}_i, \mathsf{y}_i, \mathsf{z}_i)$ and $\boldsymbol{r}_i = \boldsymbol{r}_i(x_i, y_i, z_i)$, we can write the gradient $\boldsymbol{\nabla}^2_{\mathbf{r}_i}$ in terms of internal coordinates $\boldsymbol{r}$. Let us see how it can be done for x_i component

$$\nabla_{\mathsf{x}_i} \equiv \frac{\partial}{\partial \mathsf{x}_i} = \frac{\partial x_0}{\partial \mathsf{x}_i}\frac{\partial}{\partial x_0} + \sum_{j=1}^{N-1}\frac{\partial x_j}{\partial \mathsf{x}_i}\frac{\partial}{\partial x_j}$$

$$= \frac{\partial\left(\sum_{i=1}^{N}\frac{\mathsf{m}_i \mathbf{r}_i}{\mathsf{m}_{\rm tot}}\right)}{\partial \mathsf{x}_i}\frac{\partial}{\partial x_0} + \sum_{j=1}^{N-1}\frac{\partial\left(-\mathsf{x}_1 + \mathsf{x}_{j+1}\right)}{\partial \mathsf{x}_i}\frac{\partial}{\partial x_j}.$$

From above equation we have two cases:

$$\frac{\partial}{\partial \mathsf{x}_i} = \begin{cases} \frac{\partial\left(\sum_{i=1}^{N}\frac{\mathsf{m}_i \mathbf{r}_i}{\mathsf{m}_{\rm tot}}\right)}{\partial \mathsf{x}_1}\frac{\partial}{\partial x_0} + \sum_{j=1}^{N-1}\frac{\partial(-\mathsf{x}_1+\mathsf{x}_{j+1})}{\partial \mathsf{x}_1}\frac{\partial}{\partial x_j} \\ \frac{\partial\left(\sum_{i=1}^{N}\frac{\mathsf{m}_i \mathbf{r}_i}{\mathsf{m}_{\rm tot}}\right)}{\partial \mathsf{x}_i}\frac{\partial}{\partial x_0} + \sum_{j=1}^{N-1}\frac{\partial(-\mathsf{x}_1+\mathsf{x}_{j+1})}{\partial \mathsf{x}_i}\frac{\partial}{\partial x_j} \end{cases}$$

$$= \begin{cases} \frac{\mathsf{m}_1}{\mathsf{m}_{\rm tot}}\frac{\partial}{\partial x_i} - \sum_{j=1}^{N-1}\frac{\partial}{\partial x_j} = \frac{\mathsf{m}_1}{\mathsf{m}_{\rm tot}}\nabla_0 - \sum_{i=2}^{N}\nabla_i, \quad i = 1 \\ \frac{\mathsf{m}_i}{\mathsf{m}_{\rm tot}}\frac{\partial}{\partial x_0} + \frac{\partial}{\partial x_i} = \frac{\mathsf{m}_i}{\mathsf{m}_{\rm tot}}\nabla_0 + \nabla_i, \quad i > 1 \end{cases}$$

After performing some algebraic manipulations, utilizing the provided example for the x_i component, and applying the same procedure for the y_i and z_i components, we can express the laboratory frame Hamiltonian in the following form

$$\mathcal{H} = -\frac{1}{2\mathsf{m}_{\rm tot}}\boldsymbol{\nabla}^2_{\boldsymbol{r}_N} - \sum_{i=1}^{n}\frac{1}{2\mu_i}\boldsymbol{\nabla}^2_{\boldsymbol{r}_i} - \sum_{i\neq j}^{n}\frac{1}{2m_0}\boldsymbol{\nabla}'_{\boldsymbol{r}_i}\boldsymbol{\nabla}_{\boldsymbol{r}_j} + \sum_{i=1}^{n}\frac{q_0 q_i}{r_i} + \sum_{i=1}^{n}\sum_{j>i}^{n}\frac{q_i q_j}{r_{ij}}, \tag{18}$$

where $r_{ij} = |\boldsymbol{r}_j - \boldsymbol{r}_i|$. The first term describes the motion of the center of mass (center of mass Hamiltonian $\mathcal{H}_{\rm cm}$), while other terms are called an "internal" Hamiltonian $\mathcal{H}_{\rm int}$:

$$\mathcal{H}_{\rm int} = -\sum_{i=1}^{n}\frac{1}{2\mu_i}\boldsymbol{\nabla}^2_{\boldsymbol{r}_i} - \sum_{i\neq j}^{n}\frac{1}{2m_0}\boldsymbol{\nabla}'_{\boldsymbol{r}_i}\boldsymbol{\nabla}_{\boldsymbol{r}_j} + \sum_{i=1}^{n}\frac{q_0 q_i}{r_i} + \sum_{i=1}^{n}\sum_{j>i}^{n}\frac{q_i q_j}{r_{ij}}, \tag{19}$$

$$\mathcal{H}_{\rm cm} = -\frac{1}{2\mathsf{m}_{\rm tot}}\boldsymbol{\nabla}^2_{\boldsymbol{r}_N}. \tag{20}$$

The internal Hamiltonian describes the intrinsic motion of the n pseudo-particles in the system and contains $r_{ij} = |\boldsymbol{r}_j - \boldsymbol{r}_i|$ term, which is the relative distance between the i-th and j-th pseudo-particles.

3.4 Matrix form of the internal Hamiltonian

The Hamiltonian (19) can be expressed in matrix form to simplify derivations of its matrix elements. For that purpose, we write the position and gradients of n pseudo-particles as $3n$-component vectors

$$\boldsymbol{r} = \begin{pmatrix} \boldsymbol{r}_1 \\ \boldsymbol{r}_2 \\ \vdots \\ \boldsymbol{r}_n \end{pmatrix}, \quad \boldsymbol{\nabla}_{\boldsymbol{r}} = \begin{pmatrix} \boldsymbol{\nabla}_{\boldsymbol{r}_1} \\ \boldsymbol{\nabla}_{\boldsymbol{r}_2} \\ \vdots \\ \boldsymbol{\nabla}_{\boldsymbol{r}_n} \end{pmatrix}. \tag{21}$$

The matrix form of internal Hamiltonian is

$$\mathcal{H}_{\text{int}} = -\boldsymbol{\nabla}_{\boldsymbol{r}}' \boldsymbol{M} \boldsymbol{\nabla}_{\boldsymbol{r}} + \sum_{i=1}^{n} \frac{q_0 q_i}{r_i} + \sum_{i=1}^{n} \sum_{j>i}^{n} \frac{q_i q_j}{r_{ij}}, \tag{22}$$

where $\boldsymbol{M} = M \otimes \mathbf{I}$ is the Kronecker product of $n \times n$ matrix M and 3×3 identity matrix $\mathbf{I}$. The matrix elements of M are

$$M_{ij} = \begin{cases} \frac{1}{2\mu_i}, & i = j \\ \frac{1}{2m_0}, & i \neq j \end{cases}. \tag{23}$$

4 Basis functions

The crucial aspect of high-precision bound state calculations, especially without resorting to the Born-Oppenheimer (BO) approximation [23], lies in constructing the appropriate basis set. The Born-Oppenheimer approximation assumes that nuclei are much heavier than electrons and treats them as fixed in position, simplifying the electronic wave function determination by considering the fixed positions of the nuclei as parameters. However, achieving high-accuracy calculations for quantum systems necessitates considering the coupled motions of both electrons and nuclei. Consequently, basis functions should depend not only on inter-electronic distances but also on distances between electrons and nuclei (interparticle distances, r_{ij}), with their matrix elements computable with reasonable effort, both analytically and numerically. After separating the center-of-mass motion and treating the nucleus as the center of the coordinate system 3.3, the internal Hamiltonian describes the motion of pseudo-electrons in the central field of the nucleus. Therefore, the chosen basis set must accurately capture electronic correlation effects and electron distribution around the positively charged nucleus, without relying on the simplifications of the BO approximation.

Despite the numerous conceivable types of explicitly correlated basis functions, only a handful find practical applicability. One such type is a family of explicitly correlated Gaussians (ECGs), which has gained popularity in variational calculations for various few-particle quantum mechanical systems over the past few decades [22, 23]. The use of ECG basis functions provides a relatively straightforward yet powerful tool for obtaining highly accurate solutions to the Schrödinger equation. The advantage of employing Gaussians, as opposed to other basis functions, lies in the analytical evaluation of all fundamental matrix elements for an arbitrary number of particles. In contrast, many other explicitly correlated basis functions often involve complex integrals that are challenging or impossible to evaluate and implement numerically when dealing with systems beyond three or four particles. In the realm of quantum chemical applications, explicitly correlated Gaussians were initially introduced by Boys [56] and Singer [57]. This dissertation exclusively focuses on explicitly correlated Gaussians (ECGs), delving into the specific types employed in the calculations that form the core of the summarized research.

The spatial component of ECG basis functions, which are used to describe the wave function of a system composed of particles with zero angular momenta, should exhibit spherical symmetry, meaning they are rotationally invariant. These basis functions only involve a radial exponential component and can be represented in a compact matrix format as follows [67]:

$$\phi_k = \exp\left[-\boldsymbol{r}'\left(A_k \otimes \mathbf{I}\right)\boldsymbol{r}\right]. \tag{24}$$

Here "$\otimes$" is the Kronecker product, A_k is a $n \times n$ symmetric matrix, which stores nonlinear variational parameters, and $\mathbf{I}$ is 3×3 identity matrix. Subscript k is used to indicate that, in general, matrix A_k is unique for each basis function.

In order to ensure the square-integrability of bound state wave functions, it becomes crucial to verify the positive definiteness of A_k. This criterion is automatically satisfied if A_k takes on a Cholesky-factored form, namely $A_k = L_k L_k'$, where L_k represents a lower triangular matrix. This specific representation allows for unrestricted variations in the elements of L_k within the range of $[-\infty, \infty]$ while optimizing the nonlinear parameters of the basis functions.

When characterizing few-particle systems with nonzero total orbital angular momenta, adjustments are necessary for the ECGs presented in equation (24). This adaptation involves incorporating a suitable angular factor preceding the exponent, determined through the standard rules governing the addition of angular momentum states for individual particles. In cases of multiparticle states with the total orbital angular momentum quantum number L and its projection on the z-axis M, focusing on dominant configurations involving only two particles, namely particles i and j, each with nonzero orbital angular momenta, yields the corresponding angular factors θ_{LM} in the following manner:

$$\theta_{LM}(\boldsymbol{r}_i, \boldsymbol{r}_j) = r_i^{l_i} r_j^{l_j} \sum_{\substack{m_i, m_j \\ M = m_i + m_j}} C^{LM}_{l_i m_i l_j m_j} Y_{l_i m_i}(\boldsymbol{r}_i) Y_{l_j m_j}(\boldsymbol{r}_j), \tag{25}$$

where l_i and l_j are the orbital angular momentum quantum numbers of particles i and j respectively. Y_{lm} denote the usual spherical harmonics, and $C^{LM}_{l_i m_i l_j m_j}$ denote the Clebsch-Gordan coefficients. By employing the Cartesian coordinate representation of spherical harmonics and using the Clebsch-Gordan coefficients table, it is possible to derive the angular factor θ_{LM} for any given value of the total orbital angular momentum and its

projection on the z-axis. For instance, when $L = 1$, $M = 0$, the total parity is even, and $l_i = l_j = 1$, the resulting angular factor is obtained as follows: first using the table of Clebsch-Gordan coefficients and the Cartesian coordinate representation of spherical harmonics, we expand Eq. (25)

$$\theta_{10} = \frac{1}{\sqrt{2}} Y_{11}^i Y_{1-1}^j + 0 \times Y_{10}^i Y_{10}^j - \frac{1}{\sqrt{2}} Y_{1-1}^i Y_{11}^j = \frac{1}{\sqrt{2}} \left(Y_{11}^i Y_{1-1}^j - Y_{1-1}^i Y_{11}^j \right)$$
$$= \frac{1}{\sqrt{2}} \left[\left(-\frac{1}{2} \sqrt{\frac{3}{2\pi}} \frac{(x_i + i y_i)}{r_i} \right) \left(\frac{1}{2} \sqrt{\frac{3}{2\pi}} \frac{(x_j - i y_j)}{r_j} \right) \right.$$
$$\left. - \left(\frac{1}{2} \sqrt{\frac{3}{2\pi}} \frac{(x_i - i y_i)}{r_i} \right) \left(-\frac{1}{2} \sqrt{\frac{3}{2\pi}} \frac{(x_j + i y_j)}{r_j} \right) \right] \Rightarrow$$
$$\theta_{10} = \frac{3i}{4\pi\sqrt{2}} \frac{1}{r_i^{l_i} r_j^{l_j}} [x_i y_j - x_j y_i]. \tag{26}$$

At this point, we can directly express the corresponding ECG basis function as

$$\phi_k = (x_{i_k} y_{j_k} - x_{j_k} y_{i_k}) \exp\left[-\boldsymbol{r}' \left(A_k \otimes \mathbf{I} \right) \boldsymbol{r} \right]. \tag{27}$$

Here, the integer indices i_k and j_k define a specific set of two particles with nonzero orbital angular momenta. These indices can be regarded as integer variational parameters (with values ranging from 1 to n) during the optimization of parameters for each basis function in energy minimization using the variational method. The subscript k in the indices indicates their uniqueness for each basis function.

In the case when $L = 2$, $M = 0$, and even parity, there are two distinct scenarios. In the first case, we have $l_i = l_j = 1$, and the resulting angular prefactor (25) comes out as

$$\theta_{20} = \frac{1}{\sqrt{6}} Y_{11}^i Y_{1-1}^j + \frac{2}{\sqrt{6}} Y_{10}^i Y_{10}^j + \frac{1}{\sqrt{6}} Y_{1-1}^i Y_{11}^j$$
$$= \frac{1}{\sqrt{6}} \left(-\frac{1}{2} \sqrt{\frac{3}{2\pi}} \frac{(x_i + i y_i)}{r_i} \right) \left(\frac{1}{2} \sqrt{\frac{3}{2\pi}} \frac{(x_j - i y_j)}{r_j} \right)$$
$$+ \frac{2}{\sqrt{6}} \left(\frac{\sqrt{3}}{2\sqrt{\pi}} \frac{z_i}{r_i} \right) \left(\frac{\sqrt{3}}{2\sqrt{\pi}} \frac{z_j}{r_j} \right) + \frac{1}{\sqrt{6}} \left(\frac{1}{2} \sqrt{\frac{3}{2\pi}} \frac{(x_i - i y_i)}{r_i} \right) \left(-\frac{1}{2} \sqrt{\frac{3}{2\pi}} \frac{(x_j + i y_j)}{r_j} \right) \Rightarrow$$
$$\theta_{20} = -\frac{3}{4\pi\sqrt{6}} \frac{1}{r_i r_j} [x_i x_j + y_i y_j - 2 z_i z_j]. \tag{28}$$

The corresponding basis function is

$$\phi_k = (x_{i_k} x_{j_k} + y_{i_k} y_{j_k} - 2 z_{i_k} z_{j_k}) \exp\left[-\boldsymbol{r}' \left(A_k \otimes \mathbf{I} \right) \boldsymbol{r} \right]. \tag{29}$$

In the other case, we have $l_i = 2$ and all other individual orbital angular momenta are zeros. Using the similar procedure, the resultant basis function is obtained as:

$$\phi_k = \left(x_{i_k}^2 + y_{i_k}^2 - 2z_{i_k}^2\right) \exp\left[-\boldsymbol{r}'\left(A_k \otimes \mathbf{I}\right)\boldsymbol{r}\right]. \tag{30}$$

Moreover, if we consider the case, in which $L = 0$, $M = 0$, with even parity, and $l_i = l_j = 1$, then the basis function that corresponds to this also includes an angular prefactor. However, it is rotationally invariant:

$$\phi_k = \left(x_{i_k}x_{j_k} + y_{i_k}y_{j_k} + z_{i_k}z_{j_k}\right) \exp\left[-\boldsymbol{r}'\left(A_k \otimes \mathbf{I}\right)\boldsymbol{r}\right]. \tag{31}$$

It is evident that the process of constructing angular factors for quantum numbers associated with higher orbital angular momentum can become quite extensive. Therefore, for general applications, we can utilize the following expression for the angular factor when dealing with high values of the total angular momentum number L [82]:

$$\theta_{LM}(\boldsymbol{r}_i) = v^{2K+L} Y_{LM}(\boldsymbol{v}), \tag{32}$$

where $\boldsymbol{v} = \sum_{i=1}^{n} u_i \boldsymbol{r}_i$, and $v = |\boldsymbol{v}|$ is defined as a linear combination of all pseudo-particle coordinates. In this expression, K is an integer variational parameter that can take any non-negative values and introduces an additional flexibility to improve the short-range behavior of the basis functions [82].

This dissertation covers the derivations and expressions of the matrix elements of the Hamiltonian, overlap, and the analytic energy gradient, as well as operators for leading relativistic corrections, with basis functions (27) through (31). These basis functions are suitable for high precision variational computations of the ground and excited states of various few-particle quantum systems, ranging from few-electron atoms and ions to systems composed of exotic particles and nuclei, as well as small molecules.

In further theoretical analysis concerning the derivation of matrix elements with basis functions (27)-(31), it is necessary to represent them in matrix form, combining two or three general terms as follows:

$$\begin{aligned} \phi_k &= [\boldsymbol{v}_k'\boldsymbol{r}][\boldsymbol{w}_k'\boldsymbol{r}] \exp\left[-\boldsymbol{r}'\boldsymbol{A}_k\boldsymbol{r}\right] \\ &= [(v_k \otimes \boldsymbol{\epsilon}^v)'\boldsymbol{r}][(w_k \otimes \boldsymbol{\epsilon}^w)'\boldsymbol{r}] \exp\left[-\boldsymbol{r}'\left(A_k \otimes \mathbf{I}\right)\boldsymbol{r}\right]. \end{aligned} \tag{33}$$

Here, v_k and w_k are n-component vectors with nonzero elements only in the i_k-th and j_k-th positions, respectively, both equal to unity. Meanwhile, $\boldsymbol{v}_k$ and $\boldsymbol{w}_k$ are $3n$-component vectors directly related to v_k and w_k through Kronecker products: $\boldsymbol{v}_k = v_k \otimes \boldsymbol{\epsilon}^v$ and $\boldsymbol{w}_k = w_k \otimes \boldsymbol{\epsilon}^w$. These vectors define specific products of Cartesian coordinates, such as $x_{i_k} y_{j_k}$ and $x_{i_k} x_{j_k}$, among others. Additionally, each of the two 3D unit vectors, $\boldsymbol{\epsilon}^v$ and $\boldsymbol{\epsilon}^w$, contains only one nonzero element, which is also one, defining whether the Cartesian coordinate of a pseudoparticle (x, y, or z) appears in the angular prefactor of the Gaussian. For instance, if we consider three particle system ($n = N - 1 = 2$) and the necessary angular factor is $[\boldsymbol{v}_k' \boldsymbol{r}][\boldsymbol{w}_k' \boldsymbol{r}] = x_1 y_2$, then

$$i_k = 1, \quad \boldsymbol{\epsilon}^v = \boldsymbol{\epsilon}^x, \quad j_k = 2, \quad \boldsymbol{\epsilon}^w = \boldsymbol{\epsilon}^y,$$

and the corresponding vectors are

$$\boldsymbol{v}_k = v_k \otimes \boldsymbol{\epsilon}^v = \begin{pmatrix} 1 \\ \\ 0 \end{pmatrix} \otimes \begin{pmatrix} 1 \\ \\ 0 \\ \\ 0 \end{pmatrix} = \begin{pmatrix} 1 \\ \\ 0 \\ \\ 0 \\ \\ 0 \\ \\ 0 \\ \\ 0 \end{pmatrix},$$

$$\boldsymbol{w}_k = w_k \otimes \boldsymbol{\epsilon}^w = \begin{pmatrix} 0 \\ \\ 1 \end{pmatrix} \otimes \begin{pmatrix} 0 \\ \\ 1 \\ \\ 0 \end{pmatrix} = \begin{pmatrix} 0 \\ \\ 0 \\ \\ 0 \\ \\ 0 \\ \\ 1 \\ \\ 0 \end{pmatrix}.$$

The basis function (33) can be represented in an alternative form for ease of derivations of the matrix elements

$$\phi_k \;=\; \lim_{\substack{\alpha_k \to\ 0 \\ \beta_k \to\ 0}} \frac{\partial}{\partial \alpha_k} \frac{\partial}{\partial \beta_k} \exp\left[-\boldsymbol{r}'\left(A_k \otimes \mathbf{I}\right)\boldsymbol{r} + \alpha_k \boldsymbol{v}_k'\boldsymbol{r} + \beta_k \boldsymbol{w}_k'\boldsymbol{r}\right]\Big|_{\alpha_k,\beta_k=0}. \tag{34}$$

For ease of derivations, we introduce a new function – a generating function denoted as φ_k – derivable from (34):

$$\varphi_k = \exp\left[-\boldsymbol{r}'\left(A_k \otimes \mathbf{I}\right)\boldsymbol{r} + \alpha_k \boldsymbol{v}_k'\boldsymbol{r} + \beta_k \boldsymbol{w}_k'\boldsymbol{r}\right]. \tag{35}$$

5 Symmetry considerations

In a general sense, the group-theoretical approach provides an explanation for the physics associated with various symmetries. Group representation theory serves as a purely mathematical language for characterizing the different symmetries present in the state of a physical system. Despite the non-simultaneous development of group theory mathematics and the physics of symmetries, exemplified by the Noether theorem, the close relationship between them was recognized by different authors, including Wigner and Weyl, and was clearly established as a theory before 1930. This intimate connection between group theory and the theory of symmetries in physical systems becomes explicitly apparent within the framework of quantum mechanics [83]. Specifically, the quantum mechanical wave functions that live in the Hilbert space constitute a linear vector space [80]. Symmetries inherent in the underlying physical system require specific pattern structures in these vector spaces. These particular regularities can be solely determined by group representation theory and remain independent of other details of the system.

There are various types of groups, characterized by the nature of their elements. For instance, a commonly encountered group in physics is known as continuous groups, where the group elements are continuous variables. Here, a continuous variable means that each variable or group element has a well-defined range. The mathematical theory associated with continuous groups is generally referred to as Lie groups. Another example arises when a physical system contains k identical particles, leading to the natural emergence of the symmetric group S_k that has the order of $k!$.

In atomic and molecular systems involving more than two particles, there exists a set of identical particles, comprising electrons, nuclei, or other exotic particles. The total wave functions of these systems, as well as any quantum systems, must be symmetric or antisymmetric with respect to the permutations of identical fermions and bosons, respectively. To generate highly accurate wave functions for these quantum systems, it is necessary to take into account and employ the permutational symmetry in the calculations. Let us suppose that the system of interest contains k identical particles. The Hamiltonian of the system is invariant with respect to the permutations of these identical particles. This means that the Hamiltonian commutes with the elements of the kth order

symmetric group S_k:

$$[\mathcal{H}, \mathcal{X}_i] = 0, \tag{36}$$

where $\mathcal{X}_i$ is an arbitrary element (permutation) of the symmetric group S_k. Therefore, there exist simultaneous eigenfunctions of both the Hamiltonian and the symmetric group. We can construct these simultaneous eigenstates by taking the spatial basis functions and projecting them onto the appropriate irreducible representations of the symmetric group. Only then, using these symmetry-projected basis functions, we can proceed to the energy minimization problem solved by the secular equation, as described in Section 3.1. This approach is employed to generate highly accurate wave functions and subsequently calculate the expectation values of various operators. For detailed information on the application of the symmetric group in quantum mechanical bound state calculations, refer to Ref. [83].

Because the nonrelativistic Hamiltonian expressed in equation (22) lacks spin-orbit, spin-spin, and some other small contribution interaction terms, the Hamiltonian is considered spin-free, indicating its independence on the spin of particles. The total spin operator S of this system and its projection on a selected axis (e.g., the z axis: S_z) commute with $\mathcal{H}$. As a result, the eigenstates of both the Hamiltonian and the total spin operator, along with its projection, are the same. In other words, each definite state (eigenstate) of the system can be defined by simultaneous eigenfunctions of these compatible operators. Furthermore, these eigenstates can be singlets ($S = 0$), doublets ($S = 1/2$), triplets ($S = 1$), and so on, depending on the total spin state of the system. Using the spin-free Hamiltonian implies electronic states with definite multiplicities ($2S + 1$). For instance, if a collection of identical atoms (e.g., silver atoms) passes through an inhomogeneous magnetic field, the observed outcome would be either one stream or separate streams corresponding to total spin states of $S = 0, S = 1/2$, and $S = 1$, respectively (as demonstrated in the Stern-Gerlach experiment).

In the context of spin-free formalism, as presented in references [83, 84], the Young operators associated with the irreducible representations of the symmetric group are deduced based on their corresponding Young tableaux [83, 84]. When dealing with a system consisting of k identical particles, these Young tableaux are formed by arranging a series

of k-connected vacant boxes referred to as Young frames. To illustrate, in the scenario of a system containing 4 identical particles, these Young frames might be represented as follows:

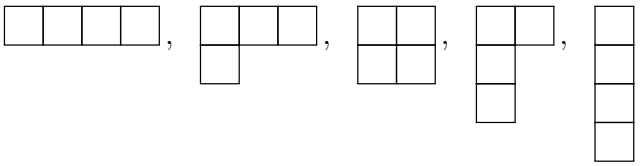

(37)

The arrangement of the suitable Young frame is contingent on various factors such as whether the identical particles under consideration are fermions or bosons, their specific spin, and the total spin of the system under consideration. In the instance of fermions with a spin of $1/2$, the Young frame associated with the spatial wave function should not exceed two columns. In contrast, for fermions possessing a spin of $3/2$, the maximum allowable number of columns is four. In the case of bosons, there is no restriction on the number of columns, but there is a constraint on the number of rows. These limitations are determined by adhering to the general principle governing the construction of Young frames [85].

To construct a Young frame for spin $1/2$ fermions with a total spin quantum number S, the symmetry quantum number p is calculated, where $p = k/2 - S$. Subsequently, a partition is expressed as $\mu = [2^p, 1^{k-2p}]$, and the Young frame is comprised of two boxes in the first p rows and one box in the remaining $k - 2p$ rows.

A Young tableau is then constructed by populating the Young frame with numbers that serve as labels for the identical particles, typically ranging from 1 to k in the case of neutral atoms. One can arrange these numbers within the boxes arbitrarily. For example, these numbers can increase either from top to bottom or from left to right in the specific Young frame. As an illustration, one can analyze the singlet D state of the beryllium atom. In this example, the number representing the identical particles or electrons is $k = 4$, and the total spin quantum number is $S = 0$. It is easy to see that $p = 2$ from the expression $p = k/2 - S$. Accordingly, the partition is denoted as $\mu = [2^2, 1^0]$. Now, let us assume that identical electrons are labeled from 1 to 4, while the fifth particle is assumed as a nucleus. Taking these assumptions, the Young tableau is populated in the following manner:

(38)

Another example is the triplet spin symmetry of the carbon atom. In this instance, the number representing the identical particles or electrons is $k = 6$, and the total spin quantum number is $S = 1$, which is a triplet multiplicity. Following the similar step from previous example, one can find that $p = 2$. Accordingly, the partition is written as $\mu = [2^2, 1^2]$. Now, let us assume that identical electrons are labeled from 2 to 7, while the first particle is assumed as a nucleus. Taking these assumptions, the Young tableau is populated in the following manner:

$$\begin{array}{|c|c|}\hline 2 & 3 \\ \hline 4 & 5 \\ \hline 6 \\ \cline{1-1} 7 \\ \cline{1-1}\end{array}\,. \tag{39}$$

By completely filling the Young tableau, one can proceed to expressing the Young symmetry projector in the following way:

$$\mathcal{Y} = \mathcal{S}\mathcal{A}. \tag{40}$$

Here, $\mathcal{S}$ and $\mathcal{A}$ represent operators for symmetrization and antisymmetrization, respectively. The definition of $\mathcal{S}$ involves a product of symmetrizers over particles in each row of the Young tableaux, while $\mathcal{A}$ is defined as a product of antisymmetrizers over particles in each column. Expressing $\mathcal{S}$ and $\mathcal{A}$ is straightforward with the use of transpositions, denoted as $\mathcal{P}_{ij}$, which represent pair permutations of particles. For example, consider the Young tableaux in Eq. (38) and (39), which give rise to the following Young operators:

$$\mathcal{Y} = \mathcal{S}_{1,2}\mathcal{S}_{3,4}\mathcal{A}_{1,3}\mathcal{A}_{2,4}\,, \tag{41}$$

$$\mathcal{Y} = \mathcal{S}_{2,3}\mathcal{S}_{4,5}\mathcal{A}_{2,4,6,7}\mathcal{A}_{3,5}\,, \tag{42}$$

In these formulas, the subscripts indicate the particles for which symmetrization or antisymmetrization is applicable. It is noteworthy to mention that, since each symmetrizer pertains to a distinct set of particles, arranging the symmetrizers in a specific order is not crucial. Similarly, specifically arranging the antisymmetrizers is also not critical. When expressed using transpositions, the $\mathcal{S}$'s and $\mathcal{A}$'s in the expressions (41) and (42) can be

represented as follows:

$$\begin{aligned}
\mathcal{S}_{1,2} &= (\mathcal{I}+\mathcal{P}_{12})\,, \\
\mathcal{S}_{3,4} &= (\mathcal{I}+\mathcal{P}_{34})\,, \\
\mathcal{A}_{1,3} &= (\mathcal{I}-\mathcal{P}_{13})\,, \\
\mathcal{A}_{2,4} &= (\mathcal{I}-\mathcal{P}_{24})\,,
\end{aligned}$$

and

$$\begin{aligned}
\mathcal{S}_{2,3} &= (\mathcal{I}+\mathcal{P}_{23})\,, \\
\mathcal{S}_{4,5} &= (\mathcal{I}+\mathcal{P}_{45})\,, \\
\mathcal{A}_{2,4,6,7} &= (\mathcal{I}-\mathcal{P}_{24})(\mathcal{I}-\mathcal{P}_{26}-\mathcal{P}_{46})(\mathcal{I}-\mathcal{P}_{27}-\mathcal{P}_{47}-\mathcal{P}_{67})\,, \\
\mathcal{A}_{3,5} &= (\mathcal{I}-\mathcal{P}_{35})
\end{aligned}$$

respectively. Here, $\mathcal{I}$ represent the identity operator.

It is important to highlight that, in variational calculations, the expectation values of operators often commute with all transpositions present in symmetrizers and antisymmetrizers (40), in addition to being Hermitian. Therefore, when evaluating the matrix elements of such quantities, due to the equality:

$$\langle \mathcal{Y}\phi_k|\mathcal{O}|\mathcal{Y}\phi_l\rangle = \langle \phi_k|\mathcal{O}|\mathcal{Y}^\dagger\mathcal{Y}\phi_l\rangle, \tag{43}$$

one can always restrict to scenarios where the Young operator is applied solely to the ket basis functions. In this equality, $\mathcal{O}$ represents the operator that commutes with all transpositions present in symmetrizers and antisymmetrizers (40). The dagger sign represents the Hermitian conjugate. For instance, $\mathcal{Y}^\dagger$ is the Hermitian conjugate of $\mathcal{Y}$. When substituted into Eq. (40), the following relation holds: $\mathcal{A}^\dagger\mathcal{S}^\dagger = \mathcal{A}\mathcal{S}$.

It is worth mentioning that the number of independent terms on the right-hand side of equation (43), resulting from the operator $\mathcal{Y}^\dagger\mathcal{Y} \propto \mathcal{A}\mathcal{S}\mathcal{A}$ acting on the ket basis function, can be reduced to $k!$ when computing the matrix element of $\mathcal{O}$. This simplification of the operator $\mathcal{A}\mathcal{S}\mathcal{A}$ involves multiplying all the transpositions term by term and combining identical terms during the summation of independent terms. While summing these independent terms, it becomes crucial to understand how the basis functions in the ket,

$|\phi_l\rangle$, are transformed when acting with the permutational transpositions in symmetrizers and antisymmetrizers. The immediate notice is the functional structure of the basis functions, which remains unchanged, with the changes occurring in the set of nonlinear variational parameters ($\boldsymbol{A}_l, \boldsymbol{v}_l$, and $\boldsymbol{w}_l$). Upon the action of an arbitrary permutational operator $\mathcal{P}$ on the laboratory frame coordinates $\mathbf{r}$ of the real particles, these coordinates experience a linear transformation. Similarly, the internal coordinates $\boldsymbol{r}$ or coordinates of the pseudoparticles undergo a linear transformation due to permutations of the real particles. This linear transformation of internal coordinates can be expressed using the permutation matrix $\boldsymbol{P} = P \otimes \mathbf{I}$. Applying $\mathcal{P}$ to the basis function (33) results in:

$$\mathcal{P}\phi_l = \mathcal{P}\frac{\partial}{\partial\alpha_l}\frac{\partial}{\partial\beta_l}\exp\left[-\boldsymbol{r}'\boldsymbol{A}_l\boldsymbol{r} + \alpha_l(\boldsymbol{v}_l)'\boldsymbol{r} + \beta_l(\boldsymbol{w}_l)'\boldsymbol{r}\right]\Big|_{\alpha_l,\beta_l=0}$$

$$= \frac{\partial}{\partial\alpha_l}\frac{\partial}{\partial\beta_l}\exp\left[-(\boldsymbol{P}\boldsymbol{r})'\boldsymbol{A}_l(\boldsymbol{P}\boldsymbol{r}) + \alpha_l(\boldsymbol{v}_l)'(\boldsymbol{P}\boldsymbol{r}) + \beta_l(\boldsymbol{w}_l)'(\boldsymbol{P}\boldsymbol{r})\right]\Big|_{\alpha_l,\beta_l=0}$$

$$= \frac{\partial}{\partial\alpha_l}\frac{\partial}{\partial\beta_l}\exp\left[-\boldsymbol{r}'(\boldsymbol{P}'\boldsymbol{A}_l\boldsymbol{P})\boldsymbol{r} + \alpha_l(\boldsymbol{P}'\boldsymbol{v}_l)'\boldsymbol{r} + \beta_l(\boldsymbol{P}'\boldsymbol{w}_l)'\boldsymbol{r}\right]\Big|_{\alpha_l,\beta_l=0}. \tag{44}$$

This expression illustrates the transformation of the nonlinear parameters of the Gaussians, namely the matrices A_l and the associated sparse vectors v_l and w_l. For clearity, we can define the following notations when deriving the matrix elements of various operators

$$\left|\tilde{\phi}_l\right\rangle \equiv \mathcal{P}\left|\phi_l\right\rangle, \quad \tilde{\boldsymbol{A}}_l \equiv \boldsymbol{P}'\boldsymbol{A}_l\boldsymbol{P}, \quad \tilde{\boldsymbol{L}}_l \equiv \boldsymbol{P}'\boldsymbol{L}_l, \quad \tilde{\boldsymbol{v}}_l \equiv \boldsymbol{P}'\boldsymbol{v}_l, \quad \tilde{\boldsymbol{w}}_l \equiv \boldsymbol{P}'\boldsymbol{w}_l. \tag{45}$$

For convenience, we can also write

$$\boldsymbol{A}_{kl} = \boldsymbol{A}_k + \boldsymbol{A}_l, \quad \tilde{\boldsymbol{A}}_{kl} = \boldsymbol{A}_k + \tilde{\boldsymbol{A}}_l. \tag{46}$$

As can be seen in the following sections, we will not be using the tilde sign defined above due to the very long and complexity of the expressions of the matrix elements. Instead, we will explicitly assume that the ket basis function can be transformed by certain particle permutations. This means that the matrices L_l, A_l, and A_{kl}, as well as the vectors v_l and w_l presented in all equations should be substituted with $\tilde{L}_l$, $\tilde{A}_l$, $\tilde{A}_{kl}$, $\tilde{v}_l$, and $\tilde{w}_l$,

respectively. Yet, to keep the expressions less confusing, we will avoid explicitly including the tilda signs.

6 Matrix elements of Hamiltonian and overlap

A couple of brief general comments need to be mentioned concerning the calculation of matrix elements. First, all the matrix element derivations will be conducted using the formalism of matrix differential calculus [78]. Let us introduce the most commonly used relations for the derivation of matrix elements in this work. These relations involve differentials with matrices:

$$\begin{aligned} \mathrm{d}\,|X| &= |X|\,\mathrm{tr}\left[X^{-1}\,\mathrm{d}\,X\right], \\ \mathrm{d}\,\mathrm{tr}\left[X\right] &= \mathrm{tr}\left[\mathrm{d}\,X\right], \\ \mathrm{d}\left(X^{-1}\right) &= -X^{-1}(\mathrm{d}\,X)X^{-1}. \end{aligned} \tag{47}$$

where the operation $|X|$ denotes the determinant of the matrix X. X^{-1} and $\mathrm{tr}\left[X\right]$ are the inverse and the trace of matrix X. Second, the following n-dimensional Gaussian integral will be used frequently

$$\int_{-\infty}^{\infty} \exp[-x'Ax + y'x]\,\mathrm{d}\,x = \frac{\pi^{n/2}}{|A|^{1/2}} \exp\left[\frac{1}{4}y'A^{-1}y\right]. \tag{48}$$

In this expression, x and y represent vectors that contain n-components. The first vector comprises n variables $(x_1, \ldots, x_n)$, while the second vector is consist of n constants $(y_1, \ldots, y_n)$. A is an $n \times n$ symmetric matrix that is positive definite.

6.1 Overlap integral

The calculation of the overlap integral for the generating functions φ_k, as defined in expression (35), is straightforwardly derived through the use of formula (48),

$$\begin{aligned} \langle\varphi_k|\varphi_l\rangle \;=\; & \int \exp\left[-\boldsymbol{r}'\boldsymbol{A}_{kl}\boldsymbol{r} + \left(\alpha_k\boldsymbol{v}_k+\beta_k\boldsymbol{w}_k+\alpha_l\boldsymbol{v}_l+\beta_l\boldsymbol{w}_l\right)'\boldsymbol{r}\right] d\boldsymbol{r} = \frac{\pi^{3n/2}}{|A_{kl}|^{3/2}} \\ & \times \exp\left[\frac{1}{4}\left(\alpha_k\boldsymbol{v}_k+\beta_k\boldsymbol{w}_k+\alpha_l\boldsymbol{v}_l+\beta_l\boldsymbol{w}_l\right)'\boldsymbol{A}_{kl}^{-1}\left(\alpha_k\boldsymbol{v}_k+\beta_k\boldsymbol{w}_k+\alpha_l\boldsymbol{v}_l+\beta_l\boldsymbol{w}_l\right)\right]. \end{aligned} \tag{49}$$

In this expression $\boldsymbol{A}_{kl} = \boldsymbol{A}_k + \boldsymbol{A}_l$, and we used the property of Kronecker product regarding the determinant of matrix A_{kl}

$$|\boldsymbol{A}_{kl}| = |A_{kl} \otimes \mathbf{I}| = |A_{kl}|^3. \tag{50}$$

The form of the overlap integral involving basis functions (33) will vary based on the particular arrangement of Cartesian coordinates in the Gaussian prefactors represented by vectors v_k and w_k. There are three specific scenarios, each resulting in a different expression, which we outline separately below.

case $(x_{i_k}x_{j_k}|x_{i_l}x_{j_l})$

In this case, it is evident that $\boldsymbol{\epsilon}^v = \boldsymbol{\epsilon}^w$. As an example, we can write $\boldsymbol{\epsilon}^v = \boldsymbol{\epsilon}^w = \boldsymbol{\epsilon}^x$. Because simple Gaussians (24) is spherically symmetric (i.e. rotationally invariant), overlap integral will be the same if we have $\boldsymbol{\epsilon}^v = \boldsymbol{\epsilon}^w = \boldsymbol{\epsilon}^y$ or $\boldsymbol{\epsilon}^v = \boldsymbol{\epsilon}^w = \boldsymbol{\epsilon}^z$.

To solve the integral, initially, we can simplify the integral (49) by reducing the size of matrix $\boldsymbol{A}_{kl}$ and vectors from $3n$ to n:

$$\begin{aligned}\langle\varphi_k|\varphi_l\rangle &= \frac{\pi^{3n/2}}{|A_{kl}|^{3/2}}\exp\Big[\frac{1}{4}\big(\alpha_k v_k+\beta_k w_k+\alpha_l v_l+\beta_l w_l\big)'\times \\ &\quad A_{kl}^{-1}\left(\alpha_k v_k+\beta_k w_k+\alpha_l v_l+\beta_l w_l\right)\Big].\end{aligned} \tag{51}$$

Note that the following property of Kronecker product is utilized above:

$$\left(a'\otimes\boldsymbol{\epsilon}^{x\prime}\right)\left(A_{kl}\otimes\mathbf{I}\right)\left(a\otimes\boldsymbol{\epsilon}^x\right)=a'A_{kl}a\otimes\boldsymbol{\epsilon}^{x\prime}\mathbf{I}\boldsymbol{\epsilon}^x=a'A_{kl}a, \tag{52}$$

where a is some vector. To find the overlap integral, we still need to take four derivatives and then evaluate the limits in the given integral:

$$\begin{aligned}\mathtt{S}_{kl} &= \frac{\partial}{\partial\beta_l}\frac{\partial}{\partial\beta_k}\frac{\partial}{\partial\alpha_l}\frac{\partial}{\partial\alpha_k}\langle\varphi_k|\varphi_l\rangle\Big|_{\alpha_k,\alpha_l,\beta_k,\beta_l=0}=\frac{\pi^{3n/2}}{|A_{kl}|^{3/2}}\frac{1}{4}\Big(\left[v_k'A_{kl}^{-1}v_l\right]\left[w_k'A_{kl}^{-1}w_l\right] \\ &\quad+\left[v_k'A_{kl}^{-1}w_k\right]\left[v_l'A_{kl}^{-1}w_l\right]+\left[v_k'A_{kl}^{-1}w_l\right]\left[w_k'A_{kl}^{-1}v_l\right]\Big).\end{aligned} \tag{53}$$

For writing the expressions in a compact form, we need to introduce the following quantities:

$$\begin{aligned}&\gamma_1=v_k'A_{kl}^{-1}v_l,\quad \gamma_2=w_k'A_{kl}^{-1}w_l,\quad \gamma_3=v_k'A_{kl}^{-1}w_k,\\ &\gamma_4=v_l'A_{kl}^{-1}w_l,\quad \gamma_5=v_k'A_{kl}^{-1}w_l,\quad \gamma_6=w_k'A_{kl}^{-1}v_l.\end{aligned} \tag{54}$$

Using these quantities, the overlap integral is

$$\mathtt{S}_{kl}=\frac{1}{4}\frac{\pi^{3n/2}}{|A_{kl}|^{3/2}}\,\gamma, \tag{55}$$

where

$$\gamma=\gamma_1\gamma_2+\gamma_3\gamma_4+\gamma_5\gamma_6. \tag{56}$$

case $(x_{i_k}y_{j_k}|y_{i_l}x_{j_l})$

Because of the property of Kronecker product we have cancellations $\boldsymbol{\epsilon}^{x\prime}\mathbf{I}\boldsymbol{\epsilon}^{y} = \boldsymbol{\epsilon}^{y\prime}\mathbf{I}\boldsymbol{\epsilon}^{x} = 0$, and therefore, expression (51) simplifies to

$$\begin{aligned}\langle\varphi_k|\varphi_l\rangle &= \frac{\pi^{3n/2}}{|A_{kl}|^{3/2}}\exp\Big[\frac{1}{4}\left(\alpha_k v_k+\alpha_l v_l\right)' A_{kl}^{-1}(\alpha_k v_k+\alpha_l v_l)\Big] \\ &\quad\times\exp\Big[\frac{1}{4}\left(\beta_k w_k+\beta_l w_l\right)' A_{kl}^{-1}\left(\beta_k w_k+\beta_l w_l\right)\Big],\end{aligned} \tag{57}$$

and following the same steps above we have

$$\mathtt{S}_{kl} = \frac{1}{4}\frac{\pi^{3n/2}}{|A_{kl}|^{3/2}}\,\gamma_1\gamma_2. \tag{58}$$

case $(x_{i_k}x_{j_k}|y_{i_l}y_{j_l})$

In this case, we have

$$\mathtt{S}_{kl} = \frac{1}{4}\frac{\pi^{3n/2}}{|A_{kl}|^{3/2}}\,\gamma_3\gamma_4. \tag{59}$$

It is evident now that the expressions and derivations of matrix elements in the three scenarios are remarkably similar. Due to this similarity, in the subsequent sections deriving other matrix elements related to kinetic energy, potential energy, and the analytical gradient, as well as operators of leading relativistic corrections, we will simply provide the final formulas for all three situations instead of reiterating nearly identical derivations several times.

6.2 Kinetic energy

case $(x_{i_k}x_{j_k}|x_{i_l}x_{j_l})$

Before solving the kinetic energy integral, let us first provide the expression for the value of an auxiliary integral involving a $3n\times 3n$ symmetric matrix $\boldsymbol{X}$. This is necessary because we will require the result of this integral several times when deriving matrix elements of

other operators. This integral represents the expectation value of $\boldsymbol{r}'\boldsymbol{X}\boldsymbol{r}$:

$$\begin{aligned}\langle\phi_k|\boldsymbol{r}'\boldsymbol{X}\boldsymbol{r}|\phi_l\rangle &= -\frac{\partial}{\partial\beta}\langle\phi_k|\exp\left[-\beta\boldsymbol{r}'\boldsymbol{X}\boldsymbol{r}\right]|\phi_l\rangle\Big|_{\beta=0} = -\frac{\partial}{\partial\beta}\frac{\pi^{3n/2}}{|A_{kl}+\beta X|^{3/2}} \\ &\times\Big(\left[v_k'(A_{kl}+\beta X)^{-1}v_l\right]\left[w_k'(A_{kl}+\beta X)^{-1}w_l\right] \\ &+\left[v_k'(A_{kl}+\beta X)^{-1}w_k\right]\left[v_l'(A_{kl}+\beta X)^{-1}w_l\right] \\ &+\left[v_k'(A_{kl}+\beta X)^{-1}w_l\right]\left[w_k'(A_{kl}+\beta X)^{-1}v_l\right]\Big)\Big|_{\beta=0}, \end{aligned} \tag{60}$$

where $\boldsymbol{X} = X \otimes \mathrm{I}_3$. By using the relations in (47) and performing some algebraic manipulations, we obtain

$$\begin{aligned}\langle\phi_k|\boldsymbol{r}'\boldsymbol{X}\boldsymbol{r}|\phi_l\rangle &= \frac{3}{2}\,\mathrm{tr}\left[A_{kl}^{-1}X\right]\mathtt{S}_{kl} + \frac{\pi^{3n/2}}{4|A_{kl}|^{3/2}}\Big(\left[v_k'A_{kl}^{-1}XA_{kl}^{-1}v_l\right]\left[w_k'A_{kl}^{-1}w_l\right] \\ &+\left[v_k'A_{kl}^{-1}v_l\right]\left[w_k'A_{kl}^{-1}XA_{kl}^{-1}w_l\right] + \left[v_k'A_{kl}^{-1}XA_{kl}^{-1}w_k\right]\left[v_l'A_{kl}^{-1}w_l\right] \\ &+\left[v_k'A_{kl}^{-1}w_k\right]\left[v_l'A_{kl}^{-1}XA_{kl}^{-1}w_l\right] + \left[v_k'A_{kl}^{-1}XA_{kl}^{-1}w_l\right]\left[w_k'A_{kl}^{-1}v_l\right] \\ &+\left[v_k'A_{kl}^{-1}w_l\right]\left[w_k'A_{kl}^{-1}XA_{kl}^{-1}v_l\right]\Big). \end{aligned} \tag{61}$$

To derive the matrix elements of the kinetic energy, we first apply $\boldsymbol{\nabla}_{\boldsymbol{r}}$ to both the bra and ket generating functions (35):

$$\boldsymbol{\nabla}_{\boldsymbol{r}}\varphi_k = \left[-2\boldsymbol{A}_k\boldsymbol{r} + \alpha_k\boldsymbol{v}_k + \beta_k\boldsymbol{w}_k\right]\varphi_k. \tag{62}$$

Multiplying the above result from both the bra and ket functions with each other yields

$$\begin{aligned}\langle\boldsymbol{\nabla}_{\boldsymbol{r}}\varphi_k|\boldsymbol{M}|\boldsymbol{\nabla}_{\boldsymbol{r}}\varphi_l\rangle &= \langle(-2\boldsymbol{A}_k\boldsymbol{r} + \alpha_k\boldsymbol{v}_k + \beta_k\boldsymbol{w}_k)\varphi_k|\boldsymbol{M}|(-2\boldsymbol{A}_l\boldsymbol{r} + \alpha_l\boldsymbol{v}_l + \beta_l\boldsymbol{w}_l)\varphi_l\rangle \\ &= 4\langle\varphi_k|\boldsymbol{r}'\boldsymbol{A}_k'\boldsymbol{M}\boldsymbol{A}_l\boldsymbol{r}|\varphi_l\rangle \\ &\quad -2\alpha_l\langle\varphi_k|\boldsymbol{r}'\boldsymbol{A}_k'\boldsymbol{M}\boldsymbol{v}_l|\varphi_l\rangle - 2\beta_l\langle\varphi_k|\boldsymbol{r}'\boldsymbol{A}_k'\boldsymbol{M}\boldsymbol{w}_l|\varphi_l\rangle \\ &\quad -2\alpha_k\langle\varphi_k|\boldsymbol{v}_k'\boldsymbol{M}\boldsymbol{A}_l\boldsymbol{r}|\varphi_l\rangle + \alpha_k\alpha_l\boldsymbol{v}_k'\boldsymbol{M}\boldsymbol{v}_l\langle\varphi_k|\varphi_l\rangle \\ &\quad +\alpha_k\beta_l\boldsymbol{v}_k'\boldsymbol{M}\boldsymbol{w}_l\langle\varphi_k|\varphi_l\rangle - 2\beta_k\langle\varphi_k|\boldsymbol{w}_k'\boldsymbol{M}\boldsymbol{A}_l\boldsymbol{r}|\varphi_l\rangle \\ &\quad +\beta_k\alpha_l\boldsymbol{w}_k'\boldsymbol{M}\boldsymbol{v}_l\langle\varphi_k|\varphi_l\rangle + \beta_k\beta_l\boldsymbol{w}_k'\boldsymbol{M}\boldsymbol{w}_l\langle\varphi_k|\varphi_l\rangle. \end{aligned} \tag{63}$$

Since it closely resembles the derivations in the previous sections, the matrix elements of the kinetic energy operator with the basis functions (33), are derived by taking four derivatives of above terms. During this process, three distinct types of integrals emerge. The first type stems from the first term on the right-hand side of (63), involving a quadratic

form. By ensuring symmetry in the matrix defining this quadratic form and employing the expression (61) with $\boldsymbol{X} = (\boldsymbol{A}_k'\boldsymbol{M}\boldsymbol{A}_l + \boldsymbol{A}_l'\boldsymbol{M}\boldsymbol{A}_k)/2$, this integral is calculated. The second type of integral arises from the second, third, fourth, and seventh terms in (63). These integrals resemble the overlap integral (55) after specific substitutions of matrices. Lastly, the third type of integral bears resemblance to the overlap integral of Gaussians with single Cartesian prefactors, a result previously derived in the work [68]. Below, we list the final results of these integrals with the signs in front, and the orders are kept as in the above expression:

- $2\frac{3}{2}\,\mathrm{tr}\left[A_{kl}^{-1}X\right]\langle\phi_k|\phi_l\rangle + 2\frac{\pi^{3n/2}}{4|A_{kl}|^{3/2}}\Big(\left[v_k'A_{kl}^{-1}XA_{kl}^{-1}v_l\right]\left[b_k'A_{kl}^{-1}b_l\right] + \left[v_k'A_{kl}^{-1}v_l\right]\left[b_k'A_{kl}^{-1}XA_{kl}^{-1}b_l\right] + \left[v_k'A_{kl}^{-1}XA_{kl}^{-1}b_k\right]\left[v_l'A_{kl}^{-1}b_l\right] + \left[v_k'A_{kl}^{-1}b_k\right]\left[v_l'A_{kl}^{-1}XA_{kl}^{-1}b_l\right] + \left[v_k'A_{kl}^{-1}XA_{kl}^{-1}b_l\right]\left[b_k'A_{kl}^{-1}v_l\right] + \left[v_k'A_{kl}^{-1}b_l\right]\left[b_k'A_{kl}^{-1}XA_{kl}^{-1}v_l\right]\Big)$
- $-2\frac{\pi^{3n/2}}{|A_{kl}|^{3/2}}\frac{1}{4}\Big(\left[v_k'A_{kl}^{-1}A_k'Mv_l\right]\left[b_k'A_{kl}^{-1}b_l\right] + \left[v_k'A_{kl}^{-1}b_k\right]\left[v_l'MA_kA_{kl}^{-1}b_l\right] + \left[v_k'A_{kl}^{-1}b_l\right]\left[b_k'A_{kl}^{-1}A_k'Mv_l\right]\Big)$
- $-2\frac{\pi^{3n/2}}{|A_{kl}|^{3/2}}\frac{1}{4}\Big(\left[v_k'A_{kl}^{-1}v_l\right]\left[b_k'A_{kl}^{-1}A_k'Mb_l\right] + \left[v_k'A_{kl}^{-1}b_k\right]\left[v_l'A_{kl}^{-1}A_k'Mb_l\right] + \left[v_k'A_{kl}^{-1}A_k'Mb_l\right]\left[b_k'A_{kl}^{-1}v_l\right]\Big)$
- $-2\frac{\pi^{3n/2}}{|A_{kl}|^{3/2}}\frac{1}{4}\Big(\left[v_k'MA_lA_{kl}^{-1}v_l\right]\left[b_k'A_{kl}^{-1}b_l\right] + \left[v_k'MA_lA_{kl}^{-1}b_k\right]\left[v_l'A_{kl}^{-1}b_l\right] + \left[v_k'MA_lA_{kl}^{-1}b_l\right]\left[b_k'A_{kl}^{-1}v_l\right]\Big)$
- $\frac{1}{2}\frac{\pi^{3n/2}}{|A_{kl}|^{3/2}}(v_k'Mv_l)(b_k'A_{kl}^{-1}b_l)$
- $\frac{1}{2}\frac{\pi^{3n/2}}{|A_{kl}|^{3/2}}(v_k'Mb_l)(b_k'A_{kl}^{-1}v_l)$
- $-2\frac{\pi^{3n/2}}{|A_{kl}|^{3/2}}\frac{1}{4}\Big(\left[v_k'A_{kl}^{-1}v_l\right]\left[b_k'MA_lA_{kl}^{-1}b_l\right] + \left[v_k'A_{kl}^{-1}A_l'Mb_k\right]\left[v_l'A_{kl}^{-1}b_l\right] + \left[v_k'A_{kl}^{-1}b_l\right]\left[b_k'MA_lA_{kl}^{-1}v_l\right]\Big)$
- $\frac{1}{2}\frac{\pi^{3n/2}}{|A_{kl}|^{3/2}}(b_k'Mv_l)(v_k'A_{kl}^{-1}b_l)$
- $\frac{1}{2}\frac{\pi^{3n/2}}{|A_{kl}|^{3/2}}(b_k'Mb_l)(v_k'A_{kl}^{-1}v_l)$

After a lengthy yet straightforward algebraic manipulations, the following final expression for the matrix elements of the kinetic energy is obtained

$$\mathtt{T}_{kl} = \mathtt{S}_{kl}\left(6\tau + \frac{4\zeta}{\gamma}\right). \tag{64}$$

Here, we introduced another set of notations (which are similar to notations in (54) and (56)) to simplify the expression:

$$\begin{aligned}
&\eta_1 = (w_k' A_{kl}^{-1} A_l' M A_k A_{kl}^{-1} w_l), \quad \eta_2 = (v_k' A_{kl}^{-1} A_l' M A_k A_{kl}^{-1} v_l),\\
&\eta_3 = (v_l' A_{kl}^{-1} A_k' M A_k A_{kl}^{-1} w_l), \quad \eta_4 = (v_k' A_{kl}^{-1} A_l' M A_l A_{kl}^{-1} w_k),\\
&\eta_5 = (w_k' A_{kl}^{-1} A_l' M A_k A_{kl}^{-1} v_l), \quad \eta_6 = (v_k' A_{kl}^{-1} A_l' M A_k A_{kl}^{-1} w_l).\\
&\tau = \mathrm{tr}\left[A_{kl}^{-1} A_l M A_k'\right], \quad \zeta = \left(\gamma_1\eta_1 + \gamma_2\eta_2 - \gamma_3\eta_3 - \gamma_4\eta_4 + \gamma_5\eta_5 + \gamma_6\eta_6\right),
\end{aligned} \tag{65}$$

case $(x_{i_k} y_{j_k} | y_{i_l} x_{j_l})$

Using the identical method applied in the privious subsection, we achieve the similar outcome

$$\mathtt{T}_{kl} = \mathtt{S}_{kl}\left(6\tau + 4\frac{\eta_2}{\gamma_1} + 4\frac{\eta_1}{\gamma_2}\right) \tag{66}$$

case $(x_{i_k} x_{j_k} | y_{i_l} y_{j_l})$

In the third case

$$\mathtt{T}_{kl} = \mathtt{S}_{kl}\left(6\tau - 4\frac{\eta_4}{\gamma_3} - 4\frac{\eta_3}{\gamma_4}\right). \tag{67}$$

6.3 Potential energy

case $(x_{i_k} x_{j_k} | x_{i_l} x_{j_l})$

We can solve the potential energy integral by employing the Gaussian integral provided below

$$\int_{-\infty}^{\infty} d\beta \exp[-\beta^2 r_{ij}^2] = 2\int_0^{\infty} d\beta \exp[-\beta^2 r_{ij}^2] = \frac{\sqrt{\pi}}{r_{ij}} \Rightarrow$$
$$\Rightarrow \frac{1}{r_{ij}} = \frac{2}{\sqrt{\pi}} \int_0^{\infty} d\beta \exp[-\beta^2 r_{ij}^2].$$

When computing the expectation value of the potential energy integral, we can substitute the new form of $\frac{1}{r_{ij}}$ as

$$\left\langle \phi_k \middle| \frac{1}{r_{ij}} \middle| \phi_l \right\rangle = \frac{2}{\sqrt{\pi}} \int_0^\infty d\beta \langle \phi_k | \exp[-\beta^2 r_{ij}^2] | \phi_l \rangle. \tag{68}$$

For further derivations we rewrite the squares of the interparticle distances in quadratic forms

$$r_i^2 = \boldsymbol{r}' \boldsymbol{J}_{ii} \boldsymbol{r}, \quad r_{ij}^2 = \boldsymbol{r}' \boldsymbol{J}_{ij} \boldsymbol{r}, \tag{69}$$

where $\boldsymbol{J}_{ij} = J_{ij} \otimes \mathbf{I}$ is a matrix with the elements defined below:

$$J_{ij} = \begin{cases} E_{ii} & \text{if } i = j \quad , \\ E_{ii} + E_{jj} - E_{ij} - E_{ji} & \text{if } i \neq j \quad . \end{cases} \tag{70}$$

In this expression, every element in the matrix E_{ij} is zero, except for the entry located in the i-th row and j-th column, which equals one. Now, using the overlap matrix elements (55) and the integral in (68), we can compute the Coulomb integrals $\langle \phi_k \, |1/r_i| \, \phi_l \rangle$ and $\langle \phi_k \, |1/r_{ij}| \, \phi_l \rangle$

$$\begin{aligned} \mathtt{R}_{kl}^{ij} &= \left\langle \phi_k \left| \frac{1}{r_{ij}} \right| \phi_l \right\rangle = \frac{2}{\sqrt{\pi}} \int_0^\infty \langle \phi_k | \exp\left[-\beta^2 \boldsymbol{r}' \boldsymbol{J}_{ij} \boldsymbol{r}\right] | \phi_l \rangle \, \mathrm{d}\beta \\ &= \frac{\pi^{\frac{3n-1}{2}}}{2} \int_0^\infty \frac{1}{|A_{kl} + \beta^2 J_{ij}|^{3/2}} \Big(\left[v_k'(A_{kl} + \beta^2 J_{ij})^{-1} v_l\right] \left[w_k'(A_{kl} + \beta^2 J_{ij})^{-1} w_l\right] \\ &\quad + \left[v_k'(A_{kl} + \beta^2 J_{ij})^{-1} w_k\right] \left[v_l'(A_{kl} + \beta^2 J_{ij})^{-1} w_l\right] \\ &\quad + \left[v_k'(A_{kl} + \beta^2 J_{ij})^{-1} w_l\right] \left[w_k'(A_{kl} + \beta^2 J_{ij})^{-1} v_l\right] \Big) \mathrm{d}\beta. \end{aligned} \tag{71}$$

Using the trace form of terms enclosed in square brackets, e.g. $[v_k'(A_{kl} + \beta^2 J_{ij})^{-1} v_l] = \mathrm{tr}\,[(A_{kl} + \beta^2 J_{ij})^{-1} v_l v_k']$, and using the Sherman-Morrison formula, we rewrite them as

$$\mathrm{tr}\left[(A_{kl} + \beta^2 J_{ij})^{-1} v_l v_k'\right] = \mathrm{tr}\left[A_{kl}^{-1} v_l v_k'\right] - \frac{\beta^2 \,\mathrm{tr}\left[A_{kl}^{-1} J_{ij} A_{kl}^{-1} v_l v_k'\right]}{1 + \beta^2 \,\mathrm{tr}\left[A_{kl}^{-1} J_{ij}\right]},$$

$$\mathrm{tr}\left[(A_{kl} + \beta^2 J_{ij})^{-1} b_l b_k'\right] = \mathrm{tr}\left[A_{kl}^{-1} b_l b_k'\right] - \frac{\beta^2 \,\mathrm{tr}\left[A_{kl}^{-1} J_{ij} A_{kl}^{-1} b_l b_k'\right]}{1 + \beta^2 \,\mathrm{tr}\left[A_{kl}^{-1} J_{ij}\right]},$$

$$\mathrm{tr}\left[(A_{kl} + \beta^2 J_{ij})^{-1} b_k v_k'\right] = \mathrm{tr}\left[A_{kl}^{-1} b_k v_k'\right] - \frac{\beta^2 \,\mathrm{tr}\left[A_{kl}^{-1} J_{ij} A_{kl}^{-1} b_k v_k'\right]}{1 + \beta^2 \,\mathrm{tr}\left[A_{kl}^{-1} J_{ij}\right]},$$

$$\operatorname{tr}\left[(A_{kl}+\beta^2 J_{ij})^{-1} b_l v_l'\right] = \operatorname{tr}\left[A_{kl}^{-1} b_l v_l'\right] - \frac{\beta^2 \operatorname{tr}\left[A_{kl}^{-1} J_{ij} A_{kl}^{-1} b_l v_l'\right]}{1+\beta^2 \operatorname{tr}\left[A_{kl}^{-1} J_{ij}\right]},$$

$$\operatorname{tr}\left[(A_{kl}+\beta^2 J_{ij})^{-1} b_l v_k'\right] = \operatorname{tr}\left[A_{kl}^{-1} b_l v_k'\right] - \frac{\beta^2 \operatorname{tr}\left[A_{kl}^{-1} J_{ij} A_{kl}^{-1} b_l v_k'\right]}{1+\beta^2 \operatorname{tr}\left[A_{kl}^{-1} J_{ij}\right]},$$

$$\operatorname{tr}\left[(A_{kl}+\beta^2 J_{ij})^{-1} v_l b_k'\right] = \operatorname{tr}\left[A_{kl}^{-1} v_l b_k'\right] - \frac{\beta^2 \operatorname{tr}\left[A_{kl}^{-1} J_{ij} A_{kl}^{-1} v_l b_k'\right]}{1+\beta^2 \operatorname{tr}\left[A_{kl}^{-1} J_{ij}\right]},$$

$$\left|A_{kl}+\beta^2 J_{ij}\right| = \left|A_{kl}\right| \left(1+\beta^2 \operatorname{tr}\left[A_{kl}^{-1} J_{ij}\right]\right).$$

Substituting these expressions we can simplify the integral (71) into elemental integrals that can be solved directly. After doing some algebraic manipulations with the results of elemental integrals we have the final expression for the Coulomb integrals,

$$\mathtt{R}_{kl}^{ij} = \frac{\pi^{(3n-1)/2}}{2\left|A_{kl}\right|^{3/2} \omega^{1/2}} \left(\gamma - \frac{\kappa}{3\omega} + \frac{\rho}{5\omega^2}\right). \tag{72}$$

In this expression, we defined new set of notations:

$$\begin{aligned}
&\rho_1 = (w_k' A_{kl}^{-1} J_{ij} A_{kl}^{-1} w_l), \quad \rho_2 = (v_k' A_{kl}^{-1} J_{ij} A_{kl}^{-1} v_l), \quad \rho_3 = (v_l' A_{kl}^{-1} J_{ij} A_{kl}^{-1} w_l),\\
&\rho_4 = (v_k' A_{kl}^{-1} J_{ij} A_{kl}^{-1} w_k), \quad \rho_5 = (w_k' A_{kl}^{-1} J_{ij} A_{kl}^{-1} v_l), \quad \rho_6 = (v_k' A_{kl}^{-1} J_{ij} A_{kl}^{-1} w_l),\\
&\rho = [\rho_1\rho_2 + \rho_3\rho_4 + \rho_5\rho_6], \quad \omega = \operatorname{tr}\left[A_{kl}^{-1} J_{ij}\right],\\
&\kappa = [\gamma_1\rho_1 + \gamma_2\rho_2 + \gamma_3\rho_3 + \gamma_4\rho_4 + \gamma_5\rho_5 + \gamma_6\rho_6].
\end{aligned} \tag{73}$$

The total potential energy matrix elements can be expressed as the sum of $\mathtt{R}_{kl}^{i}$ and $\mathtt{R}_{kl}^{ij}$:

$$\mathtt{V}_{kl} = \sum_{i=1}^{n} q_0 q_i \mathtt{R}_{kl}^{i} + \sum_{i<j}^{n} q_i q_j \mathtt{R}_{kl}^{ij}. \tag{74}$$

case $(x_{i_k} y_{j_k} | y_{i_l} x_{j_l})$

In this case, the formulation for $\mathtt{R}_{kl}^{ij}$ resembles the one in (72), with the exception that we are required to make substitutions:

$$\gamma \to \gamma_1\gamma_2, \qquad \kappa \to \gamma_1\rho_1 + \gamma_2\rho_2, \qquad \rho \to \rho_1\rho_2. \tag{75}$$

case $(x_{i_k}x_{j_k}|y_{i_l}y_{j_l})$

In this case, the substitutions are

$$\gamma \to \gamma_3\gamma_4, \qquad \kappa \to \gamma_3\rho_3 + \gamma_4\rho_4, \qquad \rho \to \rho_3\rho_4. \tag{76}$$

6.4 Matrix elements with the Dirac delta function and interpacticle distances

The Dirac delta function is one of the important quantities in computational quantum mechanics since it allows us to compute the small atomic relativistic properties as well as the higher-order quantum electrodynamics (QED) corrections to the interstate transition energies of atoms. In addition to these applications, it can help us calculate the densities of particles, pair correlation functions, and interparticle distances. If we take an arbitrary function $f(\boldsymbol{r}_{ij})$, we can express it utilizing the property of the Dirac delta-function as follows:

$$f(\boldsymbol{r}_{ij}) = \int \delta(\boldsymbol{\theta} - \boldsymbol{r}_{ij}) f(\boldsymbol{\theta}) d\boldsymbol{\theta}, \tag{77}$$

Here, the integration with respect to $\boldsymbol{\theta}$ occurs in a three-dimensional $(3D)$ space, and $\delta(\boldsymbol{\theta} - \boldsymbol{r}_{ij})$ represents a three-dimensional Dirac delta-function. Utilizing this relationship, the expectation value of f can be expressed as:

$$\langle \phi_k | f(\boldsymbol{r}_{ij}) | \phi_l \rangle = \int f(\boldsymbol{\theta}) d\boldsymbol{\theta} \langle \phi_k | \delta(\boldsymbol{\theta} - \boldsymbol{r}_{ij}) | \phi_l \rangle. \tag{78}$$

Let us consider the following form of the Dirac delta function that depend on $\boldsymbol{r}_i$:

$$\delta\big(a_1\boldsymbol{r}_1 + a_2\boldsymbol{r}_2 + \cdots + a_n\boldsymbol{r}_n - \boldsymbol{\xi}\big) = \delta\big((a \otimes \mathbf{I})'\boldsymbol{r} - \boldsymbol{\xi}\big), \tag{79}$$

where a is a vector with n-components, while $\boldsymbol{\xi}$ represents 3-component real vector. For further theoretical analysis we can use the limit representation of the delta function

$$\delta\big((a \otimes \mathbf{I})'\boldsymbol{r} - \boldsymbol{\xi}\big) \;\; = \;\; \lim_{\beta\to\infty}\left(\frac{\beta^{3/2}}{\pi^{3/2}} \exp\Big[-\beta\big((a \otimes \mathbf{I})'\boldsymbol{r} - \boldsymbol{\xi}\big)^2\Big]\right). \tag{80}$$

For the moment, let us deal with the argument of the exponent:

$$-\beta((a \otimes \mathbf{I})'\boldsymbol{r} - \boldsymbol{\xi})^2 = -\beta(a \otimes \mathbf{I})'\boldsymbol{r}(a \otimes \mathbf{I})'\boldsymbol{r} + 2\beta\boldsymbol{\xi}(a \otimes \mathbf{I})'\boldsymbol{r} - \beta\boldsymbol{\xi}^2 =$$

$$= -\beta\boldsymbol{r}'(a \otimes \mathbf{I})(a \otimes \mathbf{I})'\boldsymbol{r} + 2\beta((a \otimes \mathbf{I})\boldsymbol{\xi})'\boldsymbol{r} - \beta\boldsymbol{\xi}^2 = -\beta\boldsymbol{r}'(aa' \otimes \mathbf{I})\boldsymbol{r} + 2\beta((a \otimes \mathbf{I})\boldsymbol{\xi})'\boldsymbol{r} - \beta\boldsymbol{\xi}^2.$$

Then, we will compute the matrix elements of Dirac delta function with generating functions (35) as

$$\left\langle\varphi_k\left|\delta\big((a\otimes\mathbf{I})'\boldsymbol{r}-\boldsymbol{\xi}\big)\right|\varphi_l\right\rangle=\lim_{\beta\to\infty}\left(\frac{\beta^{3/2}}{\pi^{3/2}}\exp\left[-\beta\boldsymbol{\xi}^2\right]\right.$$
$$\left.\times\left\langle\varphi_k\right|\exp\left[-\beta\boldsymbol{r}'(aa'\otimes\mathbf{I})\boldsymbol{r}+2\beta\big((a\otimes\mathbf{I})\boldsymbol{\xi}\big)'\boldsymbol{r}\right]\left|\varphi_l\right\rangle\right). \tag{81}$$

In this expression, the matrix element within the limit closely resembles the overlap integral found in equation (49)

$$\begin{aligned}&\langle\varphi_k\left|\delta((a\otimes\mathbf{I})'\boldsymbol{r}-\boldsymbol{\xi})\right|\varphi_l\rangle\\ =\ &\lim_{\beta\to\infty}\left(\frac{\beta}{\pi}\right)^{3/2}\exp\left[-\beta\boldsymbol{\xi}^2\right]\frac{\pi^{3n/2}}{|A_{kl}+\beta aa'|^{3/2}}\exp\left[\frac{1}{4}\big(\alpha_k\boldsymbol{v}_k+\beta_k\boldsymbol{w}_k+\alpha_l\boldsymbol{v}_l+\beta_l\boldsymbol{w}_l\right.\\ &\left.+2\beta(a\otimes\mathbf{I})\boldsymbol{\xi}\big)'((A_{kl}+\beta aa')^{-1}\otimes\mathbf{I})\big(\alpha_k\boldsymbol{v}_k+\beta_k\boldsymbol{w}_k+\alpha_l\boldsymbol{v}_l+\beta_l\boldsymbol{w}_l+2\beta(a\otimes\mathbf{I})\boldsymbol{\xi}\big)\right].\end{aligned} \tag{82}$$

Expanding the exponent's argument is necessary when taking the limit of this expression as β approaches infinity. First, let us find the limit of prefactor

$$\lim_{\beta\to\infty}\left(\frac{\beta}{\pi}\right)^{3/2}\frac{\pi^{3n/2}}{|A_{kl}+\beta aa'|^{3/2}}=\lim_{\beta\to\infty}\frac{\pi^{3(n-1)/2}}{|A_{kl}|^{3/2}}\left(\frac{\beta}{1+\beta a'A_{kl}^{-1}a}\right)^{3/2}=\frac{\pi^{3(n-1)/2}}{|A_{kl}|^{3/2}}\frac{1}{(a'A_{kl}^{-1}a)^{3/2}},$$

and we will expend the argument of exponent by substituting the term $A_{kl}^{-1}-\frac{\beta A_{kl}^{-1}aa'A_{kl}^{-1}}{1+\beta a'A_{kl}^{-1}a}$ instead of $(A_{kl}+\beta aa')^{-1}$ using the Sherman-Morrison formula. Let us write the expansion by denoting the argument of two exponents in (82) together as K:

$$K=\left[\frac{1}{4}(\alpha_k\boldsymbol{v}_k+\mu_k\boldsymbol{b}_k+\alpha_l\boldsymbol{v}_l+\mu_l\boldsymbol{b}_l)'(A_{kl}^{-1}\otimes\mathbf{I})(\alpha_k\boldsymbol{v}_k+\mu_k\boldsymbol{b}_k+\alpha_l\boldsymbol{v}_l+\mu_l\boldsymbol{b}_l)-\right.$$
$$-\frac{\beta(\alpha_k\boldsymbol{v}_k+\mu_k\boldsymbol{b}_k+\alpha_l\boldsymbol{v}_l+\mu_l\boldsymbol{b}_l)'(A_{kl}^{-1}aa'A_{kl}^{-1}\otimes\mathbf{I})(\alpha_k\boldsymbol{v}_k+\mu_k\boldsymbol{b}_k+\alpha_l\boldsymbol{v}_l+\mu_l\boldsymbol{b}_l)}{4(1+\beta a'A_{kl}^{-1}a)\otimes\mathbf{I}}+$$
$$\left.\frac{\beta(\alpha_k\boldsymbol{v}_k+\mu_k\boldsymbol{b}_k+\alpha_l\boldsymbol{v}_l+\mu_l\boldsymbol{b}_l)'(A_{kl}^{-1}a\otimes\mathbf{I})\boldsymbol{\xi}-\beta\boldsymbol{\xi}^2}{(1+\beta a'A_{kl}^{-1}a)\otimes\mathbf{I}}\right].$$

Taking the limit of this expression as $\beta\to\infty$ is now straightforward.

case $(x_{i_k}x_{j_k}|x_{i_l}x_{j_l})$

Upon evaluating the limit, we derive the following expression for the matrix elements of the delta function with generator functions (35):

$$\begin{aligned}
&\left\langle \varphi_k \left| \delta\big((a\otimes \mathbf{I})'\boldsymbol{r}-\boldsymbol{\xi}\big)\right| \varphi_l\right\rangle \\
= \;& \frac{\pi^{3(n-1)/2}}{|A_{kl}|^{3/2}}\frac{1}{(a'A_{kl}^{-1}a)^{3/2}}\exp\left[\frac{1}{a'A_{kl}^{-1}a}\left(\frac{1}{4}(\alpha_k v_k+\beta_k w_k+\alpha_l v_l+\beta_l w_l)'\times\right.\right.\\
&([a'A_{kl}^{-1}a]A_{kl}^{-1}-A_{kl}^{-1}aa'A_{kl}^{-1})(\alpha_k v_k+\beta_k w_k+\alpha_l v_l+\beta_l w_l)\\
&\left.\left.+(\alpha_k v_k+\beta_k w_k+\alpha_l v_l+\beta_l w_l)'A_{kl}^{-1}a(\boldsymbol{\epsilon}^{x\prime}\boldsymbol{\xi})-\boldsymbol{\xi}^2\right)\right].
\end{aligned} \tag{83}$$

To calculate the expectation value with basis functions (33), we still need to perform a lengthy but straightforward derivative. Therefore, we will present only the final results:

$$\begin{aligned}
\left\langle \phi_k \left| \delta\big((a\otimes \mathbf{I})'\boldsymbol{r}-\boldsymbol{\xi}\big)\right| \phi_l\right\rangle \;=\; & \frac{\pi^{3(n-1)/2}}{4\,|A_{kl}|^{3/2}\,\omega^{3/2}}\exp\left[-\frac{\boldsymbol{\xi}^2}{\omega}\right]\left(\left[\gamma-\frac{\kappa}{\omega}+\frac{\rho}{\omega^2}\right]\right.\\
&\left.+\frac{2}{\omega^2}\left[\kappa-\frac{2\rho}{\omega}\right](\boldsymbol{\epsilon}^{x\prime}\boldsymbol{\xi})^2+\frac{4\rho}{3\omega^4}(\boldsymbol{\epsilon}^{x\prime}\boldsymbol{\xi})^4\right).
\end{aligned} \tag{84}$$

In this expression, we utilized the notations defined in equations (54), (56), (65), and (73) for different quantities. However, it is essential to substitute J_{ij} with aa' throughout those equations.

The formula given in expression (84) offers a general method for computing the matrix elements of pair correlation functions and particle densities, both in the center-of-mass frame and other reference frames. These values, in return, can be employed to calculate the matrix elements of operators, such as different powers of interparticle distances. For example, we can compute the matrix elements of $|\boldsymbol{r}_i|^\lambda$ and $|\boldsymbol{r}_{ij}|^\lambda$, where λ is a real number that satisfies $\lambda > -3$. This can be done by considering the partial cases of $a = j^i$ and $a = j^j - j^i$, respectively. In this context, j^i represents a vector with n components, where only the i-th component is set to one, and all other components are zero.

The matrix elements of $|\boldsymbol{r}_{ij}|^\lambda$ is

$$\begin{aligned}
\left\langle \phi_k \left| r_{ij}^\lambda\right| \phi_l\right\rangle \;=\; & \frac{\pi^{(3n-1)/2}}{2\,|A_{kl}|^{3/2}}\,\Gamma\left(\frac{\lambda+3}{2}\right)\omega^{\lambda/2}\left[\left(\gamma-\frac{\kappa}{\omega}+\frac{\rho}{\omega^2}\right)\right.\\
&\left.+\frac{\lambda+3}{3\omega}\left(\kappa-\frac{2\rho}{\omega}\right)+\frac{(\lambda+5)(\lambda+3)\rho}{15\omega^2}\right],
\end{aligned} \tag{85}$$

where $\Gamma(\dots)$ is the Euler gamma function. To proof the correctness of the formula given in (85), we need to reproduce formula (72) when $\lambda = -1$. When $\lambda = 2$, it should reproduce matrix elements of $\boldsymbol{r}'\boldsymbol{X}\boldsymbol{r}$ in (61) if we set $\boldsymbol{X} = \boldsymbol{J}_{ij}$. Lastly, in the case of $\lambda = 0$, it should yield the overlap integral in (55). As can be easily verified, all these formulas can be reproduced using the general formula (85).

case $(x_{i_k} y_{j_k} | y_{i_l} x_{j_l})$

In this case, following the steps in the previous subsection, we can derive the expressions for the matrix elements of the Dirac delta function and r_{ij}^{λ}. The results are

$$\begin{aligned}
\left\langle \phi_k \left| \delta\big((a \otimes \mathbf{I})'\boldsymbol{r} - \boldsymbol{\xi}\big) \right| \phi_l \right\rangle &= \frac{\pi^{3(n-1)/2}}{4\,|A_{kl}|^{3/2}} \frac{\gamma_1\gamma_2}{(a'A_{kl}^{-1}a)^{3/2}} \exp\left[-\frac{\boldsymbol{\xi}^2}{a'A_{kl}^{-1}a}\right] \\
&\times \left[1 + \frac{1}{a'A_{kl}^{-1}a} \frac{v_k'A_{kl}^{-1}aa'A_{kl}^{-1}v_l}{v_k'A_{kl}^{-1}v_l} \left(2\frac{(\boldsymbol{\epsilon}^{x\prime}\boldsymbol{\xi})^2}{a'A_{kl}^{-1}a} - 1\right)\right] \\
&\times \left[1 + \frac{1}{a'A_{kl}^{-1}a} \frac{w_k'A_{kl}^{-1}aa'A_{kl}^{-1}w_l}{w_k'A_{kl}^{-1}w_l} \left(2\frac{(\boldsymbol{\epsilon}^{y\prime}\boldsymbol{\xi})^2}{a'A_{kl}^{-1}a} - 1\right)\right],
\end{aligned} \tag{86}$$

$$\begin{aligned}
\left\langle \phi_k \left| r_{ij}^{\lambda} \right| \phi_l \right\rangle &= \frac{\pi^{(3n-1)/2}}{2\,|A_{kl}|^{3/2}} \Gamma\left(\frac{\lambda+3}{2}\right) \omega^{\lambda/2}\gamma_1\gamma_2 \Bigg\{ \left(1 - \frac{\rho_2}{\omega\gamma_1}\right)\left(1 - \frac{\rho_1}{\omega\gamma_2}\right) \\
&+ \left(\frac{\lambda+3}{2}\right)\frac{2}{3}\left[\left(1 - \frac{\rho_2}{\omega\gamma_1}\right)\frac{\rho_1}{\omega\gamma_2} + \frac{\rho_2}{\omega\gamma_1}\left(1 - \frac{\rho_1}{\omega\gamma_2}\right)\right] \\
&+ \frac{(\lambda+5)(\lambda+3)}{15\omega^2}\frac{\rho_1\rho_2}{\gamma_1\gamma_2}\Bigg\}.
\end{aligned} \tag{87}$$

case $(x_{i_k} x_{j_k} | y_{i_l} y_{j_l})$

Similarly, in this case we have

$$\begin{aligned}
\left\langle \phi_k \left| \delta\big((a \otimes \mathbf{I})'\boldsymbol{r} - \boldsymbol{\xi}\big) \right| \phi_l \right\rangle &= \frac{\pi^{3(n-1)/2}}{4\,|A_{kl}|^{3/2}} \frac{\gamma_3\gamma_4}{(a'A_{kl}^{-1}a)^{3/2}} \exp\left[-\frac{\boldsymbol{\xi}^2}{a'A_{kl}^{-1}a}\right] \\
&\times \left[1 + \frac{1}{a'A_{kl}^{-1}a} \frac{v_k'A_{kl}^{-1}aa'A_{kl}^{-1}w_k}{v_k'A_{kl}^{-1}w_k} \left(2\frac{(\boldsymbol{\epsilon}^{x\prime}\boldsymbol{\xi})^2}{a'A_{kl}^{-1}a} - 1\right)\right] \\
&\times \left[1 + \frac{1}{a'A_{kl}^{-1}a} \frac{v_l'A_{kl}^{-1}aa'A_{kl}^{-1}w_l}{v_l'A_{kl}^{-1}w_l} \left(2\frac{(\boldsymbol{\epsilon}^{y\prime}\boldsymbol{\xi})^2}{a'A_{kl}^{-1}a} - 1\right)\right],
\end{aligned} \tag{88}$$

The matrix elements of r_{ij}^{λ} are

$$\begin{aligned}\left\langle \phi_k \left| r_{ij}^{\lambda} \right| \phi_l \right\rangle &= \frac{\pi^{(3n-1)/2}}{2\left|A_{kl}\right|^{3/2}} \Gamma\left(\frac{\lambda+3}{2}\right) \omega^{\lambda/2} \gamma_3 \gamma_4 \Bigg\{ \left(1-\frac{\rho_4}{\omega\gamma_3}\right)\left(1-\frac{\rho_3}{\omega\gamma_4}\right) + \\ & \frac{2}{3}\left(\frac{\lambda+3}{2}\right)\left[\left(1-\frac{\rho_4}{\omega\gamma_3}\right)\frac{\rho_3}{\omega\gamma_4} + \frac{\rho_4}{\omega\gamma_3}\left(1-\frac{\rho_3}{\omega\gamma_4}\right)\right] \\ & + \frac{(\lambda+5)(\lambda+3)}{15}\frac{\rho_3\rho_4}{\omega^2\gamma_3\gamma_4}\Bigg\}. \end{aligned} \tag{89}$$

7 Matrix elements of energy gradient

The variational optimization of the nonlinear parameters of ECGs is achieved through the minimization of the Rayleigh-Rits variational energy functional (see Section 3.1). The optimization of these parameters is a highly expensive procedure. To address this and improve the basis set convergence, it is well established that one can derive and implement the gradient of the energy with respect to the nonlinear parameters of ECGs [23]. For this purpose, we first take the differential of the eigenvalue problem in Eq. (13)

$$\mathrm{d}(\mathtt{H}-\varepsilon\mathtt{S})\mathtt{c} = (\mathrm{d}\mathtt{H})\mathtt{c} - (\mathrm{d}\varepsilon)\mathtt{S}\mathtt{c} - \varepsilon(\mathrm{d}\mathtt{S})\mathtt{c} + (\mathtt{H}-\varepsilon\mathtt{S})\mathrm{d}\mathtt{c}.$$

If we multiply this equation by $\mathtt{c}'$ from the left and assume that the wave function is normalized, i.e., $\mathtt{c}'\mathtt{S}\mathtt{c}=1$, then we can have

$$\mathrm{d}\varepsilon = \mathtt{c}'(\mathrm{d}\mathtt{H} - \varepsilon\mathrm{d}\mathtt{S})\mathtt{c}, \tag{90}$$

where for general purposes we can also assume the basis functions and the linear coefficients to be complex. Let us say that the basis functions $\phi_t(\{\alpha_t\})$ depend on some nonlinear parameters α_t. Because only the t-th row and t-th column of matrices $\mathtt{H}$ and $\mathtt{S}$ depends on α_t, the derivative of any arbitrary element belonging to that row or that column of these matrices can be expressed as

$$\frac{\partial \mathtt{H}_{kl}}{\partial\alpha_t} = \frac{\partial \mathtt{H}_{kl}}{\partial\alpha_t}(\delta_{kt}+\delta_{lt}-\delta_{kt}\delta_{lt}), \quad \frac{\partial \mathtt{S}_{kl}}{\partial\alpha_t} = \frac{\partial \mathtt{S}_{kl}}{\partial\alpha_t}(\delta_{kt}+\delta_{lt}-\delta_{kt}\delta_{lt}), \quad k,l=1,\cdots,\mathcal{K}$$

Using these, and the relation in Eq. (90), the derivative of the energy ε with respect to the parameters α_t is

$$\frac{\partial\varepsilon}{\partial\alpha_t} = \mathtt{c}_t'\sum_{l=1}^{\mathcal{K}}\mathtt{c}_l\left(\frac{\partial\mathtt{H}_{tl}}{\partial\alpha_t}-\varepsilon\frac{\partial\mathtt{S}_{tl}}{\alpha_t}\right) + \mathtt{c}_t\sum_{l=1}^{\mathcal{K}}\mathtt{c}_l'\left(\frac{\partial\mathtt{H}_{lt}}{\partial\alpha_t}-\varepsilon\frac{\partial\mathtt{S}_{lt}}{\alpha_t}\right) - \mathtt{c}_t\mathtt{c}_t'\left(\frac{\partial\mathtt{H}_{tt}}{\partial\alpha_t}-\varepsilon\frac{\partial\mathtt{S}_{tt}}{\alpha_t}\right) =$$

$$= 2\mathtt{c}_t'\sum_{l=1}^{\mathcal{K}}\mathtt{c}_l\left(\frac{\partial\mathtt{H}_{tl}}{\partial\alpha_t}-\varepsilon\frac{\partial\mathtt{S}_{tl}}{\partial\alpha_t}\right) - \mathtt{c}_t\mathtt{c}_t'\left(\frac{\partial\mathtt{H}_{tt}}{\partial\alpha_t}-\varepsilon\frac{\partial\mathtt{S}_{tt}}{\partial\alpha_t}\right). \tag{91}$$

Although calculating the derivatives with respect to each α_t is necessary for obtaining the complete energy gradient, in practice, one can evaluate all the derivatives of energy

with respect to the entire vech L_k vector in a single step. This is because computing the separate differentiations for individual parameters, such as $(L_k)_{11}, \quad (L_k)_{21}, \ldots, (L_k)_{nn}$ is not efficient, and all these separate operations are identical at the same time. In short, it becomes necessary to compute the following derivatives:

$$\frac{\partial \mathtt{H}_{kl}}{\partial(\text{vech}\, L_k)}, \quad \frac{\partial \mathtt{H}_{kl}}{\partial(\text{vech}\, L_l)}, \quad \frac{\partial \mathtt{S}_{kl}}{\partial(\text{vech}\, L_k)}, \quad \frac{\partial \mathtt{S}_{kl}}{\partial(\text{vech}\, L_l)}.$$

The examples of the implementation of energy gradient in the variational optimizations of the nonlinear parameters of the basis functions can be found in the works [67, 68]. Below, we will provide the necessary expressions for the aforementioned derivatives with basis functions in Eq. (33).

7.1 Overlap gradient

Before running into details, let us first give the gradient of matrix A_{kl}

$$\mathrm{d}A_k = (\mathrm{d}L_k)L_k' + L_k \mathrm{d}L_k', \quad \mathrm{d}A_l = (\mathrm{d}L_l)L_l' + L_l(\mathrm{d}L_l'), \tag{92}$$

$$\mathrm{d}A_{kl} = (\mathrm{d}L_k)L_k' + L_k \mathrm{d}L_k' + (\mathrm{d}L_l)L_l' + L_l(\mathrm{d}L_l'). \tag{93}$$

case $(x_{i_k} x_{j_k} | x_{i_l} x_{j_l})$

In this case the differential of the overlap integral is

$$\begin{aligned} \mathrm{d}\mathtt{S}_{kl} = & -\mathtt{S}_{kl}\Bigg[\frac{3}{2}\,\mathrm{tr}\left[A_{kl}^{-1}\mathrm{d}A_{kl}\right] + \frac{1}{\gamma}\Bigg(\gamma_2\,\mathrm{tr}\left[A_{kl}^{-1}v_l v_k' A_{kl}^{-1}\mathrm{d}A_{kl}\right] + \gamma_1\,\mathrm{tr}\left[A_{kl}^{-1}w_l w_k' A_{kl}^{-1}\mathrm{d}A_{kl}\right] \\ & + \gamma_4\,\mathrm{tr}\left[A_{kl}^{-1}w_k v_k' A_{kl}^{-1}\mathrm{d}A_{kl}\right] + \gamma_3\,\mathrm{tr}\left[A_{kl}^{-1}w_l v_l' A_{kl}^{-1}\mathrm{d}A_{kl}\right] + \gamma_6\,\mathrm{tr}\left[A_{kl}^{-1}w_l v_k' A_{kl}^{-1}\mathrm{d}A_{kl}\right] \\ & + \gamma_5\,\mathrm{tr}\left[A_{kl}^{-1}v_l w_k' A_{kl}^{-1}\mathrm{d}A_{kl}\right]\Bigg)\Bigg]. \end{aligned} \tag{94}$$

To write the above expression in a compact form, we can introduce the following matrices

$$\begin{aligned} & K_{kl}^{(1)} = A_{kl}^{-1}w_l w_k' A_{kl}^{-1}, \quad K_{kl}^{(2)} = A_{kl}^{-1}v_l v_k' A_{kl}^{-1}, \quad K_{kl}^{(3)} = A_{kl}^{-1}w_l v_l' A_{kl}^{-1}, \\ & K_{kl}^{(4)} = A_{kl}^{-1}w_k v_k' A_{kl}^{-1}, \quad K_{kl}^{(5)} = A_{kl}^{-1}v_l w_k' A_{kl}^{-1}, \quad K_{kl}^{(6)} = A_{kl}^{-1}w_l v_k' A_{kl}^{-1}, \\ & K_{kl} = \left(\gamma_1 K_{kl}^{(1)} + \gamma_2 K_{kl}^{(2)} + \gamma_3 K_{kl}^{(3)} + \gamma_4 K_{kl}^{(4)} + \gamma_5 K_{kl}^{(5)} + \gamma_6 K_{kl}^{(6)}\right), \\ & F_{kl} = \frac{3}{2}A_{kl}^{-1} + \frac{K_{kl}}{\gamma}. \end{aligned} \tag{95}$$

Then, with the use of these matrices the differential of the overlap integral is

$$\mathrm{d}\mathtt{S}_{kl} = -\mathtt{S}_{kl}\,\mathrm{tr}\left[L_k'(F_{kl}+F_{kl}')\mathrm{d}L_k + L_l'(F_{kl}+F_{kl}')\mathrm{d}L_l\right]. \tag{96}$$

Now, for further analysis we need the properties of the vech operator that will be used frequently. Specifically, when X and Y represent arbitrary complex square matrices, and L denotes a lower triangular matrix, the subsequent relations are applicable:

$$\mathrm{tr}[X'Y] = (\mathrm{vec}\,X)'\,\mathrm{vec}\,Y, \quad (\mathrm{vec}\,X)'\,\mathrm{vec}\,L = (\mathrm{vech}\,X)'\,\mathrm{vech}\,L. \tag{97}$$

With these properties and some algebraic arrangements equation in (94) can be rewritten as

$$\mathrm{d}\mathtt{S}_{kl} = -\mathtt{S}_{kl}[\mathrm{vech}((F_{kl}+F_{kl}')L_k)'\mathrm{d}\,\mathrm{vech}\,L_k + \mathrm{vech}((F_{kl}+F_{kl}')L_l)'\mathrm{d}\,\mathrm{vech}\,L_l]. \tag{98}$$

From this expression, we can easily write the derivatives for the overlap integral:

$$\frac{\partial \mathtt{S}_{kl}}{\partial(\mathrm{vech}\,L_k)} = -\mathtt{S}_{kl}\,\mathrm{vech}((F_{kl}+F_{kl}')L_k), \tag{99}$$

$$\frac{\partial \mathtt{S}_{kl}}{\partial(\mathrm{vech}\,L_l)} = -\mathtt{S}_{kl}\,\mathrm{vech}((F_{kl}+F_{kl}')L_l). \tag{100}$$

case $(x_{i_k}y_{j_k}|y_{i_l}x_{j_l})$

As was the case in the derivation of the matrix elements for the Hamiltonian and overlap, the other two cases are very similar to the derivations in the previous subsection. Therefore, we only present the final results. Specifically, in the cases of $(x_{i_k}y_{j_k}|y_{i_l}x_{j_l})$ and $(x_{i_k}x_{j_k}|y_{i_l}y_{j_l})$, only the quantities γ and K_{kl} change, while the derivatives of $\mathtt{S}_{kl}$ remain the same.

$$\gamma = \gamma_1\gamma_2, \quad K_{kl} = \left(\gamma_1 K_{kl}^{(1)} + \gamma_2 K_{kl}^{(2)}\right), \tag{101}$$

case $(x_{i_k}x_{j_k}|y_{i_l}y_{j_l})$

$$\gamma = \gamma_3\gamma_4, \quad K_{kl} = \left(\gamma_3 K_{kl}^{(3)} + \gamma_4 K_{kl}^{(4)}\right). \tag{102}$$

7.2 Kinetic energy gradient

case $(x_{i_k}x_{j_k}|x_{i_l}x_{j_l})$

We begin the derivation of the matrix elements for the kinetic energy gradient by writing the differential of the kinetic energy (64):

$$\mathrm{d}\mathtt{T}_{kl} = \frac{\mathtt{T}_{kl}}{\mathtt{S}_{kl}}\mathrm{d}\mathtt{S}_{kl} + \mathtt{S}_{kl}\left(6\mathrm{d}\tau + \frac{4}{\gamma}\mathrm{d}\zeta - \frac{4\zeta}{\gamma^2}\mathrm{d}\gamma\right). \tag{103}$$

To explicitly write this expression, we need to find the differentials for γ, τ, and ζ. Note that for ζ, we need the differentials for γ's and η's (65):

$$\begin{aligned}
\mathrm{d}\gamma_1 &= -\operatorname{tr}\left[K^{(2)}_{kl}\mathrm{d}A_{kl}\right], \quad \mathrm{d}\gamma_2 = -\operatorname{tr}\left[K^{(1)}_{kl}\mathrm{d}A_{kl}\right], \quad \mathrm{d}\gamma_3 = -\operatorname{tr}\left[K^{(4)}_{kl}\mathrm{d}A_{kl}\right], \\
\mathrm{d}\gamma_4 &= -\operatorname{tr}\left[K^{(3)}_{kl}\mathrm{d}A_{kl}\right], \quad \mathrm{d}\gamma_5 = -\operatorname{tr}\left[K^{(6)}_{kl}\mathrm{d}A_{kl}\right], \quad \mathrm{d}\gamma_6 = -\operatorname{tr}\left[K^{(5)}_{kl}\mathrm{d}A_{kl}\right],
\end{aligned} \tag{104}$$

$$\begin{aligned}
\mathrm{d}\tau &= \operatorname{tr}\left[A^{-1}_{kl}A_l M A'_l A^{-1}_{kl}\mathrm{d}A'_k + A^{-1}_{kl}A_k M A'_k A^{-1}_{kl}\mathrm{d}A_l\right], \\
\mathrm{d}\eta_1 &= \operatorname{tr}\big[(K^{(1)}_{kl}A'_l M A_l A^{-1}_{kl} - A^{-1}_{kl}A'_l M A_k K^{(1)}_{kl})\mathrm{d}A'_k \\
&\quad +(A^{-1}_{kl}A'_k M A_k K^{(1)}_{kl} - K^{(1)}_{kl}A'_l M A_k A^{-1}_{kl})\mathrm{d}A_l\big], \\
\mathrm{d}\eta_2 &= \operatorname{tr}\big[(K^{(2)}_{kl}A'_l M A_l A^{-1}_{kl} - A^{-1}_{kl}A'_l M A_k K^{(2)}_{kl})\mathrm{d}A'_k \\
&\quad +(A^{-1}_{kl}A'_k M A_k K^{(2)}_{kl} - K^{(2)}_{kl}A'_l M A_k A^{-1}_{kl})\mathrm{d}A_l\big], \\
\mathrm{d}\eta_3 &= \operatorname{tr}\big[(A^{-1}_{kl}A'_l M A_k K^{(3)}_{kl} + K^{(3)}_{kl}A'_k M A_l A^{-1}_{kl})\mathrm{d}A'_k \\
&\quad -(A^{-1}_{kl}A'_k M A_k K^{(3)}_{kl} + K^{(3)}_{kl}A'_k M A_k A^{-1}_{kl})\mathrm{d}A'_l\big], \\
\mathrm{d}\eta_4 &= \operatorname{tr}\big[(A^{-1}_{kl}A'_k M A_l K^{(4)}_{kl} + K^{(4)}_{kl}A'_l M A_k A^{-1}_{kl})\mathrm{d}A_l \\
&\quad -(A^{-1}_{kl}A'_l M A_l K^{(4)}_{kl} + K^{(4)}_{kl}A'_l M A_l A^{-1}_{kl})\mathrm{d}A'_k\big], \\
\mathrm{d}\eta_5 &= \operatorname{tr}\big[(K^{(5)}_{kl}A'_l M A_l A^{-1}_{kl} - A^{-1}_{kl}A'_l M A_k K^{(5)}_{kl})\mathrm{d}A'_k \\
&\quad +(A^{-1}_{kl}A'_k M A_k K^{(5)}_{kl} - K^{(5)}_{kl}A'_l M A_k A^{-1}_{kl})\mathrm{d}A_l\big], \\
\mathrm{d}\eta_6 &= \operatorname{tr}\big[(K^{(6)}_{kl}A'_l M A_l A^{-1}_{kl} - A^{-1}_{kl}A'_l M A_k K^{(6)}_{kl})\mathrm{d}A'_k \\
&\quad +(A^{-1}_{kl}A'_k M A_k K^{(6)}_{kl} - K^{(6)}_{kl}A'_l M A_k A^{-1}_{kl})\mathrm{d}A_l\big].
\end{aligned} \tag{105}$$

To write the expressions compactly, we still need to define two more matrices,

$$U_{kl} = 6A^{-1}_{kl}A_l M A'_l A^{-1}_{kl} + \frac{4}{\gamma}X_{kl} + 4\frac{\zeta}{\gamma^2}K_{kl}, \tag{106}$$

$$W_{kl} = 6A_{kl}^{-1}A_k M A_k' A_{kl}^{-1} + \frac{4}{\gamma}Y_{kl} + 4\frac{\zeta}{\gamma^2}K_{kl}. \tag{107}$$

In these expressions, we had to define another matrices:

$$\begin{aligned} X_{kl} &= \sum_{\substack{i=1 \\ i\neq 3,4}}^{6} \gamma_i (K_{kl}^{(i)} A_l' M A_l A_{kl}^{-1} - A_{kl}^{-1} A_l' M A_k K_{kl}^{(i)}) + G_{kl} + \gamma_4 (A_{kl}^{-1} A_l' M A_l K_{kl}^{(4)} \\ &\quad + K_{kl}^{(4)} A_l' M A_l A_{kl}^{-1}) - \gamma_3 (A_{kl}^{-1} A_l' M A_k K_{kl}^{(3)} + K_{kl}^{(3)} A_k' M A_l A_{kl}^{-1}), \end{aligned} \tag{108}$$

$$\begin{aligned} Y_{kl} &= \sum_{\substack{i=1 \\ i\neq 3,4}}^{6} \gamma_i (A_{kl}^{-1} A_k' M A_k K_{kl}^{(i)} - K_{kl}^{(i)} A_l' M A_k A_{kl}^{-1}) + G_{kl} + \gamma_3 (A_{kl}^{-1} A_k' M A_k K_{kl}^{(3)} \\ &\quad + K_{kl}^{(3)} A_k' M A_k A_{kl}^{-1}) - \gamma_4 (A_{kl}^{-1} A_k' M A_l K_{kl}^{(4)} + K_{kl}^{(4)} A_l' M A_k A_{kl}^{-1}), \end{aligned} \tag{109}$$

and

$$G_{kl} = (\eta_3 K_{kl}^{(4)} + \eta_4 K_{kl}^{(3)} - \eta_1 K_{kl}^{(2)} - \eta_2 K_{kl}^{(1)} - \eta_5 K_{kl}^{(6)} - \eta_6 K_{kl}^{(5)}). \tag{110}$$

Finally, employing these notations for matrices and differentials, we can rewrite the expression in (103) as:

$$\begin{aligned} \mathrm{d}\mathtt{T}_{kl} &= \frac{\mathtt{T}_{kl}}{\mathtt{S}_{kl}} \mathrm{d}\mathtt{S}_{kl} + \mathtt{S}_{kl} \operatorname{tr}\big[\operatorname{vech}((U_{kl} + U_{kl}')L_k)' \mathrm{d} \operatorname{vech} L_k \\ &\quad + \operatorname{vech}((W_{kl} + W_{kl}')L_l)' \mathrm{d} \operatorname{vech} L_l \big]. \end{aligned} \tag{111}$$

Now, similar to the overlap gradient case, we can easily express the matrix elements of the kinetic energy gradient as follows:

$$\frac{\partial \mathtt{T}_{kl}}{\partial(\operatorname{vech} L_k)} = \frac{\mathtt{T}_{kl}}{\mathtt{S}_{kl}} \frac{\partial \mathtt{S}_{kl}}{\partial(\operatorname{vech} L_k)} + \mathtt{S}_{kl} \operatorname{vech}((U_{kl} + U_{kl}')L_k), \tag{112}$$

$$\frac{\partial \mathtt{T}_{kl}}{\partial(\operatorname{vech} L_l)} = \frac{\mathtt{T}_{kl}}{\mathtt{S}_{kl}} \frac{\partial \mathtt{S}_{kl}}{\partial(\operatorname{vech} L_l)} + \mathtt{S}_{kl} \operatorname{vech}((W_{kl} + W_{kl}')L_l). \tag{113}$$

case $(x_{i_k} y_{j_k} | y_{i_l} x_{j_l})$

In this case matrices X_{kl}, Y_{kl}, and G_{kl} change to

$$X_{kl} = G_{kl} + \sum_{i=1}^{2} \gamma_i (K_{kl}^{(i)} A_l' M A_l A_{kl}^{-1} - A_{kl}^{-1} A_l' M A_k K_{kl}^{(i)}), \tag{114}$$

$$Y_{kl} = G_{kl} + \sum_{i=1}^{2} \gamma_i (A_{kl}^{-1} A_k' M A_k K_{kl}^{(i)} - K_{kl}^{(i)} A_l' M A_k A_{kl}^{-1}), \tag{115}$$

$$G_{kl} = -\eta_1 K_{kl}^{(2)} - \eta_2 K_{kl}^{(1)}, \quad \zeta = (\gamma_1 \eta_1 + \gamma_2 \eta_2)\,. \tag{116}$$

case $(x_{i_k} x_{j_k} | y_{i_l} y_{j_l})$

In this case matrices X_{kl}, Y_{kl}, and G_{kl} change to

$$\begin{aligned} X_{kl} &= G_{kl} + \gamma_4 (A_{kl}^{-1} A_l' M A_l K_{kl}^{(4)} + K_{kl}^{(4)} A_l' M A_l A_{kl}^{-1}) \\ &\quad -\gamma_3 (A_{kl}^{-1} A_l' M A_k K_{kl}^{(3)} + K_{kl}^{(3)} A_k' M A_l A_{kl}^{-1}), \end{aligned} \tag{117}$$

$$\begin{aligned} Y_{kl} &= G_{kl} + \gamma_3 (A_{kl}^{-1} A_k' M A_k K_{kl}^{(3)} + K_{kl}^{(3)} A_k' M A_k A_{kl}^{-1}) \\ &\quad -\gamma_4 (A_{kl}^{-1} A_k' M A_l K_{kl}^{(4)} + K_{kl}^{(4)} A_l M A_k' A_{kl}^{-1}), \end{aligned} \tag{118}$$

$$G_{kl} = \eta_3 K_{kl}^{(4)} + \eta_4 K_{kl}^{(3)}, \quad \zeta = (-\gamma_3 \eta_3 - \gamma_4 \eta_4)\,. \tag{119}$$

Note the sign differences here compared to the case $(x_{i_k} y_{j_k} | y_{i_l} x_{j_l})$. Despite the expressions being identical except for the indices 3 and 4, the orders of the matrices are changed, and opposite signs appear.

7.3 Potential energy gradient

case $(x_{i_k} x_{j_k} | x_{i_l} x_{j_l})$

To derive the gradient matrix elements of the potential energy (74), we first express the differential of (72):

$$\mathrm{d}\mathtt{R}_{kl}^{ij} = \frac{\mathtt{R}_{kl}^{ij}}{\mathtt{S}_{kl}} \mathrm{d}\mathtt{S}_{kl} + \frac{2}{\sqrt{\pi}} \frac{\mathtt{S}_{kl}}{\omega^{3/2}} \Big(\frac{1}{2} \Big[\frac{\kappa}{\omega\gamma} - \frac{\rho}{\omega^2 \gamma} - 1 \Big] \mathrm{d}\omega + \Big[\frac{\kappa}{3\gamma^2} - \frac{\rho}{5\omega\gamma^2} \Big] \mathrm{d}\gamma - \frac{\mathrm{d}\kappa}{3\gamma} + \frac{\mathrm{d}\rho}{5\omega\gamma} \Big). \tag{120}$$

In this expression, it is evident that the following differentials need to be substituted

$$\mathrm{d}\rho_q = -\operatorname{tr}\left[(A_{kl}^{-1} J_{ij} K_{kl}^{(q)} + K_{kl}^{(q)} J_{ij} A_{kl}^{-1})(\mathrm{d}A_k' + \mathrm{d}A_l) \right], \quad q = 1, \ldots, 6. \tag{121}$$

$$\mathrm{d}\omega = -\operatorname{tr}\left[A_{kl}^{-1} J_{ij} A_{kl}^{-1} \mathrm{d}A_{kl} \right], \tag{122}$$

$$
\begin{aligned}
\mathrm{d}\rho &= -\Big(\rho_1 \operatorname{tr}\left[(A_{kl}^{-1}J_{ij}K_{kl}^{(2)} + K_{kl}^{(2)}J_{ij}A_{kl}^{-1})\mathrm{d}A_{kl}\right] \\
&\quad +\rho_2 \operatorname{tr}\left[(A_{kl}^{-1}J_{ij}K_{kl}^{(1)} + K_{kl}^{(1)}J_{ij}A_{kl}^{-1})\mathrm{d}A_{kl}\right] \\
&\quad +\rho_3 \operatorname{tr}\left[(A_{kl}^{-1}J_{ij}K_{kl}^{(4)} + K_{kl}^{(4)}J_{ij}A_{kl}^{-1})\mathrm{d}A_{kl}\right] \\
&\quad +\rho_4 \operatorname{tr}\left[(A_{kl}^{-1}J_{ij}K_{kl}^{(3)} + K_{kl}^{(3)}J_{ij}A_{kl}^{-1})\mathrm{d}A_{kl}\right] \\
&\quad +\rho_5 \operatorname{tr}\left[(A_{kl}^{-1}J_{ij}K_{kl}^{(6)} + K_{kl}^{(6)}J_{ij}A_{kl}^{-1})\mathrm{d}A_{kl}\right] \\
&\quad +\rho_6 \operatorname{tr}\left[(A_{kl}^{-1}J_{ij}K_{kl}^{(5)} + K_{kl}^{(5)}J_{ij}A_{kl}^{-1})\mathrm{d}A_{kl}\right]\Big),
\end{aligned} \tag{123}
$$

$$
\begin{aligned}
\mathrm{d}\kappa &= -\Big(\rho_1 \operatorname{tr}\left[K_{kl}^{(2)}\mathrm{d}A_{kl}\right] + \rho_2 \operatorname{tr}\left[K_{kl}^{(1)}\mathrm{d}A_{kl}\right] + \rho_3 \operatorname{tr}\left[K_{kl}^{(4)}\mathrm{d}A_{kl}\right] + \rho_4 \operatorname{tr}\left[K_{kl}^{(3)}\mathrm{d}A_{kl}\right] \\
&\quad +\rho_5 \operatorname{tr}\left[K_{kl}^{(6)}\mathrm{d}A_{kl}\right] + \rho_6 \operatorname{tr}\left[K_{kl}^{(5)}\mathrm{d}A_{kl}\right] \\
&\quad +\sum_{q=1}^{6}\gamma_q \operatorname{tr}\left[(A_{kl}^{-1}J_{ij}K_{kl}^{(q)} + K_{kl}^{(q)}J_{ij}A_{kl}^{-1})\mathrm{d}A_{kl}\right]\Big).
\end{aligned} \tag{124}
$$

Now, by following the steps for kinetic energy and overlap gradient, we can easily derive the necessary derivatives for the potential energy

$$
\mathrm{d}\mathtt{R}_{kl}^{ij} = \frac{\mathtt{R}_{kl}^{ij}}{\mathtt{S}_{kl}}\mathrm{d}\mathtt{S}_{kl} + \mathtt{S}_{kl}\operatorname{tr}\left[Q_{kl}(\mathrm{d}A_k' + \mathrm{d}A_l)\right], \tag{125}
$$

$$
\frac{\partial \mathtt{R}_{kl}^{ij}}{\partial(\operatorname{vech} L_k)} = \frac{\mathtt{R}_{kl}^{ij}}{\mathtt{S}_{kl}}\frac{\partial \mathtt{S}_{kl}}{\partial(\operatorname{vech} L_k)} + \mathtt{S}_{kl}\operatorname{vech}((Q_{kl} + Q_{kl}')L_k), \tag{126}
$$

$$
\frac{\partial \mathtt{R}_{kl}^{ij}}{\partial(\operatorname{vech} L_l)} = \frac{\mathtt{R}_{kl}^{ij}}{\mathtt{S}_{kl}}\frac{\partial \mathtt{S}_{kl}}{\partial(\operatorname{vech} L_l)} + \mathtt{S}_{kl}\operatorname{vech}((Q_{kl} + Q_{kl}')L_l), \tag{127}
$$

where

$$
\begin{aligned}
Q_{kl} &= \frac{2}{\sqrt{\pi}\omega^{3/2}}\Bigg(\frac{1}{2}\left[1 + \frac{\rho}{\omega^2\gamma} - \frac{\kappa}{\omega\gamma}\right]A_{kl}^{-1}J_{ij}A_{kl}^{-1} + \left[\frac{\rho}{5\omega\gamma^2} - \frac{\kappa}{3\gamma^2}\right]K_{kl} \\
&\quad +\frac{1}{3\gamma}\Bigg[\rho_1 K_{kl}^{(2)} + \rho_2 K_{kl}^{(1)} + \rho_3 K_{kl}^{(4)} + \rho_4 K_{kl}^{(3)} + \rho_5 K_{kl}^{(6)} \\
&\quad +\rho_6 K_{kl}^{(5)} + \sum_{q=1}^{6}\gamma_q(A_{kl}^{-1}J_{ij}K_{kl}^{(q)} + K_{kl}^{(q)}J_{ij}A_{kl}^{-1})\Bigg] - \frac{1}{5\omega\gamma} \\
&\quad \times\Bigg[\rho_1(A_{kl}^{-1}J_{ij}K_{kl}^{(2)} + K_{kl}^{(2)}J_{ij}A_{kl}^{-1}) + \rho_2(A_{kl}^{-1}J_{ij}K_{kl}^{(1)} + K_{kl}^{(1)}J_{ij}A_{kl}^{-1}) \\
&\quad +\rho_3(A_{kl}^{-1}J_{ij}K_{kl}^{(4)} + K_{kl}^{(4)}J_{ij}A_{kl}^{-1}) + \rho_4(A_{kl}^{-1}J_{ij}K_{kl}^{(3)} + K_{kl}^{(3)}J_{ij}A_{kl}^{-1}) \\
&\quad +\rho_5(A_{kl}^{-1}J_{ij}K_{kl}^{(6)} + K_{kl}^{(6)}J_{ij}A_{kl}^{-1}) + \rho_6(A_{kl}^{-1}J_{ij}K_{kl}^{(6)} + K_{kl}^{(6)}J_{ij}A_{kl}^{-1})\Bigg]\Bigg).
\end{aligned} \tag{128}
$$

case $(x_{i_k}y_{j_k}|y_{i_l}x_{j_l})$

All of the final formulas for derivatives of the potential energy matrix elements remain the same. However, matrices K_{kl} and Q_{kl} as well as quantities κ and γ acquire a different form:

$$\begin{aligned}
&\kappa = \gamma_1\rho_1 + \gamma_2\rho_2, \quad \rho = \rho_1\rho_2, \\
&\gamma = \gamma_1\gamma_2, \quad K_{kl} = \left(\gamma_1 K_{kl}^{(1)} + \gamma_2 K_{kl}^{(2)}\right),
\end{aligned} \tag{129}$$

$$\begin{aligned}
Q_{kl} &= \frac{2}{\sqrt{\pi}\omega^{3/2}}\left(\frac{1}{2}\left[1 + \frac{\rho}{\omega^2\gamma} - \frac{\kappa}{\omega\gamma}\right] A_{kl}^{-1} J_{ij} A_{kl}^{-1} + \left[\frac{\rho}{5\omega\gamma^2} - \frac{\kappa}{3\gamma^2}\right] K_{kl} + \frac{1}{3\gamma}\left[\rho_1 K_{kl}^{(2)}\right.\right. \\
&\left. + \rho_2 K_{kl}^{(1)} + \sum_{q=1}^{2} \gamma_q (A_{kl}^{-1} J_{ij} K_{kl}^{(q)} + K_{kl}^{(q)} J_{ij} A_{kl}^{-1})\right] - \frac{1}{5\omega\gamma} \\
&\left. \times \left[\rho_1 (A_{kl}^{-1} J_{ij} K_{kl}^{(2)} + K_{kl}^{(2)} J_{ij} A_{kl}^{-1}) + \rho_2 (A_{kl}^{-1} J_{ij} K_{kl}^{(1)} + K_{kl}^{(1)} J_{ij} A_{kl}^{-1})\right]\right).
\end{aligned} \tag{130}$$

case $(x_{i_k}x_{j_k}|y_{i_l}y_{j_l})$

In this case, we have:

$$\begin{aligned}
&\kappa = \gamma_3\rho_3 + \gamma_4\rho_4, \quad \rho = \rho_3\rho_4, \\
&\gamma = \gamma_3\gamma_4, \quad K_{kl} = \left(\gamma_3 K_{kl}^{(3)} + \gamma_4 K_{kl}^{(4)}\right),
\end{aligned} \tag{131}$$

$$\begin{aligned}
Q_{kl} &= \frac{2}{\sqrt{\pi}\omega^{3/2}}\left(\frac{1}{2}\left[1 + \frac{\rho}{\omega^2\gamma} - \frac{\kappa}{\omega\gamma}\right] A_{kl}^{-1} J_{ij} A_{kl}^{-1} + \left[\frac{\rho}{5\omega\gamma^2} - \frac{\kappa}{3\gamma^2}\right] K_{kl}\right. \\
&+ \frac{1}{3\gamma}\left[\rho_3 K_{kl}^{(4)} + \rho_4 K_{kl}^{(3)} + \sum_{q=3}^{4} \gamma_q (A_{kl}^{-1} J_{ij} K_{kl}^{(q)} + K_{kl}^{(q)} J_{ij} A_{kl}^{-1})\right] - \frac{1}{5\omega\gamma} \\
&\left. \times \left[\rho_3 (A_{kl}^{-1} J_{ij} K_{kl}^{(4)} + K_{kl}^{(4)} J_{ij} A_{kl}^{-1}) + \rho_4 (A_{kl}^{-1} J_{ij} K_{kl}^{(3)} + K_{kl}^{(3)} J_{ij} A_{kl}^{-1})\right]\right).
\end{aligned} \tag{132}$$

8 Relativistic corrections

The nonrelativistic energy, even when computed using a thoroughly optimized and large basis set, lacks the precision necessary for accurately determining the total and transition energies of atomic ground and excited states compared to experimental results. To achieve a high level of agreement, calculations must include relativistic and quantum electrodynamics (QED) effects. For instance, in the work of Morton et al. [86], which presents theoretical and experimental findings on the bound stationary states of helium, the notable level of agreement between theory and experiment in the calculations becomes apparent when relativistic and quantum electrodynamics (QED) effects are included. Another example involves the case of a molecule, specifically calculations on the H_2 molecule [1, 87–89]. These calculations revealed the necessity of including dominant α^2-dependent terms, relativistic corrections, and higher-order corrections for electronic and vibrational transition energies.

Quantum Electrodynamics (QED) is a theoretical framework that examines the interactions of quantum particles within an electromagnetic field. It provides a thorough basis for studying the effects of relativity and QED in the bound states of atoms and molecules. Nevertheless, achieving accurate calculations for even small atomic and molecular systems with a few electrons proves challenging and computationally expensive on present day computers. Additionally, the QED Dirac-Coulomb equation is correct only for a single electron in a Coulombic field, leading to approximations when dealing with systems containing more than one electron. An additional challenge arises due to the absence of a lower bound for the negative energy spectrum in the Dirac-Coulomb equation [86].

Confronted with these challenges, efforts have been directed towards developing an effective approach to including relativistic effects in light atomic and molecular systems within the perturbation theory framework. The nonrelativistic Schrodinger equation serves as the zero-order level in this approach. The perturbation Hamiltonian, representing relativistic effects, is derived based on the nonrelativistic QED theory [90, 91]. It is worth noting that a perturbation approach for accounting for relativistic corrections can also be constructed independently of nonrelativistic quantum electrodynamics, as demon-

strated by Bethe and Salpeter [92]. Nowadays, it is possible to find quantum chemistry packages routinely computing these relativistic corrections.

Relativistic corrections, proportional to powers of the fine structure constant α, are systematically included in calculations using nonrelativistic quantum electrodynamics:

$$E(\alpha) = E_{\mathrm{NR}} + \alpha^2 E_{\mathrm{REL}} + \alpha^3 E_{\mathrm{QED}} + \alpha^4 E_{\mathrm{HQED}} + \ldots \tag{133}$$

The leading terms include nonrelativistic energy E_{NR}, relativistic correction $\alpha^2 E_{\mathrm{REL}}$, and the highest-order radiative correction $\alpha^3 E_{\mathrm{REL}}$. Particularly, $\alpha^3 E_{\mathrm{REL}}$ represents the leading QED corrections and the fourth term, $\alpha^4 E_{\mathrm{HQED}}$, represent the higher-order QED corrections. Nonrelativistic QED along with corrections for nuclear structure and polarizability, stands as the most precise theoretical formalism for computing bound state energies of small atoms and molecules. In these calculations, relativistic corrections are determined through expectation values of nonrelativistic QED operators with the nonrelativistic wave function.

It should be noted that when using the infinite-nuclear-mass wave function (Born-Oppenheimer approximation), it is also important to include the recoil effects resulting from finite-nuclear-mass corrections to relativistic energy (E_{REL}). However, alternative approaches, such as those used by Stanke et al [19, 30, 32, 93–95], transform relativistic operators to an internal coordinate system, enabling automatic inclusion of recoil corrections in the relativistic energy. This approach facilitates direct calculation of how isotopic substitutions affect the relativistic energy (E_{REL}), considering contributions from both nuclear and electronic motions.

As mentioned before, the relativistic and QED corrections are computed as the expectation value of an effective operators that represent the computed term. For instance, E_{REL} is computed as the expectation value of the Dirac–Breit Hamiltonian ($\mathcal{H}_{\mathrm{REL}}$) in the Pauli approximation [92, 96]. The Dirac–Breit Hamiltonian, in turn, contains operators that are commonly interpreted as the mass–velocity, Darwin, orbit–orbit, spin-orbit, and spin–spin Hamiltonians [23]. Now, let us list the operators that are included in the relativistic and QED corrections:

$$\mathcal{H}_{\mathrm{SS}} = -\frac{8\pi}{3}\left[\sum_{i=1}^{n} \frac{q_0 q_i}{m_0 m_i}\left(\boldsymbol{s}_0'\boldsymbol{s}_i\right)\delta\left(\boldsymbol{r}_i\right) + \sum_{\substack{i,j=1\\ j>i}}^{n} \frac{q_i q_j}{m_i m_j}\left(\boldsymbol{s}_i'\boldsymbol{s}_j\right)\delta\left(\boldsymbol{r}_{ij}\right)\right] \tag{134}$$

$$\mathcal{H}_{\mathrm{D}} = -\frac{\pi}{2}\left[\sum_{i=1}^{n}\left(\frac{1}{m_0^2}+\frac{1}{m_i^2}\right)q_0 q_i \delta^3\left(\boldsymbol{r}_i\right) + \sum_{\substack{i,j=1\\ j\neq i}}^{n}\frac{1}{m_i^2}q_i q_j \delta^3\left(\boldsymbol{r}_{ij}\right)\right] \tag{135}$$

$$\begin{aligned}\mathcal{H}_{\mathrm{QED}} \;=\; & \sum_{\substack{i,j=1\\ j>i}}^{3}\left[\left(\frac{164}{15}+\frac{14}{3}\ln\alpha\right)\delta\left(\boldsymbol{r}_{ij}\right) - \frac{7}{6\pi}\mathcal{P}\left(\frac{1}{r_{ij}^3}\right)\right] \\ & + \sum_{i=1}^{3}\left(\frac{19}{30} - 2\ln\alpha - \ln k_0\right)\frac{4q_0}{3}\delta\left(\boldsymbol{r}_i\right), \end{aligned} \tag{136}$$

$$\mathcal{H}_{\mathrm{HQED}} = \pi q_0^2\left(\frac{427}{96} - 2\ln 2\right)\sum_{i=1}^{3}\delta\left(\boldsymbol{r}_i\right). \tag{137}$$

As mentioned earlier, the term H_{QED} represents the leading QED correction, encompassing effects such as two-photon exchange, vacuum polarization, and electron self-energy. The first term in the sum is the Araki-Sucher term [97–101]. Subsequently, in the same sum, we encounter the principal value $\mathcal{P}\left(\frac{1}{r_{ij}^3}\right)$, expressed as follows:

$$\left\langle \mathcal{P}\left(\frac{1}{r_{ij}^3}\right)\right\rangle = \lim_{a\to 0}\left\langle \frac{1}{r_{ij}^3}\Theta\left(r_{ij}-a\right) + 4\pi\left(\gamma+\ln a\right)\delta\left(\boldsymbol{r}_{ij}\right)\right\rangle, \tag{138}$$

where

- $\Theta(\ldots)$ is the Heaviside step function,
- $\gamma = 0.577215\ldots$ is the Euler–Mascheroni constant.

In the third sum, $\ln k_0$ represents the Bethe logarithm, which is the dominant component of the electron self-energy effect. Although accurately computing the Bethe logarithm for atomic systems is highly challenging, it is established that the primary contribution to this effect comes from inner shell electrons. Regarding the H_{HQED} operator in (137), it is an approximate operator derived by Packucki and Komasa [102, 103], including only the dominant electron-nucleus one-loop radiative correction. Other terms that are excluded are two-loop radiative, electron-electron radiative, and higher order relativistic corrections. Hence, to compute the higher order QED correction we can compute the expectation value of the approximate operator in (137).

As observed, we omit the Hamiltonians for mass-velocity and orbit-orbit corrections in the Dirac–Breit Hamiltonian ($\mathcal{H}_{\mathrm{REL}}$), as they do not involve the Dirac delta function.

Since the matrix elements of the Dirac delta function are already derived in Section (6.4), we will present the mathematical expressions for the mass-velocity and orbit-orbit Hamiltonians, along with their corresponding matrix elements using basis functions (33), in Sections 9 and 10, respectively.

A final remark regarding the relativistic operators that depend on the spin of particles, such as spin-orbit and spin-spin corrections, should be mentioned. Expectation values of these operators with the basis functions considered in this dissertation were recently accomplished with outstanding master student Pavel Rzhevskii at the Physics department, Nazarbayev University. Specific applications regarding the fine structure splittings with spin-dependent relativistic operators will be published in scientific journals once well-optimized basis functions are available.

9 Matrix elements of mass-velocity

9.1 Mass-velocity Hamiltonian

The mass-velocity Hamiltonian, as mentioned in the previous section, is part of the Dirac-Breit Hamiltonian ($\mathcal{H}_{\mathrm{REL}}$) in the Pauli approximation [92, 96], and is proportional to the sum of the fourth power of linear momenta. In the laboratory coordinate frame, the mass-velocity Hamiltonian is written as

$$\mathcal{H}_{\mathrm{MV}} = -\frac{1}{8}\sum_{i=1}^{n}\frac{\mathbf{p}_i^4}{\mathsf{m}_i^3}.$$

The linear transformation of this expression to the internal coordinate frame is straightforward and is expressed as follows:

$$\mathcal{H}_{\mathrm{MV}} = -\frac{1}{8}\left[\frac{1}{m_0^3}\left(\sum_{i=1}^{n}\boldsymbol{\nabla}_{\boldsymbol{r}_i}\right)^4 + \sum_{i=1}^{n}\frac{1}{m_i^3}\boldsymbol{\nabla}_{\boldsymbol{r}_i}^4\right]. \tag{139}$$

This transformation is not enough for computing its expectation values in the basis of ECG functions considered in this dissertation. For ease of derivation of the matrix elements for the expectation values of the mass-velocity Hamiltonian, we need to write the expression in a matrix format. This can be done by introducing new $3n \times 3n$ matrices $\boldsymbol{J} = J \otimes I_3$ and $\boldsymbol{J}_{ii} = J_{ii} \otimes I_3$. Here, J is an $n \times n$ matrix consisting entirely of elements equal to 1, whereas matrix J_{ii} is also an $n \times n$ matrix but has only a single nonzero element, which is assigned a value of 1. By employing these matrix notations, we can easily transform the expression in Eq. (139) into a matrix form:

$$\mathcal{H}_{\mathrm{MV}} = -(\boldsymbol{\nabla}_{\boldsymbol{r}}'\beta_0\boldsymbol{J}\boldsymbol{\nabla}_{\boldsymbol{r}})^2 - \sum_{i=1}^{n}(\boldsymbol{\nabla}_{\boldsymbol{r}}'\beta_i\boldsymbol{J}_{ii}\boldsymbol{\nabla}_{\boldsymbol{r}})^2. \tag{140}$$

In this expression, we define new quantities $\beta_0 = 1/\sqrt{8m_0^3}$ and $\beta_i = 1/\sqrt{8m_i^3}$.

9.2 Matrix elements

Before commencing the solution of the integral, for the sake of facilitating further analytical derivations, we first express the derivatives of the generating function φ_k:

$$\boldsymbol{\nabla}_{\boldsymbol{r}}\varphi_k = [-2\boldsymbol{A}_k\boldsymbol{r} + \alpha_k\boldsymbol{v}_k + \beta_k\boldsymbol{b}_k]\varphi_k, \quad \boldsymbol{\nabla}_{\boldsymbol{r}}'\varphi_k = [-2\boldsymbol{r}'\boldsymbol{A}_k + \alpha_k\boldsymbol{v}_k' + \beta_k\boldsymbol{b}_k']\varphi_k. \tag{141}$$

When employing the subsequent property of the nabla operator

$$\langle\varphi_k|(\boldsymbol{\nabla}'_{\boldsymbol{r}}\boldsymbol{X}\boldsymbol{\nabla}_{\boldsymbol{r}})(\boldsymbol{\nabla}'_{\boldsymbol{r}}\boldsymbol{Y}\boldsymbol{\nabla}_{\boldsymbol{r}})|\varphi_l\rangle = \langle\boldsymbol{\nabla}'_{\boldsymbol{r}}\boldsymbol{X}\boldsymbol{\nabla}_{\boldsymbol{r}}\varphi_k|\boldsymbol{\nabla}'_{\boldsymbol{r}}\boldsymbol{Y}\boldsymbol{\nabla}_{\boldsymbol{r}}\varphi_l\rangle, \tag{142}$$

it becomes evident that we also require the derivatives outlined below.

$$\boldsymbol{X}\boldsymbol{\nabla}_{\boldsymbol{r}}\varphi_k = [-2\boldsymbol{X}\boldsymbol{A}_k\boldsymbol{r} + \alpha_k\boldsymbol{X}\boldsymbol{v}_k + \beta_k\boldsymbol{X}\boldsymbol{b}_k]\varphi_k,$$

$$\begin{aligned}\boldsymbol{\nabla}'_{\boldsymbol{r}}\boldsymbol{X}\boldsymbol{\nabla}_{\boldsymbol{r}}\varphi_k &= [-2\mathrm{tr}[\boldsymbol{X}\boldsymbol{A}_k] + 4(\boldsymbol{r}'\boldsymbol{A}_k\boldsymbol{X}\boldsymbol{A}_k\boldsymbol{r}) - 4\alpha_k(\boldsymbol{v}'_k\boldsymbol{X}\boldsymbol{A}_k\boldsymbol{r}) - 4\beta_k(\boldsymbol{b}'_k\boldsymbol{X}\boldsymbol{A}_k\boldsymbol{r}) \\ &\quad +\alpha_k^2(\boldsymbol{v}'_k\boldsymbol{X}\boldsymbol{v}_k) + \beta_k^2(\boldsymbol{b}'_k\boldsymbol{X}\boldsymbol{b}_k) + 2\alpha_k\beta_k(\boldsymbol{v}'_k\boldsymbol{X}\boldsymbol{b}_k)]\varphi_k. \end{aligned}\tag{143}$$

Similarly

$$\begin{aligned}\boldsymbol{\nabla}'_{\boldsymbol{r}}\boldsymbol{Y}\boldsymbol{\nabla}_{\boldsymbol{r}}\varphi_l &= [-2\mathrm{tr}[\boldsymbol{A}_l\boldsymbol{Y}] + 4(\boldsymbol{r}'\boldsymbol{A}_l\boldsymbol{Y}\boldsymbol{A}_l\boldsymbol{r}) - 4\alpha_l(\boldsymbol{v}'_l\boldsymbol{Y}\boldsymbol{A}_l\boldsymbol{r}) - 4\beta_l(\boldsymbol{b}'_l\boldsymbol{Y}\boldsymbol{A}_l\boldsymbol{r}) \\ &\quad +\alpha_l^2(\boldsymbol{v}'_l\boldsymbol{Y}\boldsymbol{v}_l) + \beta_l^2(\boldsymbol{b}'_l\boldsymbol{Y}\boldsymbol{b}_l) + 2\alpha_l\beta_l(\boldsymbol{v}'_l\boldsymbol{Y}\boldsymbol{b}_l)]\varphi_l. \end{aligned}\tag{144}$$

Deriving the matrix elements for the expectation value of $\langle\boldsymbol{\nabla}'_{\boldsymbol{r}}\boldsymbol{X}\boldsymbol{\nabla}_{\boldsymbol{r}}\varphi_k|\boldsymbol{\nabla}'_{\boldsymbol{r}}\boldsymbol{Y}\boldsymbol{\nabla}_{\boldsymbol{r}}\varphi_l\rangle$ integral, require multiplying the equations (143) and (144) with each other one by one by neglecting the α^2 and β^2 terms. This is because theirs expectation values become zero when we take the limit with respect to α's and β's and set them equal to zero. When we multiply above two terms we will have 25 integrals with solutions written in the list for each case separately (the next page). The appeared integrals are

$$4\mathrm{tr}[\mathbf{X}\mathbf{A}_k]\mathrm{tr}[\mathbf{A}_l\mathbf{Y}] - 8\mathrm{tr}[\mathbf{X}\mathbf{A}_k](\mathbf{r}'\mathbf{A}_l\mathbf{Y}\mathbf{A}_l\mathbf{r}) + 8\alpha_l\mathrm{tr}[\mathbf{X}\mathbf{A}_k](\mathbf{v}'_l\mathbf{Y}\mathbf{A}_l\mathbf{r}) + 8\beta_l\mathrm{tr}[\mathbf{X}\mathbf{A}_k](\mathbf{w}'_l\mathbf{Y}\mathbf{A}_l\mathbf{r})$$

$$-4\alpha_l\beta_l\mathrm{tr}[\mathbf{X}\mathbf{A}_k](\mathbf{v}'_l\mathbf{Y}\mathbf{w}_l) - 8(\mathbf{r}'\mathbf{A}_k\mathbf{X}\mathbf{A}_k\mathbf{r})\mathrm{tr}[\mathbf{A}_l\mathbf{Y}] + 16(\mathbf{r}'\mathbf{A}_k\mathbf{X}\mathbf{A}_k\mathbf{r})(\mathbf{r}'\mathbf{A}_l\mathbf{Y}\mathbf{A}_l\mathbf{r})$$

$$-16\alpha_l(\mathbf{r}'\mathbf{A}_k\mathbf{X}\mathbf{A}_k\mathbf{r})(\mathbf{v}'_l\mathbf{Y}\mathbf{A}_l\mathbf{r}) - 16\beta_l(\mathbf{r}'\mathbf{A}_k\mathbf{X}\mathbf{A}_k\mathbf{r})(\mathbf{w}'_l\mathbf{Y}\mathbf{A}_l\mathbf{r}) + 8\alpha_l\beta_l(\mathbf{r}'\mathbf{A}_k\mathbf{X}\mathbf{A}_k\mathbf{r})(\mathbf{v}'_l\mathbf{Y}\mathbf{w}_l)$$

$$+8\alpha_k(\mathbf{v}'_k\mathbf{X}\mathbf{A}_k\mathbf{r})\mathrm{tr}[\mathbf{A}_l\mathbf{Y}] - 16\alpha_k(\mathbf{v}'_k\mathbf{X}\mathbf{A}_k\mathbf{r})(\mathbf{r}'\mathbf{A}_l\mathbf{Y}\mathbf{A}_l\mathbf{r}) + 16\alpha_k\alpha_l(\mathbf{v}'_k\mathbf{X}\mathbf{A}_k\mathbf{r})(\mathbf{v}'_l\mathbf{Y}\mathbf{A}_l\mathbf{r})$$

$$+16\alpha_k\beta_l(\mathbf{v}'_k\mathbf{X}\mathbf{A}_k\mathbf{r})(\mathbf{w}'_l\mathbf{Y}\mathbf{A}_l\mathbf{r}) - 8\alpha_k\alpha_l\beta_l(\mathbf{v}'_k\mathbf{X}\mathbf{A}_k\mathbf{r})(\mathbf{v}'_l\mathbf{Y}\mathbf{w}_l) + 8\beta_k(\mathbf{w}'_k\mathbf{X}\mathbf{A}_k\mathbf{r})\mathrm{tr}[\mathbf{A}_l\mathbf{Y}]$$

$$-16\beta_k(\mathbf{w}'_k\mathbf{X}\mathbf{A}_k\mathbf{r})(\mathbf{r}'\mathbf{A}_l\mathbf{Y}\mathbf{A}_l\mathbf{r}) + 16\beta_k\alpha_l(\mathbf{w}'_k\mathbf{X}\mathbf{A}_k\mathbf{r})(\mathbf{v}'_l\mathbf{Y}\mathbf{A}_l\mathbf{r}) + 16\beta_k\beta_l(\mathbf{w}'_k\mathbf{X}\mathbf{A}_k\mathbf{r})(\mathbf{w}'_l\mathbf{Y}\mathbf{A}_l\mathbf{r})$$

$$-8\beta_k\alpha_l\beta_l(\mathbf{w}'_k\mathbf{X}\mathbf{A}_k\mathbf{r})(\mathbf{v}'_l\mathbf{Y}\mathbf{w}_l) - 4\alpha_k\beta_k(\mathbf{v}'_k\mathbf{X}\mathbf{w}_k)\mathrm{tr}[\mathbf{A}_l\mathbf{Y}] + 8\alpha_k\beta_k(\mathbf{v}'_k\mathbf{X}\mathbf{w}_k)(\mathbf{r}'\mathbf{A}_l\mathbf{Y}\mathbf{A}_l\mathbf{r})$$

$$-8\alpha_k\beta_k\alpha_l(\mathbf{v}'_k\mathbf{X}\mathbf{w}_k)(\mathbf{v}'_l\mathbf{Y}\mathbf{A}_l\mathbf{r}) - 8\alpha_k\beta_k\beta_l(\mathbf{v}'_k\mathbf{X}\mathbf{w}_k)(\mathbf{w}'_l\mathbf{Y}\mathbf{A}_l\mathbf{r}) + 4\alpha_k\beta_k\alpha_l\beta_l(\mathbf{v}'_k\mathbf{X}\mathbf{w}_k)(\mathbf{v}'_l\mathbf{Y}\mathbf{w}_l)$$

In this lengthy equation and from below, it is assumed that the individual terms (integrals) formally need to include bra and ket basis functions, with one on the left and the other on the right. However, to minimize space, we will neglect this formal writing of integrals, and this should be clear from the context. Below, "a" in the list corresponds to the case $(x_{i_k}x_{j_k}|x_{i_l}x_{j_l})$, while "b" and "c" corresponds to the cases $(x_{i_k}y_{j_k}|y_{i_l}x_{j_l})$ and $(x_{i_k}x_{j_k}|y_{i_l}y_{j_l})$, respectively.

1. $4\text{tr}[\mathbf{X}\mathbf{A}_k]\text{tr}[\mathbf{A}_l\mathbf{Y}]$

   (a) $9\text{tr}[A_kX]\text{tr}[A_lY]\frac{\pi^{3n/2}}{|A_{kl}|^{3/2}}(\gamma_1\gamma_2+\gamma_3\gamma_4+\gamma_5\gamma_6) = 36\text{tr}[A_kX]\text{tr}[A_lY]\mathcal{S}_{kl}$

   (b) $9\text{tr}[A_kX]\text{tr}[A_lY]\frac{\pi^{3n/2}}{|A_{kl}|^{3/2}}\gamma_1\gamma_2 = 36\text{tr}[A_kX]\text{tr}[A_lY]\mathcal{S}_{kl}$

   (c) $9\text{tr}[A_kX]\text{tr}[A_lY]\frac{\pi^{3n/2}}{|A_{kl}|^{3/2}}\gamma_3\gamma_4 = 36\text{tr}[A_kX]\text{tr}[A_lY]\mathcal{S}_{kl}$

2. $-8\text{tr}[\mathbf{X}\mathbf{A}_k](\mathbf{r}'\mathbf{A}_l\mathbf{Y}\mathbf{A}_l\mathbf{r})$

   (a) $-24\text{tr}[A_kX]\left(\frac{3}{2}\,\text{tr}[Q]\mathcal{S}_{kl}+\frac{\pi^{3n/2}}{4|A_{kl}|^{3/2}}\left[o_1\gamma_1+o_2\gamma_2+o_3\gamma_3+o_4\gamma_4+o_5\gamma_5+o_6\gamma_6\right]\right)$

   (b) $-24\text{tr}[A_kX]\left(\frac{3}{2}\,\text{tr}[Q]\mathcal{S}_{kl}+\frac{\pi^{3n/2}}{4|A_{kl}|^{3/2}}\left[o_1\gamma_1+o_2\gamma_2\right]\right)$

   (c) $-24\text{tr}[A_kX]\left(\frac{3}{2}\,\text{tr}[Q]\mathcal{S}_{kl}+\frac{\pi^{3n/2}}{4|A_{kl}|^{3/2}}\left[o_3\gamma_3+o_4\gamma_4\right]\right)$

3. $+8\alpha_l\text{tr}[\mathbf{X}\mathbf{A}_k](\mathbf{v}_l'\mathbf{Y}\mathbf{A}_l\mathbf{r})$

   (a) $24\text{tr}[A_kX]\frac{\pi^{3n/2}}{4|A_{kl}|^{3/2}}\left(\gamma_2[v_k'A_{kl}^{-1}A_lYv_l]+\gamma_3[v_l'YA_lA_{kl}^{-1}b_l]+\gamma_5[b_k'A_{kl}^{-1}A_lYv_l]\right)$

   (b) $24\text{tr}[A_kX]\frac{\pi^{3n/2}}{4|A_{kl}|^{3/2}}\left(\gamma_2[v_k'A_{kl}^{-1}A_lYv_l]\right)$

   (c) $24\text{tr}[A_kX]\frac{\pi^{3n/2}}{4|A_{kl}|^{3/2}}\left(\gamma_3[v_l'YA_lA_{kl}^{-1}b_l]\right)$

4. $+8\beta_l\text{tr}[\mathbf{X}\mathbf{A}_k](\mathbf{w}_l'\mathbf{Y}\mathbf{A}_l\mathbf{r})$

   (a) $24\text{tr}[A_kX]\frac{\pi^{3n/2}}{4|A_{kl}|^{3/2}}\left(\gamma_1[b_k'A_{kl}^{-1}A_lYb_l]+\gamma_3[v_l'A_{kl}^{-1}A_lYb_l]+\gamma_6[v_k'A_{kl}^{-1}A_lYb_l]\right)$

   (b) $24\text{tr}[A_kX]\frac{\pi^{3n/2}}{4|A_{kl}|^{3/2}}\left(\gamma_1[b_k'A_{kl}^{-1}A_lYb_l]\right)$

   (c) $24\text{tr}[A_kX]\frac{\pi^{3n/2}}{4|A_{kl}|^{3/2}}\left(\gamma_3[v_l'A_{kl}^{-1}A_lYb_l]\right)$

5. $-4\alpha_l\beta_l\text{tr}[\mathbf{X}\mathbf{A}_k](\mathbf{v}_l'\mathbf{Y}\mathbf{w}_l)$

(a) $-12\text{tr}[A_kX](v_l'Yb_l)\frac{\pi^{3n/2}}{2|A_{kl}|^{3/2}}v_k'A_{kl}^{-1}b_k = -12\text{tr}[A_kX](v_l'Yb_l)\frac{\pi^{3n/2}}{2|A_{kl}|^{3/2}}\gamma_3$,

(b) 0

(c) $-12\text{tr}[A_kX](v_l'Yb_l)\frac{\pi^{3n/2}}{2|A_{kl}|^{3/2}}\gamma_3$,

6. $-8(\mathbf{r}'\mathbf{A}_k\mathbf{X}\mathbf{A}_k\mathbf{r})\text{tr}[\mathbf{A}_l\mathbf{Y}]$

(a) $-24\text{tr}[A_lY]\left(\frac{3}{2}\text{ tr}\left[A_{kl}^{-1}P\right]\mathcal{S}_{kl}+\frac{\pi^{3n/2}}{4|A_{kl}|^{3/2}}\left[\sigma_1\gamma_1+\sigma_2\gamma_2+\sigma_3\gamma_3+\sigma_4\gamma_4+\sigma_5\gamma_5+\sigma_6\gamma_6\right]\right)$

(b) $-24\text{tr}[A_lY]\left(\frac{3}{2}\text{ tr}\left[A_{kl}^{-1}P\right]\mathcal{S}_{kl}+\frac{\pi^{3n/2}}{4|A_{kl}|^{3/2}}\left[\sigma_1\gamma_1+\sigma_2\gamma_2\right]\right)$

(c) $-24\text{tr}[A_lY]\left(\frac{3}{2}\text{ tr}\left[A_{kl}^{-1}P\right]\mathcal{S}_{kl}+\frac{\pi^{3n/2}}{4|A_{kl}|^{3/2}}\left[\sigma_3\gamma_3+\sigma_4\gamma_4\right]\right)$

7. $16\langle\phi_k|(\boldsymbol{r}'\boldsymbol{A}_k\boldsymbol{X}\boldsymbol{A}_k\boldsymbol{r})(\boldsymbol{r}'\boldsymbol{A}_l\boldsymbol{Y}\boldsymbol{A}_l\boldsymbol{r})|\phi_l\rangle$. The result of this integral will be provided separately as its lengthy.

8. $-16\alpha_l(\mathbf{r}'\mathbf{A}_k\mathbf{X}\mathbf{A}_k\mathbf{r})(\mathbf{v}_l'\mathbf{Y}\mathbf{A}_l\mathbf{r})$

(a) $-16\frac{3}{2}\text{ tr}\left[A_{kl}^{-1}P\right]\frac{\pi^{3n/2}}{4|A_{kl}|^{3/2}}\left(\gamma_2[v_k'A_{kl}^{-1}A_lYv_l]+\gamma_3[v_l'YA_lA_{kl}^{-1}b_l]+\gamma_5[b_k'A_{kl}^{-1}A_lYv_l]\right)$

$-16\frac{\pi^{3n/2}}{4|A_{kl}|^{3/2}}\left(\gamma_2[v_kA_{kl}^{-1}PA_{kl}^{-1}A_lYv_l]+\sigma_1[v_k'A_{kl}^{-1}A_lYv_l]+\sigma_4[v_l'YA_lA_{kl}^{-1}b_l]\right.$

$\left.+\gamma_3[v_l'YA_lA_{kl}^{-1}PA_{kl}^{-1}b_l]+\sigma_6[b_k'A_{kl}^{-1}A_lYv_l]+\gamma_5[b_k'A_{kl}^{-1}PA_{kl}^{-1}A_lYv_l]\right)$

(b) $-16\frac{3}{2}\text{ tr}\left[A_{kl}^{-1}P\right]\frac{\pi^{3n/2}}{4|A_{kl}|^{3/2}}\left(\gamma_2[v_k'A_{kl}^{-1}A_lYv_l]\right)-16\frac{\pi^{3n/2}}{4|A_{kl}|^{3/2}}\left(\gamma_2[v_kA_{kl}^{-1}PA_{kl}^{-1}A_lYv_l]+\right.$
$\left.\sigma_1[v_k'A_{kl}^{-1}A_lYv_l]\right)$

(c) $-16\frac{3}{2}\text{ tr}\left[A_{kl}^{-1}P\right]\frac{\pi^{3n/2}}{4|A_{kl}|^{3/2}}\left(\gamma_3[v_l'YA_lA_{kl}^{-1}b_l]\right) - 16\frac{\pi^{3n/2}}{4|A_{kl}|^{3/2}}\left(\sigma_4[v_l'YA_lA_{kl}^{-1}b_l] + \right.$
$\left.\gamma_3[v_l'YA_lA_{kl}^{-1}PA_{kl}^{-1}b_l]\right)$

9. $-16\beta_l(\mathbf{r}'\mathbf{A}_k\mathbf{X}\mathbf{A}_k\mathbf{r})(\mathbf{w}_l'\mathbf{Y}\mathbf{A}_l\mathbf{r})$

(a) $-16\frac{3}{2}\text{ tr}[P]\frac{\pi^{3n/2}}{4|A_{kl}|^{3/2}}\left(\gamma_1[b_k'A_{kl}^{-1}A_lYb_l]+\gamma_3[v_l'A_{kl}^{-1}A_lYb_l]+\gamma_6[v_k'A_{kl}^{-1}A_lYb_l]\right)$

$-16\frac{\pi^{3n/2}}{4|A_{kl}|^{3/2}}\left(\sigma_2[b_k'A_{kl}^{-1}A_lYb_l]+\gamma_1[b_k'A_{kl}^{-1}PA_{kl}^{-1}]A_lYb_l]+\sigma_4[v_l'A_{kl}^{-1}A_lYb_l]\right.$

$\left.+\gamma_3[v_l'A_{kl}^{-1}PA_{kl}^{-1}A_lYb_l]+\gamma_6[v_k'A_{kl}^{-1}PA_{kl}^{-1}A_lYb_l]+\sigma_5[v_k'A_{kl}^{-1}A_lYb_l]\right)$

(b) $-16\frac{3}{2}\,\mathrm{tr}[P]\frac{\pi^{3n/2}}{4|A_{kl}|^{3/2}}\Big(\gamma_1[b_k'A_{kl}^{-1}A_lYb_l]\Big) \quad - \quad 16\frac{\pi^{3n/2}}{4|A_{kl}|^{3/2}}\Big(\sigma_2[b_k'A_{kl}^{-1}A_lYb_l] \quad + \quad \gamma_1[b_k'A_{kl}^{-1}PA_{kl}^{-1}A_lYb_l]\Big)$

(c) $-16\frac{3}{2}\,\mathrm{tr}[P]\frac{\pi^{3n/2}}{4|A_{kl}|^{3/2}}\Big(\gamma_3[v_l'A_{kl}^{-1}A_lYb_l]\Big) \quad - \quad 16\frac{\pi^{3n/2}}{4|A_{kl}|^{3/2}}\Big(\sigma_4[v_l'A_{kl}^{-1}A_lYb_l] \quad + \quad \gamma_3[v_l'A_{kl}^{-1}PA_{kl}^{-1}A_lYb_l]\Big)$

10. $+8\alpha_l\beta_l(\mathbf{r}'\mathbf{A}_k\mathbf{X}\mathbf{A}_k\mathbf{r})(\mathbf{v}_l'\mathbf{Y}\mathbf{w}_l)$

(a) $8(v_l'Yb_l)\frac{\pi^{3n/2}}{2|A_{kl}|^{3/2}}\left(\frac{3}{2}(v_k'A_{kl}^{-1}b_k)\mathrm{tr}[A_{kl}^{-1}A_kXA_k]+v_k'A_{kl}^{-1}A_kXA_kA_{kl}^{-1}b_k\right)$

(b) 0

(c) $8(v_l'Yb_l)\frac{\pi^{3n/2}}{2|A_{kl}|^{3/2}}\left(\frac{3}{2}(v_k'A_{kl}^{-1}b_k)\mathrm{tr}[A_{kl}^{-1}A_kXA_k]+v_k'A_{kl}^{-1}A_kXA_kA_{kl}^{-1}b_k\right)$

11. $+8\alpha_k(\mathbf{v}_k'\mathbf{X}\mathbf{A}_k\mathbf{r})\mathrm{tr}[\mathbf{A}_l\mathbf{Y}]$

(a) $24\mathrm{tr}[A_lY]\frac{\pi^{3n/2}}{4|A_{kl}|^{3/2}}\Big(\gamma_2[v_k'XA_kA_{kl}^{-1}v_l]+\gamma_4[v_k'XA_kA_{kl}^{-1}b_k]+\gamma_6[v_k'XA_kA_{kl}^{-1}b_l]\Big)$

(b) $24\mathrm{tr}[A_lY]\frac{\pi^{3n/2}}{4|A_{kl}|^{3/2}}\Big(\gamma_2[v_k'XA_kA_{kl}^{-1}v_l]\Big)$

(c) $24\mathrm{tr}[A_lY]\frac{\pi^{3n/2}}{4|A_{kl}|^{3/2}}\Big(\gamma_4[v_k'XA_kA_{kl}^{-1}b_k]\Big)$

12. $-16\alpha_k(\mathbf{v}_k'\mathbf{X}\mathbf{A}_k\mathbf{r})(\mathbf{r}'\mathbf{A}_l\mathbf{Y}\mathbf{A}_l\mathbf{r})$

(a) $-16\frac{3}{2}\,\mathrm{tr}[Q]\frac{\pi^{3n/2}}{4|A_{kl}|^{3/2}}\Big(\gamma_2[v_k'XA_kA_{kl}^{-1}v_l]+\gamma_4[v_k'XA_kA_{kl}^{-1}b_k]+\gamma_6[v_k'XA_kA_{kl}^{-1}b_l]\Big)$

$-16\frac{\pi^{3n/2}}{4|A_{kl}|^{3/2}}\Big(\gamma_2[v_k'XA_kA_{kl}^{-1}QA_{kl}^{-1}v_l]+o_1[v_k'XA_kA_{kl}^{-1}v_l]+\gamma_4[v_k'XA_kA_{kl}^{-1}QA_{kl}^{-1}b_k]$

$+o_3[v_k'XA_kA_{kl}^{-1}b_k]+\gamma_6[v_k'XA_kA_{kl}^{-1}QA_{kl}^{-1}b_l]+o_5[v_k'XA_kA_{kl}^{-1}b_l]\Big)$

(b) $-16\frac{3}{2}\,\mathrm{tr}[Q]\frac{\pi^{3n/2}}{4|A_{kl}|^{3/2}}\Big(\gamma_2[v_k'XA_kA_{kl}^{-1}v_l]\Big) \; - \; 16\frac{\pi^{3n/2}}{4|A_{kl}|^{3/2}}\Big(\gamma_2[v_k'XA_kA_{kl}^{-1}QA_{kl}^{-1}v_l] \; + \; o_1[v_k'XA_kA_{kl}^{-1}v_l]\Big)$

(c) $-16\frac{3}{2}\,\mathrm{tr}[Q]\frac{\pi^{3n/2}}{4|A_{kl}|^{3/2}}\Big(\gamma_2[\gamma_4[v_k'XA_kA_{kl}^{-1}b_k]\Big)-16\frac{\pi^{3n/2}}{4|A_{kl}|^{3/2}}\Big(\gamma_4[v_k'XA_kA_{kl}^{-1}QA_{kl}^{-1}b_k]+ o_3[v_k'XA_kA_{kl}^{-1}b_k]\Big)$

13. $+16\alpha_k\alpha_l(\mathbf{v}_k'\mathbf{X}\mathbf{A}_k\mathbf{r})(\mathbf{v}_l'\mathbf{Y}\mathbf{A}_l\mathbf{r})$

(a) $16\frac{\pi^{3n/2}}{4|A_{kl}|^{3/2}}\Big(\gamma_2[v_k'XA_kA_{kl}^{-1}A_lYv_l]+[v_k'XA_kA_{kl}^{-1}b_k][v_l'YA_lA_{kl}^{-1}b_l]$

$+[v_k'XA_kA_{kl}^{-1}b_l][b_k'A_{kl}^{-1}A_lYv_l]\Big)$

(b) $16\frac{\pi^{3n/2}}{4|A_{kl}|^{3/2}}\big(\gamma_2[v_k'XA_kA_{kl}^{-1}A_lYv_l]\big)$

(c) $16\frac{\pi^{3n/2}}{4|A_{kl}|^{3/2}}\big([v_k'XA_kA_{kl}^{-1}b_l][b_k'A_{kl}^{-1}A_lYv_l]\big)$

14. $+16\alpha_k\beta_l(\mathbf{v}_k'\mathbf{X}\mathbf{A}_k\mathbf{r})(\mathbf{w}_l'\mathbf{Y}\mathbf{A}_l\mathbf{r})$

(a) $16\frac{\pi^{3n/2}}{4|A_{kl}|^{3/2}}\Big([v_k'XA_kA_{kl}^{-1}v_l][b_k'A_{kl}^{-1}A_lYb_l]+[v_k'XA_kA_{kl}^{-1}b_k][v_l'A_{kl}^{-1}A_lYb_l]$

$+\gamma_6[v_k'XA_kA_{kl}^{-1}A_lYb_l]\Big),$

(b) $16\frac{\pi^{3n/2}}{4|A_{kl}|^{3/2}}\big([v_k'XA_kA_{kl}^{-1}v_l][b_k'A_{kl}^{-1}A_lYb_l]\big)$

(c) $16\frac{\pi^{3n/2}}{4|A_{kl}|^{3/2}}\big(\gamma_6[v_k'XA_kA_{kl}^{-1}A_lYb_l]\big)$

15. $-8\alpha_k\alpha_l\beta_l(\mathbf{v}_k'\mathbf{X}\mathbf{A}_k\mathbf{r})(\mathbf{v}_l'\mathbf{Y}\mathbf{w}_l)$

(a) $-8(v_lYb_l)\frac{\pi^{3n/2}}{2|A_{kl}|^{3/2}}(v_k'XA_kA_{kl}^{-1}b_k)$

(b) 0

(c) $-8(v_lYb_l)\frac{\pi^{3n/2}}{2|A_{kl}|^{3/2}}(v_k'XA_kA_{kl}^{-1}b_k)$

16. $+8\beta_k(\mathbf{w}_k'\mathbf{X}\mathbf{A}_k\mathbf{r})\mathrm{tr}[\mathbf{A}_l\mathbf{Y}]$

(a) $24\mathrm{tr}[A_lY]\frac{\pi^{3n/2}}{4|A_{kl}|^{3/2}}\Big(\gamma_1[b_k'XA_kA_{kl}^{-1}b_l]+\gamma_4[v_k'A_{kl}^{-1}A_k'Xb_k]+\gamma_5[b_k'XA_kA_{kl}^{-1}v_l]\Big)$

(b) $24\mathrm{tr}[A_lY]\frac{\pi^{3n/2}}{4|A_{kl}|^{3/2}}\Big(\gamma_1[b_k'XA_kA_{kl}^{-1}b_l]\Big)$

(c) $24\mathrm{tr}[A_lY]\frac{\pi^{3n/2}}{4|A_{kl}|^{3/2}}\Big(\gamma_4[v_k'A_{kl}^{-1}A_k'Xb_k]\Big)$

17. $-16\beta_k(\mathbf{w}_k'\mathbf{X}\mathbf{A}_k\mathbf{r})(\mathbf{r}'\mathbf{A}_l\mathbf{Y}\mathbf{A}_l\mathbf{r})$

(a) $-16\frac{3}{2}\,\mathrm{tr}[Q]\frac{\pi^{3n/2}}{4|A_{kl}|^{3/2}}\Big(\gamma_1[b_k'XA_kA_{kl}^{-1}b_l]+\gamma_4[v_k'A_{kl}^{-1}A_k'Xb_k]+\gamma_5[b_k'XA_kA_{kl}^{-1}v_l]\Big)$

$-16\frac{\pi^{3n/2}}{4|A_{kl}|^{3/2}}\Big(o_2[b_k'XA_kA_{kl}^{-1}b_l]+\gamma_1[b_k'XA_kA_{kl}^{-1}QA_{kl}^{-1}b_l]+\gamma_4[v_k'A_{kl}^{-1}QA_{kl}^{-1}A_k'Xb_k]$

$+o_3[v_k'A_{kl}^{-1}A_kXb_k]+o_6[b_k'XA_kA_{kl}^{-1}v_l]+\gamma_5[b_k'XA_kA_{kl}^{-1}QA_{kl}^{-1}v_l]\Big)$

(b) $-16\frac{3}{2}\,\mathrm{tr}[Q]\frac{\pi^{3n/2}}{4|A_{kl}|^{3/2}}\Big(\gamma_1[b_k'XA_kA_{kl}^{-1}b_l]\Big) \quad - \quad 16\frac{\pi^{3n/2}}{4|A_{kl}|^{3/2}}\Big(o_2[b_k'XA_kA_{kl}^{-1}b_l] \quad + \gamma_1[b_k'XA_kA_{kl}^{-1}QA_{kl}^{-1}b_l]\Big)$

(c) $-16\frac{3}{2}\,\mathrm{tr}[Q]\frac{\pi^{3n/2}}{4|A_{kl}|^{3/2}}\Big(\gamma_4[v_k'A_{kl}^{-1}A_k'Xb_k]\Big) \; - \; 16\frac{\pi^{3n/2}}{4|A_{kl}|^{3/2}}\Big(\gamma_4[v_k'A_{kl}^{-1}QA_{kl}^{-1}A_k'Xb_k] \; + \; o_3[v_k'A_{kl}^{-1}A_kXb_k]\Big)$

18. $+16\beta_k\alpha_l(\mathbf{w}_k'\mathbf{X}\mathbf{A}_k\mathbf{r})(\mathbf{v}_l'\mathbf{Y}\mathbf{A}_l\mathbf{r})$

(a) $16\frac{\pi^{3n/2}}{4|A_{kl}|^{3/2}}\Big([v_k'A_{kl}^{-1}A_lYv_l][b_k'XA_kA_{kl}^{-1}b_l] + [v_k'A_{kl}^{-1}A_kXb_k][v_l'YA_lA_{kl}^{-1}b_l] + \gamma_5[b_k'XA_kA_{kl}^{-1}A_lYv_l]\Big)$

(b) $16\frac{\pi^{3n/2}}{4|A_{kl}|^{3/2}}\Big([v_k'A_{kl}^{-1}A_lYv_l][b_k'XA_kA_{kl}^{-1}b_l]\Big)$

(c) $16\frac{\pi^{3n/2}}{4|A_{kl}|^{3/2}}\Big(\gamma_5[b_k'XA_kA_{kl}^{-1}A_lYv_l]\Big)$

19. $+16\beta_k\beta_l(\mathbf{w}_k'\mathbf{X}\mathbf{A}_k\mathbf{r})(\mathbf{w}_l'\mathbf{Y}\mathbf{A}_l\mathbf{r})$

(a) $16\frac{\pi^{3n/2}}{4|A_{kl}|^{3/2}}\Big(\gamma_1[b_k'XA_kA_{kl}^{-1}A_lYb_l] + [v_k'A_{kl}^{-1}A_kXb_k][v_l'A_{kl}^{-1}A_lYb_l] + [v_k'A_{kl}^{-1}A_lYb_l][b_k'XA_kA_{kl}^{-1}b_l]\Big)$

(b) $16\frac{\pi^{3n/2}}{4|A_{kl}|^{3/2}}\Big(\gamma_1[b_k'XA_kA_{kl}^{-1}A_lYb_l]\Big)$

(c) $16\frac{\pi^{3n/2}}{4|A_{kl}|^{3/2}}\Big([v_k'A_{kl}^{-1}A_lYb_l][b_k'XA_kA_{kl}^{-1}b_l]\Big)$

20. $-8\beta_k\alpha_l\beta_l(\mathbf{w}_k'\mathbf{X}\mathbf{A}_k\mathbf{r})(\mathbf{v}_l'\mathbf{Y}\mathbf{w}_l)$

(a) $-8(v_lYb_l)\frac{\pi^{3n/2}}{2|A_{kl}|^{3/2}}(v_k'A_{kl}^{-1}A_k'Xb_k)$

(b) 0

(c) $-8(v_lYb_l)\frac{\pi^{3n/2}}{2|A_{kl}|^{3/2}}(v_k'A_{kl}^{-1}A_k'Xb_k)$

21. $-4\alpha_k\beta_k(\mathbf{v}_k'\mathbf{X}\mathbf{w}_k)\mathrm{tr}[\mathbf{A}_l\mathbf{Y}]$

(a) $-12\mathrm{tr}[A_lY](v_k'Xb_k)\frac{\pi^{3n/2}}{2|A_{kl}|^{3/2}}\gamma_4$

(b) 0

(c) $-12\text{tr}[A_l Y](v_k' X b_k)\frac{\pi^{3n/2}}{2|A_{kl}|^{3/2}}\gamma_4$

22. $+8\alpha_k\beta_k(\mathbf{v}_k'\mathbf{X}\mathbf{w}_k)(\mathbf{r}'\mathbf{A}_l\mathbf{Y}\mathbf{A}_l\mathbf{r})$

(a) $8(v_k' X b_k)\frac{\pi^{3n/2}}{2|A_{kl}|^{3/2}}\left(\frac{3}{2}(v_l' A_{kl}^{-1} b_l)\text{tr}[A_{kl}^{-1}A_l Y A_l] + v_l' A_{kl}^{-1} A_l Y A_l A_{kl}^{-1} b_l\right)$

(b) 0

(c) $8(v_k' X b_k)\frac{\pi^{3n/2}}{2|A_{kl}|^{3/2}}\left(\frac{3}{2}(v_l' A_{kl}^{-1} b_l)\text{tr}[A_{kl}^{-1}A_l Y A_l] + v_l' A_{kl}^{-1} A_l Y A_l A_{kl}^{-1} b_l\right)$

23. $-8\alpha_k\beta_k\alpha_l(\mathbf{v}_k'\mathbf{X}\mathbf{w}_k)(\mathbf{v}_l'\mathbf{Y}\mathbf{A}_l\mathbf{r})$

(a) $-8(v_k' X b_k)\frac{\pi^{3n/2}}{2|A_{kl}|^{3/2}}(v_l' Y A_l A_{kl}^{-1} b_l)$

(b) 0

(c) $-8(v_k' X b_k)\frac{\pi^{3n/2}}{2|A_{kl}|^{3/2}}(v_l' Y A_l A_{kl}^{-1} b_l)$

24. $-8\alpha_k\beta_k\beta_l(\mathbf{v}_k'\mathbf{X}\mathbf{w}_k)(\mathbf{w}_l'\mathbf{Y}\mathbf{A}_l\mathbf{r})$

(a) $-8(v_k' X b_k)\frac{\pi^{3n/2}}{2|A_{kl}|^{3/2}}(v_l' A_{kl}^{-1} A_l Y b_l)$

(b) 0

(c) $-8(v_k' X b_k)\frac{\pi^{3n/2}}{2|A_{kl}|^{3/2}}(v_l' A_{kl}^{-1} A_l Y b_l)$

25. $+4\alpha_k\beta_k\alpha_l\beta_l(\mathbf{v}_k'\mathbf{X}\mathbf{w}_k)(\mathbf{v}_l'\mathbf{Y}\mathbf{w}_l)$

(a) $4(v_k' X b_k)(v_l' Y b_l)\frac{\pi^{3n/2}}{|A_{kl}|^{3/2}}$

(b) 0

(c) $4(v_k' X b_k)(v_l' Y b_l)\frac{\pi^{3n/2}}{|A_{kl}|^{3/2}}$

The seventh integral $\langle\phi_k|(\boldsymbol{r}'\boldsymbol{P}\boldsymbol{r})(\boldsymbol{r}'\boldsymbol{Q}\boldsymbol{r})|\phi_l\rangle$ is difficult and the solution is

1. $\langle\phi_k|(\boldsymbol{r}'\boldsymbol{P}\boldsymbol{r})(\boldsymbol{r}'\boldsymbol{Q}\boldsymbol{r})|\phi_l\rangle =$

(a)

$$\frac{\pi^{3n/2}}{4|A_{kl}|^{3/2}}\left(\sum_{i=1}^{6}\left[\frac{3}{2}\text{tr}[Q]\sigma_i\gamma_i + \frac{3}{2}\text{tr}[P]o_i\gamma_i + o\sigma_i\gamma_i + \sigma o_i\gamma_i\right] + \left(\gamma_1\gamma_2+\gamma_3\gamma_4+\gamma_5\gamma_6\right)\right.$$
$$\left.\times\left(\frac{3}{2}\text{tr}[QP] + \frac{9}{4}\text{tr}[Q]\text{tr}[P]\right) + (o_1\sigma_2 + o_2\sigma_1 + o_3\sigma_4 + o_4\sigma_3 + o_5\sigma_6 + o_6\sigma_5)\right)$$

(b)

$$\frac{\pi^{3n/2}}{4|A_{kl}|^{3/2}}\Bigg(\sum_{i=1}^{2}\left[\frac{3}{2}\mathrm{tr}[Q]\sigma_i\gamma_i+\frac{3}{2}\mathrm{tr}[P]o_i\gamma_i+o\sigma_i\gamma_i+\sigma o_i\gamma_i\right]$$
$$+\gamma_1\gamma_2\left(\frac{3}{2}\mathrm{tr}[QP]+\frac{9}{4}\mathrm{tr}[Q]\mathrm{tr}[P]\right)+(o_1\sigma_2+o_2\sigma_1)\Bigg)$$

(c)

$$\frac{\pi^{3n/2}}{4|A_{kl}|^{3/2}}\Bigg(\sum_{i=3}^{4}\left[\frac{3}{2}\mathrm{tr}[Q]\sigma_i\gamma_i+\frac{3}{2}\mathrm{tr}[P]o_i\gamma_i+o\sigma_i\gamma_i+\sigma o_i\gamma_i\right]$$
$$+\gamma_3\gamma_4\left(\frac{3}{2}\mathrm{tr}[QP]+\frac{9}{4}\mathrm{tr}[Q]\mathrm{tr}[P]\right)+(o_3\sigma_4+o_4\sigma_3)\Bigg)$$

Here the following set of notations are defined:

$$\begin{aligned}
&\gamma_1=v_k'A_{kl}^{-1}v_l,\quad \gamma_2=b_k'A_{kl}^{-1}b_l,\quad \gamma_3=v_k'A_{kl}^{-1}b_k,\\
&\gamma_4=v_l'A_{kl}^{-1}b_l,\quad \gamma_5=v_k'A_{kl}^{-1}b_l,\quad \gamma_6=b_k'A_{kl}^{-1}v_l,\\
&\gamma=\gamma_1\gamma_2+\gamma_3\gamma_4+\gamma_5\gamma_6,\quad \tau=\mathrm{tr}\left[A_{kl}^{-1}A_lMA_k'\right],\\
&\mathrm{tr}[QP]=\mathrm{tr}\left[A_{kl}^{-1}QA_{kl}^{-1}P\right],\quad \mathrm{tr}[P]=\mathrm{tr}\left[A_{kl}^{-1}P\right],\quad \mathrm{tr}[Q]=\mathrm{tr}\left[A_{kl}^{-1}Q\right]
\end{aligned}\tag{145}$$

$$\begin{aligned}
&\sigma_1=b_k'A_{kl}^{-1}PA_{kl}^{-1}b_l,\quad \sigma_2=v_k'A_{kl}^{-1}PA_{kl}^{-1}v_l,\quad \sigma_3=v_l'A_{kl}^{-1}PA_{kl}^{-1}b_l,\\
&\sigma_4=v_k'A_{kl}^{-1}PA_{kl}^{-1}b_k,\quad \sigma_5=b_k'A_{kl}^{-1}PA_{kl}^{-1}v_l,\quad \sigma_6=v_k'A_{kl}^{-1}PA_{kl}^{-1}b_l,\\
&o_1=b_k'A_{kl}^{-1}QA_{kl}^{-1}b_l,\quad o_2=v_k'A_{kl}^{-1}QA_{kl}^{-1}v_l,\quad o_3=v_l'A_{kl}^{-1}QA_{kl}^{-1}b_l,\\
&o_4=v_k'A_{kl}^{-1}QA_{kl}^{-1}b_k,\quad o_5=b_k'A_{kl}^{-1}QA_{kl}^{-1}v_l,\quad o_6=v_k'A_{kl}^{-1}QA_{kl}^{-1}b_l,
\end{aligned}\tag{146}$$

$$\begin{aligned}
&\sigma o_1=b_k'A_{kl}^{-1}PA_{kl}^{-1}QA_{kl}^{-1}b_l,\quad \sigma o_2=v_k'A_{kl}^{-1}PA_{kl}^{-1}QA_{kl}^{-1}v_l,\\
&\sigma o_3=v_l'A_{kl}^{-1}PA_{kl}^{-1}QA_{kl}^{-1}b_l,\quad \sigma o_4=v_k'A_{kl}^{-1}PA_{kl}^{-1}QA_{kl}^{-1}b_k,\\
&\sigma o_5=b_k'A_{kl}^{-1}PA_{kl}^{-1}QA_{kl}^{-1}v_l,\quad \sigma o_6=v_k'A_{kl}^{-1}PA_{kl}^{-1}QA_{kl}^{-1}b_l,\\
&o\sigma_1=b_k'A_{kl}^{-1}QA_{kl}^{-1}PA_{kl}^{-1}b_l,\quad o\sigma_2=v_k'A_{kl}^{-1}QA_{kl}^{-1}PA_{kl}^{-1}v_l,\\
&o\sigma_3=v_l'A_{kl}^{-1}QA_{kl}^{-1}PA_{kl}^{-1}b_l,\quad o\sigma_4=v_k'A_{kl}^{-1}QA_{kl}^{-1}PA_{kl}^{-1}b_k,\\
&o\sigma_5=b_k'A_{kl}^{-1}QA_{kl}^{-1}PA_{kl}^{-1}v_l,\quad o\sigma_6=v_k'A_{kl}^{-1}QA_{kl}^{-1}PA_{kl}^{-1}b_l.
\end{aligned}\tag{147}$$

As observed, we have presented derivations for the matrix elements of the mass-velocity Hamiltonian (140) with basis functions (33) for three cases: $(x_{i_k}x_{j_k}|x_{i_l}x_{j_l})$, $(x_{i_k}y_{j_k}|y_{i_l}x_{j_l})$, and $(x_{i_k}x_{j_k}|y_{i_l}y_{j_l})$. Despite following the same procedure and leading to

nearly identical final results, we presented three cases separately to be clear and avoid any confusion.

This similarity also holds true when deriving the matrix elements of the orbit-orbit Hamiltonian (148). Consequently, we choose not to articulate the matrix elements separately for each of the three cases. Instead, we present the final results for the other two cases when deriving the matrix elements of some lengthy operators encountered in orbit-orbit Hamiltonian.

10 Matrix elements of Orbit-Orbit correction

10.1 Orbit-Orbit Hamiltonian

The matrix notation of the Orbit-Orbit interaction operator is

$$\begin{aligned}
&\langle \phi_k | \mathcal{H}_{\mathrm{OO}} | \phi_l \rangle = \\
&-\frac{1}{2}\sum_{i=1}^{n} \frac{q_0 q_i}{m_0 m_i} \left\langle \phi_k \left| \frac{1}{r_i} \boldsymbol{\nabla}' \boldsymbol{E}_{ii} \boldsymbol{\nabla} - (\boldsymbol{r}' \boldsymbol{E}_{ii})^{\lambda} \left(\boldsymbol{\nabla}' \boldsymbol{E}_{ii} \frac{1}{r_i} \right)^{\sigma} (\boldsymbol{E}_{ii} \boldsymbol{\nabla})_{\sigma} (\boldsymbol{E}_{ii} \boldsymbol{\nabla})_{\lambda} \right| \phi_l \right\rangle \\
&-\frac{1}{2}\sum_{i=1}^{n}\sum_{j\neq i}^{n} \frac{q_0 q_i}{m_0 m_i} \left\langle \phi_k \left| \frac{1}{r_i} \boldsymbol{\nabla}' \boldsymbol{E}_{ij} \boldsymbol{\nabla} - (\boldsymbol{r}' \boldsymbol{E}_{ii})^{\lambda} \left(\boldsymbol{\nabla}' \boldsymbol{E}_{ij} \frac{1}{r_i} \right)^{\sigma} (\boldsymbol{E}_{jj} \boldsymbol{\nabla})_{\sigma} (\boldsymbol{E}_{ii} \boldsymbol{\nabla})_{\lambda} \right| \phi_l \right\rangle + \\
&\frac{1}{2}\sum_{i=1}^{n}\sum_{j>i}^{n} \frac{q_i q_j}{m_i m_j} \left\langle \phi_k \left| \frac{1}{r_{ij}} \boldsymbol{\nabla}' \boldsymbol{E}_{ij} \boldsymbol{\nabla} + (\boldsymbol{r}' (\boldsymbol{E}_{ij} - \boldsymbol{E}_{jj}))^{\lambda} \left(\boldsymbol{\nabla}' \boldsymbol{E}_{ji} \frac{1}{r_{ij}} \right)^{\sigma} (\boldsymbol{E}_{ii} \boldsymbol{\nabla})_{\sigma} (\boldsymbol{E}_{jj} \boldsymbol{\nabla})_{\lambda} \right| \phi_l \right\rangle .
\end{aligned} \tag{148}$$

To streamline the calculation of the expectation value of $\mathcal{H}_{\mathrm{OO}}$, we employ the subsequent generic integral for each of the three components present in the expectation value:

$$\begin{aligned}
&\left\langle \phi_k \left| \frac{1}{r_g} \boldsymbol{\nabla}' \boldsymbol{B} \boldsymbol{\nabla} \right| \phi_l \right\rangle - \left\langle \phi_k \left| (\boldsymbol{r}' \boldsymbol{K})^{\lambda} \left(\boldsymbol{\nabla}' \boldsymbol{D} \frac{1}{r_g} \right)^{\sigma} (\boldsymbol{F} \boldsymbol{\nabla})_{\sigma} (\boldsymbol{G} \boldsymbol{\nabla})_{\lambda} \right| \phi_l \right\rangle = \frac{\partial}{\partial \alpha_k} \frac{\partial}{\partial \alpha_l} \frac{\partial}{\partial \beta_k} \frac{\partial}{\partial \beta_l} \\
&\times \left[\left\langle \varphi_k \left| \frac{1}{r_g} \boldsymbol{\nabla}' \boldsymbol{B} \boldsymbol{\nabla} \right| \varphi_l \right\rangle - \left\langle \varphi_k \left| (\boldsymbol{r}' \boldsymbol{K})^{\lambda} \left(\boldsymbol{\nabla}' \boldsymbol{D} \frac{1}{r_g} \right)^{\sigma} (\boldsymbol{F} \boldsymbol{\nabla})_{\sigma} (\boldsymbol{G} \boldsymbol{\nabla})_{\lambda} \right| \varphi_l \right\rangle \right]_{\alpha_{k,l}, \beta_{k,l} = 0},
\end{aligned}$$

where

for the first sum: $g = i$, $\boldsymbol{B} = \boldsymbol{E}_{ii}$, $\boldsymbol{K} = \boldsymbol{E}_{ii}$, $\boldsymbol{D} = \boldsymbol{E}_{ii}$, $\boldsymbol{F} = \boldsymbol{E}_{ii}$, $\boldsymbol{G} = \boldsymbol{E}_{ii}$;

for the second sum $g = i$, $\boldsymbol{B} = \boldsymbol{E}_{ij}$, $\boldsymbol{K} = \boldsymbol{E}_{ii}$, $\boldsymbol{D} = \boldsymbol{E}_{ij}$, $\boldsymbol{F} = \boldsymbol{E}_{jj}$, $\boldsymbol{G} = \boldsymbol{E}_{ii}$;

for the third sum: $g = ij$, $\boldsymbol{B} = \boldsymbol{E}_{ij}$, $\boldsymbol{K} = (\boldsymbol{E}_{ij} - \boldsymbol{E}_{jj})$, $\boldsymbol{D} = \boldsymbol{E}_{ji}$, $\boldsymbol{F} = \boldsymbol{E}_{ii}$, $\boldsymbol{G} = \boldsymbol{E}_{jj}$.

Subsequently, the integrals present in the aforementioned matrix elements are reformulated in relation to more fundamental integrals. Following this, the elemental integrals are computed.

10.2 Matrix elements

First let us define some useful notations and derivatives [104]

$$\boldsymbol{\nabla}_{\boldsymbol{r}}^{\lambda} \varphi_k \equiv \boldsymbol{\nabla}^{\lambda} \varphi_k \equiv \partial^{\lambda} \varphi_k, \quad \boldsymbol{\nabla}_{\boldsymbol{r}\lambda} \varphi_k \equiv \boldsymbol{\nabla}_{\lambda} \varphi_k \equiv \partial_{\lambda} \varphi_k. \tag{149}$$

where we have a gradient $\boldsymbol{\nabla}_{\boldsymbol{r}} = [\partial_x, \partial_y, \partial_z]$ taken with respect to $\boldsymbol{r}$, which is the vector of the coordinates .

$$\boldsymbol{\nabla}^{\lambda}\varphi_k \equiv \partial^{\lambda}\varphi_k = [-2\boldsymbol{r}'\boldsymbol{A}_k + \alpha_k\boldsymbol{v}_k' + \beta_k\boldsymbol{b}_k']^{\lambda}\varphi_k,$$

$$\boldsymbol{\nabla}_{\lambda}\varphi_k \equiv \partial_{\lambda}\varphi_k = [-2\boldsymbol{A}_k\boldsymbol{r} + \alpha_k\boldsymbol{v}_k + \beta_k\boldsymbol{b}_k]_{\lambda}\varphi_k.$$

$$(\boldsymbol{D}\boldsymbol{\nabla})_{\sigma}\varphi_k = \boldsymbol{D}_{\sigma}^{\lambda}\partial_{\lambda}\varphi_k = [-2\boldsymbol{D}\boldsymbol{A}_k\boldsymbol{r} + \alpha_k\boldsymbol{D}\boldsymbol{v}_k + \beta_k\boldsymbol{D}\boldsymbol{b}_k]_{\sigma}\varphi_k.$$

$$(\boldsymbol{\nabla}'\boldsymbol{D})^{\sigma}\varphi_k = \boldsymbol{D}_{\lambda}^{\sigma}\partial^{\lambda}\varphi_k = [-2\boldsymbol{r}'\boldsymbol{A}_k\boldsymbol{D} + \alpha_k\boldsymbol{v}_k'\boldsymbol{D} + \beta_k\boldsymbol{b}_k'\boldsymbol{D}]^{\sigma}\varphi_k.$$

$$\begin{aligned}\boldsymbol{\nabla}_{\boldsymbol{r}}'\boldsymbol{D}\boldsymbol{\nabla}_{\boldsymbol{r}}\varphi_k &= [-2\mathrm{tr}[\boldsymbol{A}_k\boldsymbol{D}] + 4(\boldsymbol{r}'\boldsymbol{A}_k\boldsymbol{D}\boldsymbol{A}_k\boldsymbol{r}) - 4\alpha_k(\boldsymbol{v}_k'\boldsymbol{D}\boldsymbol{A}_k\boldsymbol{r}) - 4\beta_k(\boldsymbol{b}_k'\boldsymbol{D}\boldsymbol{A}_k\boldsymbol{r}) \\ &\quad +\alpha_k^2(\boldsymbol{v}_k'\boldsymbol{D}\boldsymbol{v}_k) + \beta_k^2(\boldsymbol{b}_k'\boldsymbol{D}\boldsymbol{b}_k) + 2\alpha_k\beta_k(\boldsymbol{v}_k'\boldsymbol{D}\boldsymbol{b}_k)]\varphi_k. \qquad (150)\end{aligned}$$

$$\begin{aligned}\partial^{\lambda}\partial_{\sigma}\varphi_k &= \boldsymbol{\nabla}^{\lambda}\boldsymbol{\nabla}_{\sigma}\varphi_k = \Big[-2\left(\boldsymbol{A}_k\right)_{\sigma}^{\lambda} + 4\left(\boldsymbol{r}'\boldsymbol{A}_k\right)^{\lambda}\left(\boldsymbol{A}_k\boldsymbol{r}\right)_{\sigma} - 2\alpha_k\left(\boldsymbol{r}'\boldsymbol{A}_k\right)^{\lambda}\left(\boldsymbol{v}_k\right)_{\sigma} \\ &\quad -2\beta_k\left(\boldsymbol{r}'\boldsymbol{A}_k\right)^{\lambda}\left(\boldsymbol{b}_k\right)_{\sigma} - 2\alpha_k(\boldsymbol{v}_k)^{\lambda}\left(\boldsymbol{A}_k\boldsymbol{r}\right)_{\sigma} + \alpha_k^2(\boldsymbol{v}_k)^{\lambda}\left(\boldsymbol{v}_k\right)_{\sigma} + \alpha_k\beta_k(\boldsymbol{v}_k)^{\lambda}\left(\boldsymbol{b}_k\right)_{\sigma} \\ &\quad -2\beta_k(\boldsymbol{b}_k)^{\lambda}\left(\boldsymbol{A}_k\boldsymbol{r}\right)_{\sigma} + \beta_k\alpha_k(\boldsymbol{b}_k)^{\lambda}\left(\boldsymbol{v}_k\right)_{\sigma} + \beta_k^2(\boldsymbol{b}_k)^{\lambda}\left(\boldsymbol{b}_k\right)_{\sigma}\Big]\varphi_k. \qquad (151)\end{aligned}$$

$$\begin{aligned}\partial_{\lambda}\partial_{\sigma}\varphi_k &= \boldsymbol{\nabla}_{\lambda}\boldsymbol{\nabla}_{\sigma}\varphi_k = \Big[-2\left(\boldsymbol{A}_k\right)_{\lambda\sigma} + 4\left(\boldsymbol{A}_k\boldsymbol{r}\right)_{\lambda}\left(\boldsymbol{A}_k\boldsymbol{r}\right)_{\sigma} - 2\alpha_k\left(\boldsymbol{A}_k\boldsymbol{r}\right)_{\lambda}\left(\boldsymbol{v}_k\right)_{\sigma} \\ &\quad -2\beta_k\left(\boldsymbol{A}_k\boldsymbol{r}\right)_{\lambda}\left(\boldsymbol{b}_k\right)_{\sigma} - 2\alpha_k(\boldsymbol{v}_k)_{\lambda}\left(\boldsymbol{A}_k\boldsymbol{r}\right)_{\sigma} + \alpha_k^2(\boldsymbol{v}_k)_{\lambda}\left(\boldsymbol{v}_k\right)_{\sigma} + \alpha_k\beta_k(\boldsymbol{v}_k)_{\lambda}\left(\boldsymbol{b}_k\right)_{\sigma} \\ &\quad -2\beta_k(\boldsymbol{b}_k)_{\lambda}\left(\boldsymbol{A}_k\boldsymbol{r}\right)_{\sigma} + \beta_k\alpha_k(\boldsymbol{b}_k)_{\lambda}\left(\boldsymbol{v}_k\right)_{\sigma} + \beta_k^2(\boldsymbol{b}_k)_{\lambda}\left(\boldsymbol{b}_k\right)_{\sigma}\Big]\varphi_k. \qquad (152)\end{aligned}$$

In the derivatives below, we will exclude the the terms that have quadratic λ's and σ's because their expectation values become zero when we take the limit with respect to λ's and σ's and set them equal to zero:

$$\begin{aligned}&\partial^{\rho}\partial_{\sigma}\partial_{\lambda}\varphi_k \\ &= \Big[4\left(\boldsymbol{A}_k\right)_{\lambda}^{\rho}\left(\boldsymbol{A}_k\boldsymbol{r}\right)_{\sigma} + 4\left(\boldsymbol{A}_k\right)_{\sigma}^{\rho}\left(\boldsymbol{A}_k\boldsymbol{r}\right)_{\lambda} - 2\alpha_k\left(\boldsymbol{A}_k\right)_{\lambda}^{\rho}\left(\boldsymbol{v}_k\right)_{\sigma} - 2\beta_k\left(\boldsymbol{A}_k\right)_{\lambda}^{\rho}\left(\boldsymbol{b}_k\right)_{\sigma} \\ &\quad -2\alpha_k\left(\boldsymbol{A}_k\right)_{\sigma}^{\rho}\left(\boldsymbol{v}_k\right)_{\lambda} - 2\beta_k\left(\boldsymbol{A}_k\right)_{\sigma}^{\rho}\left(\boldsymbol{b}_k\right)_{\lambda} + 4\left(\boldsymbol{A}_k\right)_{\lambda\sigma}\left(\boldsymbol{r}'\boldsymbol{A}_k\right)^{\rho} - 8\left(\boldsymbol{A}_k\boldsymbol{r}\right)_{\lambda}\left(\boldsymbol{A}_k\boldsymbol{r}\right)_{\sigma}\left(\boldsymbol{r}'\boldsymbol{A}_k\right)^{\rho} \\ &\quad +4\alpha_k\left(\boldsymbol{A}_k\boldsymbol{r}\right)_{\lambda}\left(\boldsymbol{v}_k\right)_{\sigma}\left(\boldsymbol{r}'\boldsymbol{A}_k\right)^{\rho} + 4\beta_k\left(\boldsymbol{A}_k\boldsymbol{r}\right)_{\lambda}\left(\boldsymbol{b}_k\right)_{\sigma}\left(\boldsymbol{r}'\boldsymbol{A}_k\right)^{\rho} + 4\alpha_k(\boldsymbol{v}_k)_{\lambda}\left(\boldsymbol{A}_k\boldsymbol{r}\right)_{\sigma}\left(\boldsymbol{r}'\boldsymbol{A}_k\right)^{\rho} \\ &\quad -2\alpha_k\beta_k(\boldsymbol{v}_k)_{\lambda}\left(\boldsymbol{b}_k\right)_{\sigma}\left(\boldsymbol{r}'\boldsymbol{A}_k\right)^{\rho} + 4\beta_k(\boldsymbol{b}_k)_{\lambda}\left(\boldsymbol{A}_k\boldsymbol{r}\right)_{\sigma}\left(\boldsymbol{r}'\boldsymbol{A}_k\right)^{\rho} - 2\beta_k\alpha_k(\boldsymbol{b}_k)_{\lambda}\left(\boldsymbol{v}_k\right)_{\sigma}\left(\boldsymbol{r}'\boldsymbol{A}_k\right)^{\rho} \\ &\quad -2\alpha_k\left(\boldsymbol{v}_k\right)^{\rho}\left(\boldsymbol{A}_k\right)_{\lambda\sigma} + 4\alpha_k\left(\boldsymbol{v}_k\right)^{\rho}\left(\boldsymbol{A}_k\boldsymbol{r}\right)_{\lambda}\left(\boldsymbol{A}_k\boldsymbol{r}\right)_{\sigma} - 2\beta_k\alpha_k\left(\boldsymbol{v}_k\right)^{\rho}\left(\boldsymbol{A}_k\boldsymbol{r}\right)_{\lambda}\left(\boldsymbol{b}_k\right)_{\sigma} \\ &\quad -2\beta_k\alpha_k\left(\boldsymbol{v}_k\right)^{\rho}\left(\boldsymbol{b}_k\right)_{\lambda}\left(\boldsymbol{A}_k\boldsymbol{r}\right)_{\sigma} - 2\beta_k\left(\boldsymbol{b}_k\right)^{\rho}\left(\boldsymbol{A}_k\right)_{\lambda\sigma} + 4\beta_k\left(\boldsymbol{b}_k\right)^{\rho}\left(\boldsymbol{A}_k\boldsymbol{r}\right)_{\lambda}\left(\boldsymbol{A}_k\boldsymbol{r}\right)_{\sigma} \\ &\quad -2\alpha_k\beta_k\left(\boldsymbol{b}_k\right)^{\rho}\left(\boldsymbol{A}_k\boldsymbol{r}\right)_{\lambda}\left(\boldsymbol{v}_k\right)_{\sigma} - 2\alpha_k\beta_k\left(\boldsymbol{b}_k\right)^{\rho}\left(\boldsymbol{v}_k\right)_{\lambda}\left(\boldsymbol{A}_k\boldsymbol{r}\right)_{\sigma}\Big]\varphi_k. \qquad (153)\end{aligned}$$

10.3 Integral $\langle\phi_k|\frac{\boldsymbol{\nabla}'\boldsymbol{B}\boldsymbol{\nabla}}{r_g}|\phi_l\rangle$

First let us write the following

$$\left\langle \phi_k \left| \frac{\boldsymbol{\nabla}'\boldsymbol{B}\boldsymbol{\nabla}}{r_g} \right| \phi_l \right\rangle = \frac{\partial}{\partial\alpha_k}\frac{\partial}{\partial\alpha_l}\frac{\partial}{\partial\beta_k}\frac{\partial}{\partial\beta_l} \left\langle \varphi_k \left| \frac{1}{r_g}\boldsymbol{\nabla}'\boldsymbol{B}\boldsymbol{\nabla} \right| \varphi_l \right\rangle \Big|_{\alpha_{k,l},\beta_{k,l}=0}$$

Using the following derivative we will have

$$\begin{aligned} \boldsymbol{\nabla}'_{\boldsymbol{r}}\boldsymbol{B}\boldsymbol{\nabla}_{\boldsymbol{r}}\varphi_l &= [-2\mathrm{tr}[\boldsymbol{A}_l\boldsymbol{B}] + 4(\boldsymbol{r}'\boldsymbol{A}_l\boldsymbol{B}\boldsymbol{A}_l\boldsymbol{r}) - 4\alpha_l(\boldsymbol{v}'_l\boldsymbol{B}\boldsymbol{A}_l\boldsymbol{r}) - 4\beta_l(\boldsymbol{b}'_l\boldsymbol{B}\boldsymbol{A}_l\boldsymbol{r}) \\ &\quad +\alpha_l^2(\boldsymbol{v}'_l\boldsymbol{B}\boldsymbol{v}_l) + \beta_l^2(\boldsymbol{b}'_l\boldsymbol{B}\boldsymbol{b}_l) + 2\alpha_l\beta_l(\boldsymbol{v}'_l\boldsymbol{B}\boldsymbol{b}_l)]\varphi_l. \end{aligned} \tag{154}$$

After taking the derivative we will have

$$\begin{aligned} &\frac{\partial}{\partial\alpha_k}\frac{\partial}{\partial\alpha_l}\frac{\partial}{\partial\beta_k}\frac{\partial}{\partial\beta_l} \left\langle \varphi_k \left| \frac{1}{r_g}\boldsymbol{\nabla}'\boldsymbol{B}\boldsymbol{\nabla} \right| \varphi_l \right\rangle \Big|_{\alpha_{k,l},\beta_{k,l}=0} \\ = \; & -6\,\mathrm{tr}[A_lB] \left\langle \phi_k \left| \frac{1}{r_g} \right| \phi_l \right\rangle + 4 \left\langle \phi_k \left| \frac{\boldsymbol{r}'\boldsymbol{A}_l\boldsymbol{B}\boldsymbol{A}_l\boldsymbol{r}}{r_g} \right| \phi_l \right\rangle - 4 \left\langle \phi_k \left| \frac{1}{r_g} \right| \phi_l \right\rangle_{(v_l->A'_lBv_l)} \\ & -4 \left\langle \phi_k \left| \frac{1}{r_g} \right| \phi_l \right\rangle_{(b_l->A'_lBb_l)} + 2v_lBb_l \left\langle \phi_k \left| \frac{1}{r_g} \right| \phi_l \right\rangle_{L=1,v_kAb_k}. \end{aligned} \tag{155}$$

Integral $\left\langle \phi_k \left| \frac{\boldsymbol{r}'\boldsymbol{X}\boldsymbol{r}}{r_{ij}} \right| \phi_l \right\rangle$

In order to compute this integral, we use the following relation for a symmetric matrix $\boldsymbol{X} = X \otimes I_3$:

$$\boldsymbol{r}'\boldsymbol{X}\boldsymbol{r} = -\frac{\partial}{\partial\alpha}\exp[-\alpha\boldsymbol{r}'\boldsymbol{X}\boldsymbol{r}]\Big|_{\alpha=0}. \tag{156}$$

For simplicity of taking the derivatives of different terms, we can list the following derivatives as an example for further analysis:

1. $\frac{\partial}{\partial\alpha}\left(\mathrm{tr}[(A_{kl}+\alpha X)^{-1}J_{ij}]\right)^{-1/2} = \frac{1}{2}\frac{\mathrm{tr}[A_{kl}^{-1}XA_{kl}^{-1}J_{ij}]}{\mathrm{tr}[A_{kl}^{-1}J_{ij}]^{3/2}}$,
2. $\frac{\partial}{\partial\alpha}\left(\mathrm{tr}[(A_{kl}+\alpha X)^{-1}J_{ij}]\right)^{-3/2} = \frac{3}{2}\frac{\mathrm{tr}[A_{kl}^{-1}XA_{kl}^{-1}J_{ij}]}{\mathrm{tr}[A_{kl}^{-1}J_{ij}]^{5/2}}$,
3. $\frac{\partial}{\partial\alpha}\left(\mathrm{tr}[(A_{kl}+\alpha X)^{-1}J_{ij}]\right)^{-5/2} = \frac{5}{2}\frac{\mathrm{tr}[A_{kl}^{-1}XA_{kl}^{-1}J_{ij}]}{\mathrm{tr}[A_{kl}^{-1}J_{ij}]^{7/2}}$,
4. $\frac{\partial}{\partial\alpha}|A_{kl}+\alpha X|^{-3/2} = -\frac{3}{2}|A_{kl}|^{-3/2}\,\mathrm{tr}[A_{kl}^{-1}X]$,
5. $\frac{\partial}{\partial\alpha}\,\mathrm{tr}[(A_{kl}+\alpha X)^{-1}v_lv'_k] = -\,\mathrm{tr}[A_{kl}^{-1}XA_{kl}^{-1}v_lv'_k] = -\chi_2$,

6. $\frac{\partial}{\partial\alpha}\operatorname{tr}[(A_{kl}+\alpha X)^{-1}J_{ij}(A_{kl}+\alpha X)^{-1}v_l v_k']$
$= -\operatorname{tr}[A_{kl}^{-1}XA_{kl}^{-1}J_{ij}A_{kl}^{-1}v_l v_k' + A_{kl}^{-1}J_{ij}A_{kl}^{-1}XA_{kl}^{-1}v_l v_k'] = -\chi\xi_2 - \xi\chi_2.$

It is important to note that the integral $\left\langle \phi_k \left| \frac{\boldsymbol{r}'\boldsymbol{X}\boldsymbol{r}}{r_{ij}} \right| \phi_l \right\rangle$ is identical to integral of $\mathtt{R}_{kl}^{ij}$ in (72). Therefore, we substitute the value $A_{kl} \equiv A_{kl} + \alpha X$ everywhere for the matrix elements in equation (72) and find the derivative. Before that, we need to define some set of notations that will be used further

- $(\mu\xi_1) = \mu\xi_1 + \xi\mu_1$
- $(\mu\xi_2) = \mu\xi_2 + \xi\mu_2$
- $(\mu\xi_3) = \mu\xi_3 + \xi\mu_3$
- $(\mu\xi_4) = \mu\xi_4 + \xi\mu_4$
- $(\mu\xi_5) = \mu\xi_5 + \xi\mu_5$
- $(\mu\xi_6) = \mu\xi_6 + \xi\mu_6$

- $\chi\mu\xi_1 = \mu\chi\xi_1 + \chi\mu\xi_1 + \chi\xi\mu_1 + \mu\xi\chi_1 + \xi\mu\chi_1 + \xi\chi\mu_1$
- $\chi\mu\xi_2 = \mu\chi\xi_2 + \chi\mu\xi_2 + \chi\xi\mu_2 + \mu\xi\chi_2 + \xi\mu\chi_2 + \xi\chi\mu_2$
- $\chi\mu\xi_3 = \mu\chi\xi_3 + \chi\mu\xi_3 + \chi\xi\mu_3 + \mu\xi\chi_3 + \xi\mu\chi_3 + \xi\chi\mu_3$
- $\chi\mu\xi_4 = \mu\chi\xi_4 + \chi\mu\xi_4 + \chi\xi\mu_4 + \mu\xi\chi_4 + \xi\mu\chi_4 + \xi\chi\mu_4$
- $\chi\mu\xi_5 = \mu\chi\xi_5 + \chi\mu\xi_5 + \chi\xi\mu_5 + \mu\xi\chi_5 + \xi\mu\chi_5 + \xi\chi\mu_5$
- $\chi\mu\xi_6 = \mu\chi\xi_6 + \chi\mu\xi_6 + \chi\xi\mu_6 + \mu\xi\chi_6 + \xi\mu\chi_6 + \xi\chi\mu_6$

- $\mu_1 = \operatorname{tr}[A_{kl}^{-1}YA_{kl}^{-1}w_l w_k']$
- $\mu_2 = \operatorname{tr}[A_{kl}^{-1}YA_{kl}^{-1}v_l v_k']$
- $\mu_3 = \operatorname{tr}[A_{kl}^{-1}YA_{kl}^{-1}w_l v_l']$
- $\mu_4 = \operatorname{tr}[A_{kl}^{-1}YA_{kl}^{-1}w_k v_k']$
- $\mu_5 = \operatorname{tr}[A_{kl}^{-1}YA_{kl}^{-1}v_l w_k']$
- $\mu_6 = \operatorname{tr}[A_{kl}^{-1}YA_{kl}^{-1}w_l v_k']$

- $\chi_1 = \operatorname{tr}[A_{kl}^{-1}XA_{kl}^{-1}w_l w_k']$

- $\chi_2 = \mathrm{tr}[A_{kl}^{-1} X A_{kl}^{-1} v_l v_k']$
- $\chi_3 = \mathrm{tr}[A_{kl}^{-1} X A_{kl}^{-1} w_l v_l']$
- $\chi_4 = \mathrm{tr}[A_{kl}^{-1} X A_{kl}^{-1} w_k v_k']$
- $\chi_5 = \mathrm{tr}[A_{kl}^{-1} X A_{kl}^{-1} v_l w_k']$
- $\chi_6 = \mathrm{tr}[A_{kl}^{-1} X A_{kl}^{-1} w_l v_k']$

- $\mu\chi_1 = \mathrm{tr}[A_{kl}^{-1} Y A_{kl}^{-1} X A_{kl}^{-1} w_l w_k']$
- $\mu\chi_2 = \mathrm{tr}[A_{kl}^{-1} Y A_{kl}^{-1} X A_{kl}^{-1} v_l v_k']$
- $\mu\chi_3 = \mathrm{tr}[A_{kl}^{-1} Y A_{kl}^{-1} X A_{kl}^{-1} w_l v_l']$
- $\mu\chi_4 = \mathrm{tr}[A_{kl}^{-1} Y A_{kl}^{-1} X A_{kl}^{-1} w_k v_k']$
- $\mu\chi_5 = \mathrm{tr}[A_{kl}^{-1} Y A_{kl}^{-1} X A_{kl}^{-1} v_l w_k']$
- $\mu\chi_6 = \mathrm{tr}[A_{kl}^{-1} Y A_{kl}^{-1} X A_{kl}^{-1} w_l v_k']$

- $\mu\xi_1 = \mathrm{tr}[A_{kl}^{-1} Y A_{kl}^{-1} \xi A_{kl}^{-1} w_l w_k']$
- $\mu\xi_2 = \mathrm{tr}[A_{kl}^{-1} Y A_{kl}^{-1} \xi A_{kl}^{-1} v_l v_k']$
- $\mu\xi_3 = \mathrm{tr}[A_{kl}^{-1} Y A_{kl}^{-1} \xi A_{kl}^{-1} w_l v_l']$
- $\mu\xi_4 = \mathrm{tr}[A_{kl}^{-1} Y A_{kl}^{-1} \xi A_{kl}^{-1} w_k v_k']$
- $\mu\xi_5 = \mathrm{tr}[A_{kl}^{-1} Y A_{kl}^{-1} \xi A_{kl}^{-1} v_l w_k']$
- $\mu\xi_6 = \mathrm{tr}[A_{kl}^{-1} Y A_{kl}^{-1} \xi A_{kl}^{-1} w_l v_k']$

- $\mu\chi\xi_1 = \mathrm{tr}[A_{kl}^{-1} Y A_{kl}^{-1} X A_{kl}^{-1} J_{ij} A_{kl}^{-1} w_l w_k']$
- $\mu\chi\xi_2 = \mathrm{tr}[A_{kl}^{-1} Y A_{kl}^{-1} X A_{kl}^{-1} J_{ij} A_{kl}^{-1} v_l v_k']$
- $\mu\chi\xi_3 = \mathrm{tr}[A_{kl}^{-1} Y A_{kl}^{-1} X A_{kl}^{-1} J_{ij} A_{kl}^{-1} w_l v_l']$
- $\mu\chi\xi_4 = \mathrm{tr}[A_{kl}^{-1} Y A_{kl}^{-1} X A_{kl}^{-1} J_{ij} A_{kl}^{-1} w_k v_k']$
- $\mu\chi\xi_5 = \mathrm{tr}[A_{kl}^{-1} Y A_{kl}^{-1} X A_{kl}^{-1} J_{ij} A_{kl}^{-1} v_l w_k']$
- $\mu\chi\xi_6 = \mathrm{tr}[A_{kl}^{-1} Y A_{kl}^{-1} X A_{kl}^{-1} J_{ij} A_{kl}^{-1} w_l v_k']$

- $\mathrm{tr}[YXJ] = \mathrm{tr}[A_{kl}^{-1} Y A_{kl}^{-1} X A_{kl}^{-1} J_{ij}], \quad \mathrm{tr}[XYJ] = \mathrm{tr}[XYJ] + \mathrm{tr}[YXJ],$

Now, using these notations we substitute the value $A_{kl} \equiv A_{kl}+\alpha X$ everywhere for the matrix elements in equation (72) and find the derivative for each three cases separately as it is done below:

case $(x_{i_k}x_{j_k}|x_{i_l}x_{j_l})$

$$-\frac{\partial}{\partial\alpha}\frac{\pi^{(3n-1)/2}}{2\,|A_{kl}+\alpha X|^{3/2}}\left(\frac{\gamma_1\gamma_2+\gamma_3\gamma_4+\gamma_5\gamma_6}{\omega^{1/2}}-\frac{\gamma_1\rho_1+\gamma_2\rho_2+\gamma_3\rho_3+\gamma_4\rho_4+\gamma_5\rho_5+\gamma_6\rho_6}{3\omega^{3/2}}\right.$$

$$\left.+\frac{\rho_1\rho_2+\rho_3\rho_4+\rho_5\rho_6}{5\omega^{5/2}}\right)\Rightarrow$$

$$\left\langle\phi_k\left|\frac{\boldsymbol{r}'\boldsymbol{X}\boldsymbol{r}}{r_{ij}}\right|\phi_l\right\rangle=\frac{\pi^{(3n-1)/2}}{2|A_{kl}|^{3/2}}\left[\left(\frac{3}{2}\,\mathrm{tr}[A_{kl}^{-1}X]\right)\left(\frac{\gamma}{\omega^{1/2}}-\frac{\gamma\rho}{3\omega^{3/2}}+\frac{\rho}{5\omega^{5/2}}\right)-\frac{\gamma\,\mathrm{tr}[XJ]}{2\omega^{3/2}}\right.$$

$$+\frac{(\gamma\xi)}{\omega^{1/2}}+\frac{(\gamma\rho)\,\mathrm{tr}[XJ]}{2\omega^{5/2}}-\frac{\chi_2\rho_1+\chi_1\rho_2+\chi_4\rho_3+\chi_3\rho_4+\chi_6\rho_5+\chi_5\rho_6+\gamma(\chi\xi)}{3\omega^{3/2}}$$

$$\left.-\frac{\rho\,\mathrm{tr}[XJ]}{2\omega^{7/2}}+\frac{\rho_2(\chi\xi_1)+\rho_1(\chi\xi_2)+\rho_4(\chi\xi_3)+\rho_3(\chi\xi_4)+\rho_6(\chi\xi_5)+\rho_5(\chi\xi_6)}{5\omega^{5/2}}\right]. \tag{157}$$

In this case, we defined the following notations:

- $\gamma\xi=\gamma_1\chi_1+\gamma_2\chi_2+\gamma_3\chi_3+\gamma_4\chi_4+\gamma_5\chi_5+\gamma_6\chi_6$,
- $\gamma\mu=\gamma_1\mu_1+\gamma_2\mu_2+\gamma_3\mu_3+\gamma_4\mu_4+\gamma_5\mu_5+\gamma_6\mu_6$,
- $\gamma\rho=\gamma_1\rho_1+\gamma_2\rho_2+\gamma_3\rho_3+\gamma_4\rho_4+\gamma_5\rho_5+\gamma_6\rho_6$,
- $\gamma(\chi\xi)=\gamma_1(\chi\xi_1)+\gamma_2(\chi\xi_2)+\gamma_3(\chi\xi_3)+\gamma_4(\chi\xi_4)+\gamma_5(\chi\xi_5)+\gamma_6(\chi\xi_6)$,
- $\gamma(\mu\xi)=\gamma_1(\mu\xi_1)+\gamma_2(\mu\xi_2)+\gamma_3(\mu\xi_3)+\gamma_4(\mu\xi_4)+\gamma_5(\mu\xi_5)+\gamma_6(\mu\xi_6)$,
- $\gamma(\mu\chi)=\gamma_1(\mu\chi_1)+\gamma_2(\mu\chi_2)+\gamma_3(\mu\chi_3)+\gamma_4(\mu\chi_4)+\gamma_5(\mu\chi_5)+\gamma_6(\mu\chi_6)$.

case $(x_{i_k}y_{j_k}|y_{i_l}x_{j_l})$

$$-\frac{\partial}{\partial\alpha}\frac{\pi^{(3n-1)/2}}{2\left|A_{kl}+\alpha X\right|^{3/2}}\left(\frac{\gamma_1\gamma_2}{\omega^{1/2}}-\frac{\gamma_1\rho_1+\gamma_2\rho_2}{3\omega^{3/2}}+\frac{\rho_1\rho_2}{5\omega^{5/2}}\right)\Rightarrow$$

$$\left\langle\phi_k\left|\frac{\boldsymbol{r}'\boldsymbol{X}\boldsymbol{r}}{r_{ij}}\right|\phi_l\right\rangle=\frac{\pi^{(3n-1)/2}}{2|A_{kl}|^{3/2}}\left[\left(\frac{3}{2}\operatorname{tr}[A_{kl}^{-1}X]\right)\left(\frac{\gamma_1\gamma_2}{\omega^{1/2}}-\frac{\gamma\rho}{3\omega^{3/2}}+\frac{\rho_1\rho_2}{5\omega^{5/2}}\right)\right.$$

$$-\frac{\gamma_1\gamma_2\operatorname{tr}[XJ]}{2\omega^{3/2}}+\frac{(\gamma\xi)}{\omega^{1/2}}+\frac{(\gamma\rho)\operatorname{tr}[XJ]}{2\omega^{5/2}}$$

$$\left.-\frac{\chi_2\rho_1+\chi_1\rho_2+\gamma(\chi\xi)}{3\omega^{3/2}}-\frac{\rho_1\rho_2\operatorname{tr}[XJ]}{2\omega^{7/2}}+\frac{\rho_2(\chi\xi_1)+\rho_1(\chi\xi_2)}{5\omega^{5/2}}\right]. \tag{158}$$

In this case, we defined the following notations:

- $\gamma\xi=\gamma_1\chi_1+\gamma_2\chi_2,\quad \gamma\mu=\gamma_1\mu_1+\gamma_2\mu_2,$
- $\gamma\rho=\gamma_1\rho_1+\gamma_2\rho_2,\quad \gamma(\chi\xi)=\gamma_1(\chi\xi_1)+\gamma_2(\chi\xi_2),$
- $\gamma(\mu\xi)=\gamma_1(\mu\xi_1)+\gamma_2(\mu\xi_2),\quad \gamma(\mu\chi)=\gamma_1(\mu\chi_1)+\gamma_2(\mu\chi_2).$

case $(x_{i_k}x_{j_k}|y_{i_l}y_{j_l})$

$$-\frac{\partial}{\partial\alpha}\frac{\pi^{(3n-1)/2}}{2\left|A_{kl}+\alpha X\right|^{3/2}}\left(\frac{\gamma_3\gamma_4}{\omega^{1/2}}-\frac{\gamma_3\rho_3+\gamma_4\rho_4}{3\omega^{3/2}}+\frac{\rho_3\rho_4}{5\omega^{5/2}}\right)\Rightarrow$$

$$\left\langle\phi_k\left|\frac{\boldsymbol{r}'\boldsymbol{X}\boldsymbol{r}}{r_{ij}}\right|\phi_l\right\rangle=\frac{\pi^{(3n-1)/2}}{2|A_{kl}|^{3/2}}\left[\left(\frac{3}{2}\operatorname{tr}[A_{kl}^{-1}X]\right)\left(\frac{\gamma_3\gamma_4}{\omega^{1/2}}-\frac{\gamma\rho}{3\omega^{3/2}}+\frac{\rho_3\rho_4}{5\omega^{5/2}}\right)\right.$$

$$-\frac{\gamma_3\gamma_4\operatorname{tr}[XJ]}{2\omega^{3/2}}+\frac{(\gamma\xi)}{\omega^{1/2}}+\frac{(\gamma\rho)\operatorname{tr}[XJ]}{2\omega^{5/2}}$$

$$\left.-\frac{\chi_4\rho_3+\chi_3\rho_4+\gamma(\chi\xi)}{3\omega^{3/2}}-\frac{\rho_3\rho_4\operatorname{tr}[XJ]}{2\omega^{7/2}}+\frac{\rho_2(\chi\xi_1)+\rho_1(\chi\xi_2)}{5\omega^{5/2}}\right]. \tag{159}$$

In this case, we defined the following notations:

- $\gamma\chi=\gamma_3\chi_3+\gamma_4\chi_4,\quad \gamma\mu=\gamma_3\mu_3+\gamma_4\mu_4,$
- $\gamma\rho=\gamma_3\rho_3+\gamma_4\rho_4,\quad \gamma(\chi\xi)=\gamma_3(\chi\xi_3)+\gamma_4(\chi\xi_4),$
- $\gamma(\mu\xi)=\gamma_3(\mu\xi_3)+\gamma_4(\mu\xi_4),\quad \gamma(\mu\chi)=\gamma_3(\mu\chi_3)+\gamma_4(\mu\chi_4).$

Integral $\left\langle \phi_k \left| \frac{(\boldsymbol{r}'\boldsymbol{X}\boldsymbol{r})(\boldsymbol{r}'\boldsymbol{Y}\boldsymbol{r})}{r_{ij}} \right| \phi_l \right\rangle$

As we did in the previous subsection, we just substitute the value $A_{kl} \equiv A_{kl} + \alpha Y$ everywhere in the matrix elements of integral $\left\langle \phi_k \left| \frac{\boldsymbol{r}'\boldsymbol{X}\boldsymbol{r}}{r_{ij}} \right| \phi_l \right\rangle$ and find the derivative. First, we present the examples of useful derivatives below:

1. $\frac{\partial}{\partial\alpha}|A_{kl} + \alpha Y|^{-3/2} = -\frac{3}{2}|A_{kl}|^{-3/2}\,\mathrm{tr}[A_{kl}^{-1}Y]$,
2. $\frac{\partial}{\partial\alpha}\,\mathrm{tr}[(A_{kl} + \alpha Y)^{-1}X] = -\,\mathrm{tr}[A_{kl}^{-1}YA_{kl}^{-1}X] = -\,\mathrm{tr}[YX]$,
3. $\frac{\partial}{\partial\alpha}\frac{1}{c^{p/2}} = \frac{\partial}{\partial\alpha}\left(\mathrm{tr}[(A_{kl} + \alpha Y)^{-1}J_{ij}]\right)^{-p/2} = \frac{p}{2}\frac{\mathrm{tr}[A_{kl}^{-1}YA_{kl}^{-1}J_{ij}]}{\mathrm{tr}[A_{kl}^{-1}J_{ij}]^{(p+1)/2}}$, where p is the odd integer.
4. $\frac{\partial}{\partial\alpha}\gamma_1 = \frac{\partial}{\partial\alpha}\,\mathrm{tr}[(A_{kl} + \alpha Y)^{-1}v_lv_k'] = -\,\mathrm{tr}[A_{kl}^{-1}YA_{kl}^{-1}v_lv_k'] = -\mu_2$,
5. $\frac{\partial}{\partial\alpha}\gamma_2 = -\mu_1$,
6. $\frac{\partial}{\partial\alpha}\mu_2 = \frac{\partial}{\partial\alpha}\,\mathrm{tr}[(A_{kl} + \alpha Y)^{-1}J_{ij}(A_{kl} + \alpha Y)^{-1}v_lv_k'] = -\,\mathrm{tr}[A_{kl}^{-1}YA_{kl}^{-1}J_{ij}A_{kl}^{-1}v_lv_k' + A_{kl}^{-1}J_{ij}A_{kl}^{-1}YA_{kl}^{-1}v_lv_k'] = -\mu\xi_2 - \xi\mu_2$,
7. $\frac{\partial}{\partial\alpha}\mu_1 = -\mu\xi_1 - \xi\mu_1$,
8. $\frac{\partial}{\partial\alpha}\chi_2 = \frac{\partial}{\partial\alpha}\,\mathrm{tr}[(A_{kl} + \alpha Y)^{-1}X(A_{kl} + \alpha Y)^{-1}v_lv_k'] = -\,\mathrm{tr}[A_{kl}^{-1}YA_{kl}^{-1}XA_{kl}^{-1}v_lv_k' + A_{kl}^{-1}XA_{kl}^{-1}YA_{kl}^{-1}v_lv_k'] = -\mu\chi_2 - \chi\mu_2$,
9. $\frac{\partial}{\partial\alpha}\chi_1 = -\mu\chi_1 - \chi\mu_1$,
10. $\frac{\partial}{\partial\alpha}\,\mathrm{tr}[XJ] = \frac{\partial}{\partial\alpha}\,\mathrm{tr}[(A_{kl} + \alpha Y)^{-1}X(A_{kl} + \alpha Y)^{-1}J_{ij}] = -\,\mathrm{tr}[A_{kl}^{-1}YA_{kl}^{-1}XA_{kl}^{-1}J_{ij} + A_{kl}^{-1}XA_{kl}^{-1}YA_{kl}^{-1}J_{ij}] = -\,\mathrm{tr}[YXJ] - \mathrm{tr}[XYJ]$,
11. $\frac{\partial}{\partial\alpha}\chi\xi_2 = \frac{\partial}{\partial\alpha}\,\mathrm{tr}[(A_{kl} + \alpha Y)^{-1}X(A_{kl} + \alpha Y)^{-1}J_{ij}(A_{kl} + \alpha Y)^{-1}v_lv_k'] = -\,\mathrm{tr}[A_{kl}^{-1}YA_{kl}^{-1}XA_{kl}^{-1}J_{ij}A_{kl}^{-1}v_lv_k' + A_{kl}^{-1}XA_{kl}^{-1}YA_{kl}^{-1}J_{ij}A_{kl}^{-1}v_lv_k' + A_{kl}^{-1}XA_{kl}^{-1}J_{ij}A_{kl}^{-1}YA_{kl}^{-1}v_lv_k'] = -\mu\chi\xi_2 - \chi\mu\xi_2 - \chi\xi\mu_2$,
12. $\frac{\partial}{\partial\alpha}\chi\xi_1 = -\mu\chi\xi_1 - \chi\mu\xi_1 - \chi\xi\mu_1$.

Now, using the notations defined in 10.3, we substitute the value $A_{kl} \equiv A_{kl} + \alpha Y$ everywhere for the results of integral $\left\langle \phi_k \left| \frac{\boldsymbol{r}'\boldsymbol{X}\boldsymbol{r}}{r_{ij}} \right| \phi_l \right\rangle$ in the previous subsection and find the derivative for each three cases separately as it is done below:

case $(x_{i_k}x_{j_k}|x_{i_l}x_{j_l})$

$$-\frac{\partial}{\partial\alpha}\frac{\pi^{(3n-1)/2}}{2|A_{kl}+\alpha Y|^{3/2}}\left[\left(\frac{3}{2}\operatorname{tr}[(A_{kl}+\alpha Y)^{-1}X]\right)\left(\frac{\gamma}{\omega^{1/2}}-\frac{\kappa}{3\omega^{3/2}}+\frac{\rho}{5\omega^{5/2}}\right)\right.$$

$$-\frac{\gamma\operatorname{tr}[XJ]}{2\omega^{3/2}}+\frac{(\gamma_1\chi_1+\gamma_2\chi_2+\gamma_3\chi_3+\gamma_4\chi_4+\gamma_5\chi_5+\gamma_6\chi_6)}{\omega^{1/2}}+\frac{\kappa\operatorname{tr}[XJ]}{2\omega^{5/2}}$$

$$-\frac{\chi_2\rho_1+\chi_1\rho_2+\gamma_1\chi\xi_1+\gamma_1\xi\chi_1+\gamma_2\chi\xi_2+\gamma_2\xi\chi_2}{3\omega^{3/2}}-\frac{\rho\operatorname{tr}[XJ]}{2\omega^{7/2}}$$

$$-\frac{\chi_4\rho_3+\chi_3\rho_4+\gamma_3\chi\xi_3+\gamma_3\xi\chi_3+\gamma_4\chi\xi_4+\gamma_4\xi\chi_4}{3\omega^{3/2}}$$

$$-\frac{\chi_6\rho_5+\chi_5\rho_6+\gamma_5\chi\xi_5+\gamma_5\xi\chi_5+\gamma_6\chi\xi_6+\gamma_6\xi\chi_6}{3\omega^{3/2}}$$

$$+\frac{\rho_2(\chi\xi_1+\xi\chi_1)+\rho_1(\chi\xi_2+\xi\chi_2)}{5\omega^{5/2}}+\frac{\rho_4(\chi\xi_3+\xi\chi_3)+\rho_3(\chi\xi_4+\xi\chi_4)}{5\omega^{5/2}}$$

$$\left.+\frac{\rho_6(\chi\xi_5+\xi\chi_5)+\rho_5(\chi\xi_6+\xi\chi_6)}{5\omega^{5/2}}\right]\Rightarrow\left\langle\phi_k\left|\frac{(\boldsymbol{r}'\boldsymbol{X}\boldsymbol{r})(\boldsymbol{r}'\boldsymbol{Y}\boldsymbol{r})}{r_{ij}}\right|\phi_l\right\rangle$$

$$=\frac{3}{2}\operatorname{tr}[A_{kl}^{-1}Y]\left\langle\phi_k\left|\frac{(\boldsymbol{r}'\boldsymbol{X}\boldsymbol{r})}{r_{ij}}\right|\phi_l\right\rangle-\frac{\pi^{(3n-1)/2}}{2|A_{kl}|^{3/2}}\left[\left(-\frac{3}{2}\operatorname{tr}[YX]\right)\left(\frac{\gamma}{\omega^{1/2}}-\frac{\gamma\rho}{3\omega^{3/2}}+\frac{\rho}{5\omega^{5/2}}\right)\right.$$

$$+\frac{3}{2}\operatorname{tr}[A_{kl}^{-1}X]\left(\frac{1}{2}\frac{\operatorname{tr}[YJ]}{\omega^{3/2}}\gamma-\frac{\gamma\mu}{\omega^{1/2}}-\frac{1}{2}\frac{\operatorname{tr}[YJ]}{\omega^{5/2}}(\gamma\rho)+\frac{\mu_2\rho_1+\mu_1\rho_2+\mu_4\rho_3+\mu_3\rho_4+\mu_6\rho_5+\mu_5\rho_6+\gamma(\mu\xi)}{3\omega^{3/2}}\right.$$

$$\left.\left.+\frac{\operatorname{tr}[YJ]}{2\omega^{7/2}}\rho-\frac{\rho_2(\mu\xi_1)+\rho_1(\mu\xi_2)+\rho_4(\mu\xi_3)+\rho_3(\mu\xi_4)+\rho_6(\mu\xi_5)+\rho_5(\mu\xi_6)}{5\omega^{5/2}}\right)\right.$$

$$-\frac{3\gamma\operatorname{tr}[XJ]\operatorname{tr}[YJ]}{4\omega^{5/2}}+\frac{(\gamma\xi)\operatorname{tr}[YJ]}{2\omega^{3/2}}+\frac{\gamma\mu\operatorname{tr}[XJ]+\gamma(\operatorname{tr}[XYJ])}{2\omega^{3/2}}$$

$$-\frac{\mu_2\chi_1+\mu_1\chi_2+\mu_4\chi_3+\mu_3\chi_4+\mu_6\chi_5+\mu_5\chi_6+\gamma(\mu\chi)}{\omega^{1/2}}+\frac{5(\gamma\rho)\operatorname{tr}[XJ]\operatorname{tr}[YJ]}{4\omega^{7/2}}$$

$$-\frac{(\gamma\rho)(\mathrm{tr}[XYJ])+\mathrm{tr}[XJ](\mu_2\rho_1+\mu_1\rho_2+\mu_4\rho_3+\mu_3\rho_4+\mu_6\rho_5+\mu_5\rho_6+\gamma(\mu\xi))}{2\omega^{5/2}}$$

$$-\frac{\mathrm{tr}[YJ](\chi_2\rho_1+\chi_1\rho_2+\chi_4\rho_3+\chi_3\rho_4+\chi_6\rho_5+\chi_5\rho_6+\gamma(\chi\xi))}{2\omega^{5/2}}$$

$$+\frac{1}{3\omega^{3/2}}\Bigg(\rho_1(\mu\chi_2)+\chi_2(\mu\xi_1)+\rho_2(\mu\chi_1)+\chi_1(\mu\xi_2)+\mu_2(\chi\xi_1)+\mu_1(\chi\xi_2)+\gamma_1(\chi\mu\xi_1)$$

$$+\gamma_2(\chi\mu\xi_2)\Bigg)+\frac{1}{3\omega^{3/2}}\Bigg(\rho_3(\mu\chi_4)+\chi_4(\mu\xi_3)+\rho_4(\mu\chi_3)+\chi_3(\mu\xi_4)$$

$$+\mu_4(\chi\xi_3)+\mu_3(\chi\xi_4)+\gamma_3(\chi\mu\xi_3)+\gamma_4(\chi\mu\xi_4)\Bigg)$$

$$+\frac{1}{3\omega^{3/2}}\Bigg(\rho_5(\mu\chi_6)+\chi_6(\mu\xi_5)+\rho_6(\mu\chi_5)+\chi_5(\mu\xi_6)+\mu_6(\chi\xi_5)$$

$$+\mu_5(\chi\xi_6)+\gamma_5(\chi\mu\xi_5)+\gamma_6(\chi\mu\xi_6)\Bigg)-\frac{7\,\mathrm{tr}[YJ]\,\mathrm{tr}[XJ]\rho}{4\omega^{9/2}}$$

$$+\frac{\rho(\mathrm{tr}[XYJ])+\mathrm{tr}[XJ](\rho_1(\mu\xi_2)+\rho_2(\mu\xi_1)+\rho_3(\mu\xi_4)+\rho_4(\mu\xi_3)+\rho_5(\mu\xi_6)+\rho_6(\mu\xi_5))}{2\omega^{7/2}}$$

$$+\frac{\mathrm{tr}[YJ]}{2\omega^{7/2}}\left[\rho_2(\chi\xi_1)+\rho_1(\chi\xi_2)+\rho_4(\chi\xi_3)+\rho_3(\chi\xi_4)+\rho_6(\chi\xi_5)+\rho_5(\chi\xi_6)\right]$$

$$-\frac{1}{5\omega^{5/2}}\Bigg((\chi\xi_1)(\mu\xi_2)+(\chi\xi_2)(\mu\xi_1)+\rho_2(\chi\mu\xi_1)+\rho_1(\chi\mu\xi_2)\Bigg)$$

$$-\frac{1}{5\omega^{5/2}}\Bigg((\chi\xi_3)(\mu\xi_4)+(\chi\xi_4)(\mu\xi_3)+\rho_4(\chi\mu\xi_3)+\rho_3(\chi\mu\xi_4)\Bigg)$$

$$-\frac{1}{5\omega^{5/2}}\Bigg((\chi\xi_5)(\mu\xi_6)+(\chi\xi_6)(\mu\xi_5)+\rho_6(\chi\mu\xi_5)+\rho_5(\chi\mu\xi_6)\Bigg)\Bigg]. \tag{160}$$

case $(x_{i_k}y_{j_k}|y_{i_l}x_{j_l})$

$$-\frac{\partial}{\partial\alpha}\frac{\pi^{(3n-1)/2}}{2|A_{kl}+\alpha Y|^{3/2}}\Bigg[\left(\frac{3}{2}\operatorname{tr}[(A_{kl}+\alpha Y)^{-1}X]\right)\left(\frac{\gamma_1\gamma_2}{\omega^{1/2}}-\frac{\gamma_1\rho_1+\gamma_2\rho_2}{3\omega^{3/2}}+\frac{\rho_1\rho_2}{5\omega^{5/2}}\right)$$

$$-\frac{\gamma_1\gamma_2\operatorname{tr}[XJ]}{2\omega^{3/2}}+\frac{(\gamma_2\chi_2+\gamma_1\chi_1)}{\omega^{1/2}}+\frac{(\gamma_1\rho_1+\gamma_2\rho_2)\operatorname{tr}[XJ]}{2\omega^{5/2}}$$

$$-\frac{\chi_2\rho_1+\chi_1\rho_2+\gamma_1\chi\xi_1+\gamma_1\xi\chi_1+\gamma_2\chi\xi_2+\gamma_2\xi\chi_2}{3\omega^{3/2}}-\frac{\rho_1\rho_2\operatorname{tr}[XJ]}{2\omega^{7/2}}$$

$$+\frac{\rho_2(\chi\xi_1+\xi\chi_1)+\rho_1(\chi\xi_2+\xi\chi_2)}{5\omega^{5/2}}\Bigg]\Rightarrow\left\langle\phi_k\left|\frac{(\boldsymbol{r}'\boldsymbol{X}\boldsymbol{r})(\boldsymbol{r}'\boldsymbol{Y}\boldsymbol{r})}{r_{ij}}\right|\phi_l\right\rangle$$

$$=\frac{3}{2}\operatorname{tr}[A_{kl}^{-1}Y]\left\langle\phi_k\left|\frac{(\boldsymbol{r}'\boldsymbol{X}\boldsymbol{r})}{r_{ij}}\right|\phi_l\right\rangle-\frac{\pi^{(3n-1)/2}}{2|A_{kl}|^{3/2}}\Bigg[\left(-\frac{3}{2}\operatorname{tr}[YX]\right)\left(\frac{\gamma_1\gamma_2}{\omega^{1/2}}-\frac{\gamma\rho}{3\omega^{3/2}}+\frac{\rho_1\rho_2}{5\omega^{5/2}}\right)$$

$$+\frac{3}{2}\operatorname{tr}[A_{kl}^{-1}X]\left(\frac{1}{2}\frac{\operatorname{tr}[YJ]}{\omega^{3/2}}\gamma_1\gamma_2-\frac{\gamma\mu}{\omega^{1/2}}-\frac{1}{2}\frac{\operatorname{tr}[YJ]}{\omega^{5/2}}(\gamma\rho)+\frac{\mu_2\rho_1+\mu_1\rho_2+\gamma(\mu\xi)}{3\omega^{3/2}}\right.$$

$$\left.+\frac{\operatorname{tr}[YJ]}{2\omega^{7/2}}\rho_1\rho_2-\frac{\rho_2(\mu\xi_1)+\rho_1(\mu\xi_2)}{5\omega^{5/2}}\right)-\frac{3\gamma_1\gamma_2\operatorname{tr}[XJ]\operatorname{tr}[YJ]}{4\omega^{5/2}}+\frac{(\gamma\xi)\operatorname{tr}[YJ]}{2\omega^{3/2}}$$

$$+\frac{\gamma\mu\operatorname{tr}[XJ]+\gamma_1\gamma_2(\operatorname{tr}[XYJ])}{2\omega^{3/2}}-\frac{\mu_2\chi_1+\mu_1\chi_2+\gamma(\mu\chi)}{\omega^{1/2}}+\frac{5(\gamma\rho)\operatorname{tr}[XJ]\operatorname{tr}[YJ]}{4\omega^{7/2}}$$

$$-\frac{(\gamma\rho)(\operatorname{tr}[XYJ])+\operatorname{tr}[XJ](\mu_2\rho_1+\mu_1\rho_2+\gamma(\mu\xi))}{2\omega^{5/2}}-\frac{\operatorname{tr}[YJ](\chi_2\rho_1+\chi_1\rho_2+\gamma(\chi\xi))}{2\omega^{5/2}}$$

$$+\frac{1}{3\omega^{3/2}}\Bigg(\rho_1(\mu\chi_2)+\chi_2(\mu\xi_1)+\rho_2(\mu\chi_1)+\chi_1(\mu\xi_2)+\mu_2(\chi\xi_1)+\mu_1(\chi\xi_2)+\gamma_1(\chi\mu\xi_1)$$

$$+\gamma_2(\chi\mu\xi_2)\Bigg)-\frac{7\operatorname{tr}[YJ]\operatorname{tr}[XJ]\rho_1\rho_2}{4\omega^{9/2}}+\frac{\rho_1\rho_2(\operatorname{tr}[XYJ])+\operatorname{tr}[XJ](\rho_1(\mu\xi_2)+\rho_2(\mu\xi_1))}{2\omega^{7/2}}$$

$$+\frac{\operatorname{tr}[YJ]}{2\omega^{7/2}}\left[\rho_2(\chi\xi_1)+\rho_1(\chi\xi_2)\right]-\frac{1}{5\omega^{5/2}}\Bigg((\chi\xi_1)(\mu\xi_2)+(\chi\xi_2)(\mu\xi_1)+\rho_2(\chi\mu\xi_1)+\rho_1(\chi\mu\xi_2)\Bigg)\Bigg]. \tag{161}$$

case $(x_{i_k}x_{j_k}|y_{i_l}y_{j_l})$

$$-\frac{\partial}{\partial\alpha}\frac{\pi^{(3n-1)/2}}{2|A_{kl}+\alpha Y|^{3/2}}\Bigg[\left(\frac{3}{2}\operatorname{tr}[(A_{kl}+\alpha Y)^{-1}X]\right)\left(\frac{\gamma_3\gamma_4}{\omega^{1/2}}-\frac{\gamma_3\rho_3+\gamma_4\rho_4}{3\omega^{3/2}}+\frac{\rho_3\rho_4}{5\omega^{5/2}}\right)$$

$$-\frac{\gamma_3\gamma_4\operatorname{tr}[XJ]}{2\omega^{3/2}}+\frac{(\gamma_4\chi_4+\gamma_3\chi_3)}{\omega^{1/2}}+\frac{(\gamma_3\rho_3+\gamma_4\rho_4)\operatorname{tr}[XJ]}{2\omega^{5/2}}$$

$$-\frac{\chi_4\rho_3+\chi_3\rho_4+\gamma_3\chi\xi_3+\gamma_3\xi\chi_3+\gamma_4\chi\xi_4+\gamma_4\xi\chi_4}{3\omega^{3/2}}-\frac{\rho_3\rho_4\operatorname{tr}[XJ]}{2\omega^{7/2}}$$

$$+\frac{\rho_4(\chi\xi_3+\xi\chi_3)+\rho_3(\chi\xi_4+\xi\chi_4)}{5\omega^{5/2}}\Bigg]\Rightarrow\left\langle\phi_k\left|\frac{(\boldsymbol{r}'\boldsymbol{X}\boldsymbol{r})(\boldsymbol{r}'\boldsymbol{Y}\boldsymbol{r})}{r_{ij}}\right|\phi_l\right\rangle$$

$$=\frac{3}{2}\operatorname{tr}[A_{kl}^{-1}Y]\left\langle\phi_k\left|\frac{(\boldsymbol{r}'\boldsymbol{X}\boldsymbol{r})}{r_{ij}}\right|\phi_l\right\rangle-\frac{\pi^{(3n-1)/2}}{2|A_{kl}|^{3/2}}\Bigg[\left(-\frac{3}{2}\operatorname{tr}[YX]\right)\left(\frac{\gamma_3\gamma_4}{\omega^{1/2}}-\frac{\gamma\rho}{3\omega^{3/2}}+\frac{\rho_3\rho_4}{5\omega^{5/2}}\right)$$

$$+\frac{3}{2}\operatorname{tr}[A_{kl}^{-1}X]\left(\frac{1}{2}\frac{\operatorname{tr}[YJ]}{\omega^{3/2}}\gamma_3\gamma_4-\frac{\gamma\mu}{\omega^{1/2}}-\frac{1}{2}\frac{\operatorname{tr}[YJ]}{\omega^{5/2}}(\gamma\rho)+\frac{\mu_4\rho_3+\mu_3\rho_4+\gamma(\mu\xi)}{3\omega^{3/2}}\right.$$

$$\left.+\frac{\operatorname{tr}[YJ]}{2\omega^{7/2}}\rho_3\rho_4-\frac{\rho_4(\mu\xi_3)+\rho_3(\mu\xi_4)}{5\omega^{5/2}}\right)-\frac{3\gamma_3\gamma_4\operatorname{tr}[XJ]\operatorname{tr}[YJ]}{4\omega^{5/2}}+\frac{(\gamma\xi)\operatorname{tr}[YJ]}{2\omega^{3/2}}$$

$$+\frac{\gamma\mu\operatorname{tr}[XJ]+\gamma_3\gamma_4(\operatorname{tr}[XYJ])}{2\omega^{3/2}}-\frac{\mu_4\chi_3+\mu_3\chi_4+\gamma(\mu\chi)}{\omega^{1/2}}+\frac{5(\gamma\rho)\operatorname{tr}[XJ]\operatorname{tr}[YJ]}{4\omega^{7/2}}$$

$$-\frac{(\gamma\rho)(\operatorname{tr}[XYJ])+\operatorname{tr}[XJ](\mu_4\rho_3+\mu_3\rho_4+\gamma(\mu\xi))}{2\omega^{5/2}}-\frac{\operatorname{tr}[YJ](\chi_4\rho_3+\chi_3\rho_4+\gamma(\chi\xi))}{2\omega^{5/2}}$$

$$+\frac{1}{3\omega^{3/2}}\Bigg(\rho_3(\mu\chi_4)+\chi_4(\mu\xi_3)+\rho_4(\mu\chi_3)+\chi_3(\mu\xi_4)+\mu_4(\chi\xi_3)+\mu_3(\chi\xi_4)+\gamma_3(\chi\mu\xi_3)$$

$$+\gamma_4(\chi\mu\xi_4)\Bigg)-\frac{7\operatorname{tr}[YJ]\operatorname{tr}[XJ]\rho_3\rho_4}{4\omega^{9/2}}+\frac{\rho_3\rho_4(\operatorname{tr}[XYJ])+\operatorname{tr}[XJ](\rho_3(\mu\xi_4)+\rho_4(\mu\xi_3))}{2\omega^{7/2}}$$

$$+\frac{\operatorname{tr}[YJ]}{2\omega^{7/2}}\left[\rho_4(\chi\xi_3)+\rho_3(\chi\xi_4)\right]-\frac{1}{5\omega^{5/2}}\Bigg((\chi\xi_3)(\mu\xi_4)+(\chi\xi_4)(\mu\xi_3)+\rho_4(\chi\mu\xi_3)+\rho_3(\chi\mu\xi_4)\Bigg)\Bigg]. \tag{162}$$

10.4 Integral $\left\langle \phi_k \left| (\mathbf{r'K})^\lambda \left(\boldsymbol{\nabla}' \mathbf{D} \frac{1}{r_g}\right)^\beta (\mathbf{F}\boldsymbol{\nabla})_\beta (\mathbf{G}\boldsymbol{\nabla})_\lambda \right| \phi_l \right\rangle$

$$\begin{aligned} & \left\langle \phi_k \left| (\boldsymbol{r'K})^\lambda \left(\boldsymbol{\nabla}' \boldsymbol{D} \frac{1}{r_g}\right)^\beta (\boldsymbol{F}\boldsymbol{\nabla})_\beta (\boldsymbol{G}\boldsymbol{\nabla})_\lambda \right| \phi_l \right\rangle \\ = & \frac{\partial}{\partial\alpha_k}\frac{\partial}{\partial\alpha_l}\frac{\partial}{\partial\beta_k}\frac{\partial}{\partial\beta_l} \left\langle \varphi_k \left| (\boldsymbol{r'K})^\lambda \left(\boldsymbol{\nabla}' \boldsymbol{D} \frac{1}{r_g}\right)^\beta (\boldsymbol{F}\boldsymbol{\nabla})_\beta (\boldsymbol{G}\boldsymbol{\nabla})_\lambda \right| \varphi_l \right\rangle \Big|_{\alpha_{k,l},\beta_{k,l}=0} . \quad (163) \end{aligned}$$

we rewrite this integral in the following way:

$$\left\langle \varphi_k \left| (\boldsymbol{r'K})^\lambda \left(\boldsymbol{\nabla}' \boldsymbol{D} \frac{1}{r_g}\right)^\beta (\boldsymbol{F}\boldsymbol{\nabla})_\beta (\boldsymbol{G}\boldsymbol{\nabla})_\lambda \right| \varphi_l \right\rangle = -\int \mathrm{d}\boldsymbol{r} \frac{1}{r_g} (\boldsymbol{\nabla}'\boldsymbol{D})^\beta \{\varphi_k (\boldsymbol{r'K})^\lambda (\boldsymbol{F}\boldsymbol{\nabla})_\beta (\boldsymbol{G}\boldsymbol{\nabla})_\lambda \varphi_l\}.$$

The integral can be split into three terms:

$$-\int \mathrm{d}\boldsymbol{r} \frac{1}{r_g} (\boldsymbol{\nabla}'\boldsymbol{D})^\beta \{\varphi_k (\boldsymbol{r'K})^\lambda (\boldsymbol{F}\boldsymbol{\nabla})_\beta (\boldsymbol{G}\boldsymbol{\nabla})_\lambda \varphi_l\}$$

$$= -\int \mathrm{d}\boldsymbol{r} \frac{1}{r_g} \{(\boldsymbol{\nabla}'\boldsymbol{D})^\beta \varphi_k\} (\boldsymbol{r'KG\nabla}) (\boldsymbol{F}\boldsymbol{\nabla})_\beta \varphi_l = \text{first term}$$

$$-\int \mathrm{d}\boldsymbol{r} \frac{1}{r_g} \varphi_k \{(\boldsymbol{\nabla}'\boldsymbol{D})^\beta (\boldsymbol{r'K})^\lambda\} (\boldsymbol{F}\boldsymbol{\nabla})_\beta (\boldsymbol{G}\boldsymbol{\nabla})_\lambda \varphi_l = \text{second term}$$

$$-\int \mathrm{d}\boldsymbol{r} \frac{1}{r_g} \varphi_k (\boldsymbol{r'K})^\lambda \{(\boldsymbol{\nabla}'\boldsymbol{D})^\beta (\boldsymbol{F}\boldsymbol{\nabla})_\beta (\boldsymbol{G}\boldsymbol{\nabla})_\lambda \varphi_l\} = \text{third term}$$

Term 1: $\int \mathrm{d}\boldsymbol{r} \frac{1}{r_g} \{(\boldsymbol{\nabla}'\boldsymbol{D})^\beta \varphi_k\} (\boldsymbol{r'KG\nabla}) (\boldsymbol{F}\boldsymbol{\nabla})_\beta \varphi_l$

$$\{(\boldsymbol{\nabla}'\boldsymbol{D})^\beta \varphi_k\} (\boldsymbol{r'KG\nabla}) (\boldsymbol{F}\boldsymbol{\nabla})_\beta \varphi_l = \{\boldsymbol{D}_\gamma^\beta \partial^\gamma \varphi_k\} [(\boldsymbol{r'KG})^\lambda \boldsymbol{F}_\beta^\rho \partial_\lambda \partial_\rho \varphi_l]$$

$$= \boldsymbol{D}_\gamma^\beta [-2\boldsymbol{r'A}_k + \alpha_k \boldsymbol{v}_k' + \beta_k \boldsymbol{b}_k']^\gamma \varphi_k (\boldsymbol{r'KG})^\lambda \boldsymbol{F}_\beta^\rho$$

$$\Big[-2 (\boldsymbol{A}_l)_{\lambda\rho} + 4 (\boldsymbol{A}_l \boldsymbol{r})_\lambda (\boldsymbol{A}_l \boldsymbol{r})_\rho - 2\alpha_l (\boldsymbol{A}_l \boldsymbol{r})_\lambda (\boldsymbol{v}_l)_\rho - 2\beta_l (\boldsymbol{A}_l \boldsymbol{r})_\lambda (\boldsymbol{b}_l)_\rho$$

$$-2\alpha_l (\boldsymbol{v}_l)_\lambda (\boldsymbol{A}_l \boldsymbol{r})_\rho + \alpha_l \beta_l (\boldsymbol{v}_l)_\lambda (\boldsymbol{b}_l)_\rho - 2\beta_l (\boldsymbol{b}_l)_\lambda (\boldsymbol{A}_l \boldsymbol{r})_\rho + \beta_l \alpha_l (\boldsymbol{b}_l)_\lambda (\boldsymbol{v}_l)_\rho \Big] \varphi_l.$$

1. $(\boldsymbol{r'KG})^\lambda \boldsymbol{F}_\beta^\rho \big[-2 (\boldsymbol{A}_l)_{\lambda\rho} \big] \boldsymbol{D}_\gamma^\beta [-2(\boldsymbol{r'A}_k)^\gamma] = 4(\boldsymbol{r'KGA}_l \boldsymbol{F'D'A}_k \boldsymbol{r})$,

2. $(\boldsymbol{r'KG})^\lambda \boldsymbol{F}_\beta^\rho \big[4 (\boldsymbol{A}_l \boldsymbol{r})_\lambda (\boldsymbol{A}_l \boldsymbol{r})_\rho \big] \boldsymbol{D}_\gamma^\beta [-2(\boldsymbol{r'A}_k)^\gamma] = -8(\boldsymbol{r'KGA}_l \boldsymbol{r})(\boldsymbol{r'A}_k \boldsymbol{DFA}_l \boldsymbol{r})$,

3. $(\boldsymbol{r'KG})^\lambda \boldsymbol{F}_\beta^\rho \big[-2\alpha_l (\boldsymbol{A}_l \boldsymbol{r})_\lambda (\boldsymbol{v}_l)_\rho \big] \boldsymbol{D}_\gamma^\beta [-2(\boldsymbol{r'A}_k)^\gamma] = 4\alpha_l (\boldsymbol{r'KGA}_l \boldsymbol{r})(\boldsymbol{r'A}_k \boldsymbol{DFv}_l)$,

4. $(\boldsymbol{r}'\boldsymbol{K}\boldsymbol{G})^{\lambda}\boldsymbol{F}_{\beta}^{\rho}\big[-2\beta_l\left(\boldsymbol{A}_l\boldsymbol{r}\right)_{\lambda}\left(\boldsymbol{b}_l\right)_{\rho}\big]\boldsymbol{D}_{\gamma}^{\beta}[-2(\boldsymbol{r}'\boldsymbol{A}_k)^{\gamma}] = 4\beta_l(\boldsymbol{r}'\boldsymbol{K}\boldsymbol{G}\boldsymbol{A}_l\boldsymbol{r})(\boldsymbol{r}'\boldsymbol{A}_k\boldsymbol{D}\boldsymbol{F}\boldsymbol{b}_l)$,

5. $(\boldsymbol{r}'\boldsymbol{K}\boldsymbol{G})^{\lambda}\boldsymbol{F}_{\beta}^{\rho}\big[-2\alpha_l(\boldsymbol{v}_l)_{\lambda}\left(\boldsymbol{A}_l\boldsymbol{r}\right)_{\rho}\big]\boldsymbol{D}_{\gamma}^{\beta}[-2(\boldsymbol{r}'\boldsymbol{A}_k)^{\gamma}] = 4\alpha_l(\boldsymbol{r}'\boldsymbol{K}\boldsymbol{G}\boldsymbol{v}_l)(\boldsymbol{r}'\boldsymbol{A}_k\boldsymbol{D}\boldsymbol{F}\boldsymbol{A}_l\boldsymbol{r})$,

6. $(\boldsymbol{r}'\boldsymbol{K}\boldsymbol{G})^{\lambda}\boldsymbol{F}_{\beta}^{\rho}\big[\alpha_l\beta_l(\boldsymbol{v}_l)_{\lambda}\left(\boldsymbol{b}_l\right)_{\rho}\big]\boldsymbol{D}_{\gamma}^{\beta}[-2(\boldsymbol{r}'\boldsymbol{A}_k)^{\gamma}] = -2\alpha_l\beta_l(\boldsymbol{r}'\boldsymbol{K}\boldsymbol{G}\boldsymbol{v}_l)(\boldsymbol{r}'\boldsymbol{A}_k\boldsymbol{D}\boldsymbol{F}\boldsymbol{b}_l)$,

7. $(\boldsymbol{r}'\boldsymbol{K}\boldsymbol{G})^{\lambda}\boldsymbol{F}_{\beta}^{\rho}\big[-2\beta_l(\boldsymbol{b}_l)_{\lambda}\left(\boldsymbol{A}_l\boldsymbol{r}\right)_{\rho}\big]\boldsymbol{D}_{\gamma}^{\beta}[-2(\boldsymbol{r}'\boldsymbol{A}_k)^{\gamma}] = 4\beta_l(\boldsymbol{r}'\boldsymbol{K}\boldsymbol{G}\boldsymbol{b}_l)(\boldsymbol{r}'\boldsymbol{A}_k\boldsymbol{D}\boldsymbol{F}\boldsymbol{A}_l\boldsymbol{r})$,

8. $(\boldsymbol{r}'\boldsymbol{K}\boldsymbol{G})^{\lambda}\boldsymbol{F}_{\beta}^{\rho}\big[\beta_l\alpha_l(\boldsymbol{b}_l)_{\lambda}\left(\boldsymbol{v}_l\right)_{\rho}\big]\boldsymbol{D}_{\gamma}^{\beta}[-2(\boldsymbol{r}'\boldsymbol{A}_k)^{\gamma}] = -2\alpha_l\beta_l(\boldsymbol{r}'\boldsymbol{K}\boldsymbol{G}\boldsymbol{b}_l)(\boldsymbol{r}'\boldsymbol{A}_k\boldsymbol{D}\boldsymbol{F}\boldsymbol{v}_l)$,

9. $(\boldsymbol{r}'\boldsymbol{K}\boldsymbol{G})^{\lambda}\boldsymbol{F}_{\beta}^{\rho}\big[-2\left(\boldsymbol{A}_l\right)_{\lambda\rho}\big]\boldsymbol{D}_{\gamma}^{\beta}[\alpha_k(\boldsymbol{v}_k')^{\gamma}] = -2\alpha_k(\boldsymbol{r}'\boldsymbol{K}\boldsymbol{G}\boldsymbol{A}_l\boldsymbol{F}'\boldsymbol{D}'\boldsymbol{v}_k)$,

10. $(\boldsymbol{r}'\boldsymbol{K}\boldsymbol{G})^{\lambda}\boldsymbol{F}_{\beta}^{\rho}\big[4\left(\boldsymbol{A}_l\boldsymbol{r}\right)_{\lambda}\left(\boldsymbol{A}_l\boldsymbol{r}\right)_{\rho}\big]\boldsymbol{D}_{\gamma}^{\beta}[\alpha_k(\boldsymbol{v}_k')^{\gamma}] = 4\alpha_k(\boldsymbol{r}'\boldsymbol{K}\boldsymbol{G}\boldsymbol{A}_l\boldsymbol{r})(\boldsymbol{v}_k'\boldsymbol{D}\boldsymbol{F}\boldsymbol{A}_l\boldsymbol{r})$,

11. $(\boldsymbol{r}'\boldsymbol{K}\boldsymbol{G})^{\lambda}\boldsymbol{F}_{\beta}^{\rho}\big[-2\alpha_l\left(\boldsymbol{A}_l\boldsymbol{r}\right)_{\lambda}\left(\boldsymbol{v}_l\right)_{\rho}\big]\boldsymbol{D}_{\gamma}^{\beta}[\alpha_k(\boldsymbol{v}_k')^{\gamma}] = -2\alpha_k\alpha_l(\boldsymbol{r}'\boldsymbol{K}\boldsymbol{G}\boldsymbol{A}_l\boldsymbol{r})(\boldsymbol{v}_k'\boldsymbol{D}\boldsymbol{F}\boldsymbol{v}_l)$,

12. $(\boldsymbol{r}'\boldsymbol{K}\boldsymbol{G})^{\lambda}\boldsymbol{F}_{\beta}^{\rho}\big[-2\beta_l\left(\boldsymbol{A}_l\boldsymbol{r}\right)_{\lambda}\left(\boldsymbol{b}_l\right)_{\rho}\big]\boldsymbol{D}_{\gamma}^{\beta}[\alpha_k(\boldsymbol{v}_k')^{\gamma}] = -2\alpha_k\beta_l(\boldsymbol{r}'\boldsymbol{K}\boldsymbol{G}\boldsymbol{A}_l\boldsymbol{r})(\boldsymbol{v}_k'\boldsymbol{D}\boldsymbol{F}\boldsymbol{b}_l)$,

13. $(\boldsymbol{r}'\boldsymbol{K}\boldsymbol{G})^{\lambda}\boldsymbol{F}_{\beta}^{\rho}\big[-2\alpha_l(\boldsymbol{v}_l)_{\lambda}\left(\boldsymbol{A}_l\boldsymbol{r}\right)_{\rho}\big]\boldsymbol{D}_{\gamma}^{\beta}[\alpha_k(\boldsymbol{v}_k')^{\gamma}] = -2\alpha_k\alpha_l(\boldsymbol{r}'\boldsymbol{K}\boldsymbol{G}\boldsymbol{v}_l)(\boldsymbol{v}_k'\boldsymbol{D}\boldsymbol{F}\boldsymbol{A}_l\boldsymbol{r})$,

14. $(\boldsymbol{r}'\boldsymbol{K}\boldsymbol{G})^{\lambda}\boldsymbol{F}_{\beta}^{\rho}\big[\alpha_l\beta_l(\boldsymbol{v}_l)_{\lambda}\left(\boldsymbol{b}_l\right)_{\rho}\big]\boldsymbol{D}_{\gamma}^{\beta}[\alpha_k(\boldsymbol{v}_k')^{\gamma}] = \alpha_k\alpha_l\beta_l(\boldsymbol{r}'\boldsymbol{K}\boldsymbol{G}\boldsymbol{v}_l)(\boldsymbol{v}_k'\boldsymbol{D}\boldsymbol{F}\boldsymbol{b}_l)$,

15. $(\boldsymbol{r}'\boldsymbol{K}\boldsymbol{G})^{\lambda}\boldsymbol{F}_{\beta}^{\rho}\big[-2\beta_l(\boldsymbol{b}_l)_{\lambda}\left(\boldsymbol{A}_l\boldsymbol{r}\right)_{\rho}\big]\boldsymbol{D}_{\gamma}^{\beta}[\alpha_k(\boldsymbol{v}_k')^{\gamma}] = -2\alpha_k\beta_l(\boldsymbol{r}'\boldsymbol{K}\boldsymbol{G}\boldsymbol{b}_l)(\boldsymbol{v}_k'\boldsymbol{D}\boldsymbol{F}\boldsymbol{A}_l\boldsymbol{r})$,

16. $(\boldsymbol{r}'\boldsymbol{K}\boldsymbol{G})^{\lambda}\boldsymbol{F}_{\beta}^{\rho}\big[\beta_l\alpha_l(\boldsymbol{b}_l)_{\lambda}\left(\boldsymbol{v}_l\right)_{\rho}\big]\boldsymbol{D}_{\gamma}^{\beta}[\alpha_k(\boldsymbol{v}_k')^{\gamma}] = \alpha_k\alpha_l\beta_l(\boldsymbol{r}'\boldsymbol{K}\boldsymbol{G}\boldsymbol{b}_l)(\boldsymbol{v}_k'\boldsymbol{D}\boldsymbol{F}\boldsymbol{v}_l)$,

17. $(\boldsymbol{r}'\boldsymbol{K}\boldsymbol{G})^{\lambda}\boldsymbol{F}_{\beta}^{\rho}\big[-2\left(\boldsymbol{A}_l\right)_{\lambda\rho}\big]\boldsymbol{D}_{\gamma}^{\beta}[\beta_k(\boldsymbol{b}_k')^{\gamma}] = -2\beta_k(\boldsymbol{r}'\boldsymbol{K}\boldsymbol{G}\boldsymbol{A}_l\boldsymbol{F}'\boldsymbol{D}'\boldsymbol{b}_k)$,

18. $(\boldsymbol{r}'\boldsymbol{K}\boldsymbol{G})^{\lambda}\boldsymbol{F}_{\beta}^{\rho}\big[4\left(\boldsymbol{A}_l\boldsymbol{r}\right)_{\lambda}\left(\boldsymbol{A}_l\boldsymbol{r}\right)_{\rho}\big]\boldsymbol{D}_{\gamma}^{\beta}[\beta_k(\boldsymbol{b}_k')^{\gamma}] = 4\beta_k(\boldsymbol{r}'\boldsymbol{K}\boldsymbol{G}\boldsymbol{A}_l\boldsymbol{r})(\boldsymbol{b}_k'\boldsymbol{D}\boldsymbol{F}\boldsymbol{A}_l\boldsymbol{r})$,

19. $(\boldsymbol{r}'\boldsymbol{K}\boldsymbol{G})^{\lambda}\boldsymbol{F}_{\beta}^{\rho}\big[-2\alpha_l\left(\boldsymbol{A}_l\boldsymbol{r}\right)_{\lambda}\left(\boldsymbol{v}_l\right)_{\rho}\big]\boldsymbol{D}_{\gamma}^{\beta}[\beta_k(\boldsymbol{b}_k')^{\gamma}] = -2\beta_k\alpha_l(\boldsymbol{r}'\boldsymbol{K}\boldsymbol{G}\boldsymbol{A}_l\boldsymbol{r})(\boldsymbol{b}_k'\boldsymbol{D}\boldsymbol{F}\boldsymbol{v}_l)$,

20. $(\boldsymbol{r}'\boldsymbol{K}\boldsymbol{G})^{\lambda}\boldsymbol{F}_{\beta}^{\rho}\big[-2\beta_l\left(\boldsymbol{A}_l\boldsymbol{r}\right)_{\lambda}\left(\boldsymbol{b}_l\right)_{\rho}\big]\boldsymbol{D}_{\gamma}^{\beta}[\beta_k(\boldsymbol{b}_k')^{\gamma}] = -2\beta_k\beta_l(\boldsymbol{r}'\boldsymbol{K}\boldsymbol{G}\boldsymbol{A}_l\boldsymbol{r})(\boldsymbol{b}_k'\boldsymbol{D}\boldsymbol{F}\boldsymbol{b}_l)$,

21. $(\boldsymbol{r}'\boldsymbol{K}\boldsymbol{G})^{\lambda}\boldsymbol{F}_{\beta}^{\rho}\big[-2\alpha_l(\boldsymbol{v}_l)_{\lambda}\left(\boldsymbol{A}_l\boldsymbol{r}\right)_{\rho}\big]\boldsymbol{D}_{\gamma}^{\beta}[\beta_k(\boldsymbol{b}_k')^{\gamma}] = -2\beta_k\alpha_l(\boldsymbol{r}'\boldsymbol{K}\boldsymbol{G}\boldsymbol{v}_l)(\boldsymbol{b}_k'\boldsymbol{D}\boldsymbol{F}\boldsymbol{A}_l\boldsymbol{r})$,

22. $(\boldsymbol{r}'\boldsymbol{K}\boldsymbol{G})^{\lambda}\boldsymbol{F}_{\beta}^{\rho}\big[\alpha_l\beta_l(\boldsymbol{v}_l)_{\lambda}\left(\boldsymbol{b}_l\right)_{\rho}\big]\boldsymbol{D}_{\gamma}^{\beta}[\beta_k(\boldsymbol{b}_k')^{\gamma}] = \beta_k\alpha_l\beta_l(\boldsymbol{r}'\boldsymbol{K}\boldsymbol{G}\boldsymbol{v}_l)(\boldsymbol{b}_k'\boldsymbol{D}\boldsymbol{F}\boldsymbol{b}_l)$,

23. $(\boldsymbol{r}'\boldsymbol{K}\boldsymbol{G})^{\lambda}\boldsymbol{F}_{\beta}^{\rho}\big[-2\beta_l(\boldsymbol{b}_l)_{\lambda}\left(\boldsymbol{A}_l\boldsymbol{r}\right)_{\rho}\big]\boldsymbol{D}_{\gamma}^{\beta}[\beta_k(\boldsymbol{b}_k')^{\gamma}] = -2\beta_k\beta_l(\boldsymbol{r}'\boldsymbol{K}\boldsymbol{G}\boldsymbol{b}_l)(\boldsymbol{b}_k'\boldsymbol{D}\boldsymbol{F}\boldsymbol{A}_l\boldsymbol{r})$,

24. $(\boldsymbol{r}'\boldsymbol{K}\boldsymbol{G})^{\lambda}\boldsymbol{F}_{\beta}^{\rho}\big[+\beta_l\alpha_l(\boldsymbol{b}_l)_{\lambda}\left(\boldsymbol{v}_l\right)_{\rho}\big]\boldsymbol{D}_{\gamma}^{\beta}[\beta_k(\boldsymbol{b}_k')^{\gamma}] = \beta_k\alpha_l\beta_l(\boldsymbol{r}'\boldsymbol{K}\boldsymbol{G}\boldsymbol{b}_l)(\boldsymbol{b}_k'\boldsymbol{D}\boldsymbol{F}\boldsymbol{v}_l)$,

Term 2: $\int \mathrm{d}\boldsymbol{r}\frac{1}{r_g}\varphi_k\{(\boldsymbol{\nabla}'\boldsymbol{D})^\beta(\boldsymbol{r}'\boldsymbol{K})^\lambda\}(\boldsymbol{F}\boldsymbol{\nabla})_\beta(\boldsymbol{G}\boldsymbol{\nabla})_\lambda\varphi_l$

We note that

$$\{(\boldsymbol{\nabla}'\boldsymbol{D})^\beta(\boldsymbol{r}'\boldsymbol{K})^\lambda\}(\boldsymbol{F}\boldsymbol{\nabla})_\beta(\boldsymbol{G}\boldsymbol{\nabla})_\lambda\varphi_l = (\boldsymbol{D}\boldsymbol{F}\boldsymbol{\nabla})_\gamma(\boldsymbol{K}\boldsymbol{G}\boldsymbol{\nabla})^\gamma\varphi_l = (\boldsymbol{\nabla}'\boldsymbol{G}'\boldsymbol{K}'\boldsymbol{D}\boldsymbol{F}\boldsymbol{\nabla})\varphi_l.$$

Hence the expression is analogous to (154): $\boldsymbol{\nabla}'_{\boldsymbol{r}}\boldsymbol{B}\boldsymbol{\nabla}_{\boldsymbol{r}}\varphi_l$, hence we can use that result.

Term 3: $\int \mathrm{d}\boldsymbol{r}\frac{1}{r_g}\varphi_k(\boldsymbol{r}'\boldsymbol{K})^\lambda\{(\boldsymbol{\nabla}'\boldsymbol{D})^\beta(\boldsymbol{F}\boldsymbol{\nabla})_\beta(\boldsymbol{G}\boldsymbol{\nabla})_\lambda\varphi_l\}$

First we make few simple transformations:

$$(\boldsymbol{r}'\boldsymbol{K})^\lambda\{(\boldsymbol{\nabla}'\boldsymbol{D})^\beta(\boldsymbol{F}\boldsymbol{\nabla})_\beta(\boldsymbol{G}\boldsymbol{\nabla})_\lambda\varphi_l\} = (\boldsymbol{r}'\boldsymbol{K}\boldsymbol{G})^\lambda(\boldsymbol{D}\boldsymbol{F})^\beta_\rho\partial^\rho\partial_\beta\partial_\lambda\varphi_l.$$

We will use this result (153) and list the resulted integrals below for easier computer implementation:

1. $(\boldsymbol{r}'\boldsymbol{K}\boldsymbol{G})^\lambda(\boldsymbol{D}\boldsymbol{F})^\beta_\rho[4\,(\boldsymbol{A}_l)^\rho_\lambda\,(\boldsymbol{A}_l\boldsymbol{r})_\beta] = 4(\boldsymbol{r}'\boldsymbol{K}\boldsymbol{G}\boldsymbol{A}_l\boldsymbol{D}\boldsymbol{F}\boldsymbol{A}_l\boldsymbol{r})$,
2. $(\boldsymbol{r}'\boldsymbol{K}\boldsymbol{G})^\lambda(\boldsymbol{D}\boldsymbol{F})^\beta_\rho[4\,(\boldsymbol{A}_l)^\rho_\beta\,(\boldsymbol{A}_l\boldsymbol{r})_\lambda] = 12\,\mathrm{tr}[A_lDF](\boldsymbol{r}'\boldsymbol{K}\boldsymbol{G}\boldsymbol{A}_l\boldsymbol{r})$,
3. $(\boldsymbol{r}'\boldsymbol{K}\boldsymbol{G})^\lambda(\boldsymbol{D}\boldsymbol{F})^\beta_\rho[-2\alpha_l\,(\boldsymbol{A}_l)^\rho_\lambda\,(\boldsymbol{v}_l)_\beta] = -2\alpha_l(\boldsymbol{r}'\boldsymbol{K}\boldsymbol{G}\boldsymbol{A}_l\boldsymbol{D}\boldsymbol{F}\boldsymbol{v}_l)$,
4. $(\boldsymbol{r}'\boldsymbol{K}\boldsymbol{G})^\lambda(\boldsymbol{D}\boldsymbol{F})^\beta_\rho[-2\beta_l\,(\boldsymbol{A}_l)^\rho_\lambda\,(\boldsymbol{b}_l)_\beta] = -2\beta_l(\boldsymbol{r}'\boldsymbol{K}\boldsymbol{G}\boldsymbol{A}_l\boldsymbol{D}\boldsymbol{F}\boldsymbol{b}_l)$,
5. $(\boldsymbol{r}'\boldsymbol{K}\boldsymbol{G})^\lambda(\boldsymbol{D}\boldsymbol{F})^\beta_\rho[-2\alpha_l\,(\boldsymbol{A}_l)^\rho_\beta\,(\boldsymbol{v}_l)_\lambda] = -6\alpha_l\,\mathrm{tr}[A_lDF](\boldsymbol{r}'\boldsymbol{K}\boldsymbol{G}\boldsymbol{v}_l)$,
6. $(\boldsymbol{r}'\boldsymbol{K}\boldsymbol{G})^\lambda(\boldsymbol{D}\boldsymbol{F})^\beta_\rho[-2\beta_l\,(\boldsymbol{A}_l)^\rho_\beta\,(\boldsymbol{b}_l)_\lambda] = -6\beta_l\,\mathrm{tr}[A_lDF](\boldsymbol{r}'\boldsymbol{K}\boldsymbol{G}\boldsymbol{b}_l)$,
7. $(\boldsymbol{r}'\boldsymbol{K}\boldsymbol{G})^\lambda(\boldsymbol{D}\boldsymbol{F})^\beta_\rho[4\,(\boldsymbol{A}_l)_{\lambda\beta}\,(\boldsymbol{r}'\boldsymbol{A}_l)^\rho] = 4(\boldsymbol{r}'\boldsymbol{K}\boldsymbol{G}\boldsymbol{A}_l\boldsymbol{F}'\boldsymbol{D}'\boldsymbol{A}_l\boldsymbol{r})$,
8. $(\boldsymbol{r}'\boldsymbol{K}\boldsymbol{G})^\lambda(\boldsymbol{D}\boldsymbol{F})^\beta_\rho[-8\,(\boldsymbol{A}_l\boldsymbol{r})_\lambda\,(\boldsymbol{A}_l\boldsymbol{r})_\beta\,(\boldsymbol{r}'\boldsymbol{A}_l)^\rho] = -8(\boldsymbol{r}'\boldsymbol{K}\boldsymbol{G}\boldsymbol{A}_l\boldsymbol{r})(\boldsymbol{r}'\boldsymbol{A}_l\boldsymbol{D}\boldsymbol{F}\boldsymbol{A}_l\boldsymbol{r})$,
9. $(\boldsymbol{r}'\boldsymbol{K}\boldsymbol{G})^\lambda(\boldsymbol{D}\boldsymbol{F})^\beta_\rho[4\alpha_l\,(\boldsymbol{A}_l\boldsymbol{r})_\lambda\,(\boldsymbol{v}_l)_\beta\,(\boldsymbol{r}'\boldsymbol{A}_l)^\rho] = 4\alpha_l(\boldsymbol{r}'\boldsymbol{K}\boldsymbol{G}\boldsymbol{A}_l\boldsymbol{r})(\boldsymbol{r}'\boldsymbol{A}_l\boldsymbol{D}\boldsymbol{F}\boldsymbol{v}_l)$,
10. $(\boldsymbol{r}'\boldsymbol{K}\boldsymbol{G})^\lambda(\boldsymbol{D}\boldsymbol{F})^\beta_\rho[4\beta_l\,(\boldsymbol{A}_l\boldsymbol{r})_\lambda\,(\boldsymbol{b}_l)_\beta\,(\boldsymbol{r}'\boldsymbol{A}_l)^\rho] = 4\beta_l(\boldsymbol{r}'\boldsymbol{K}\boldsymbol{G}\boldsymbol{A}_l\boldsymbol{r})(\boldsymbol{r}'\boldsymbol{A}_l\boldsymbol{D}\boldsymbol{F}\boldsymbol{b}_l)$,
11. $(\boldsymbol{r}'\boldsymbol{K}\boldsymbol{G})^\lambda(\boldsymbol{D}\boldsymbol{F})^\beta_\rho[4\alpha_l(\boldsymbol{v}_l)_\lambda\,(\boldsymbol{A}_l\boldsymbol{r})_\beta\,(\boldsymbol{r}'\boldsymbol{A}_l)^\rho] = 4\alpha_l(\boldsymbol{r}'\boldsymbol{K}\boldsymbol{G}\boldsymbol{v}_l)(\boldsymbol{r}'\boldsymbol{A}_l\boldsymbol{D}\boldsymbol{F}\boldsymbol{A}_l\boldsymbol{r})$,
12. $(\boldsymbol{r}'\boldsymbol{K}\boldsymbol{G})^\lambda(\boldsymbol{D}\boldsymbol{F})^\beta_\rho[-2\alpha_l\beta_l(\boldsymbol{v}_l)_\lambda\,(\boldsymbol{b}_l)_\beta\,(\boldsymbol{r}'\boldsymbol{A}_l)^\rho] = -2\alpha_l\beta_l(\boldsymbol{r}'\boldsymbol{K}\boldsymbol{G}\boldsymbol{v}_l)(\boldsymbol{r}'\boldsymbol{A}_l\boldsymbol{D}\boldsymbol{F}\boldsymbol{b}_l)$,

13. $(\boldsymbol{r}'\boldsymbol{K}\boldsymbol{G})^{\lambda}(\boldsymbol{D}\boldsymbol{F})^{\beta}_{\rho}[4\beta_l(\boldsymbol{b}_l)_{\lambda}\left(\boldsymbol{A}_l\boldsymbol{r}\right)_{\beta}\left(\boldsymbol{r}'\boldsymbol{A}_l\right)^{\rho}] = 4\beta_l(\boldsymbol{r}'\boldsymbol{K}\boldsymbol{G}\boldsymbol{b}_l)(\boldsymbol{r}'\boldsymbol{A}_l\boldsymbol{D}\boldsymbol{F}\boldsymbol{A}_l\boldsymbol{r})$,

14. $(\boldsymbol{r}'\boldsymbol{K}\boldsymbol{G})^{\lambda}(\boldsymbol{D}\boldsymbol{F})^{\beta}_{\rho}[-2\beta_l\alpha_l(\boldsymbol{b}_l)_{\lambda}\left(\boldsymbol{v}_l\right)_{\beta}\left(\boldsymbol{r}'\boldsymbol{A}_l\right)^{\rho}] = -2\alpha_l\beta_l(\boldsymbol{r}'\boldsymbol{K}\boldsymbol{G}\boldsymbol{b}_l)(\boldsymbol{r}'\boldsymbol{A}_l\boldsymbol{D}\boldsymbol{F}\boldsymbol{v}_l)$,

15. $(\boldsymbol{r}'\boldsymbol{K}\boldsymbol{G})^{\lambda}(\boldsymbol{D}\boldsymbol{F})^{\beta}_{\rho}[-2\alpha_l\left(\boldsymbol{v}_l\right)^{\rho}\left(\boldsymbol{A}_l\right)_{\lambda\beta}] = -2\alpha_l(\boldsymbol{r}'\boldsymbol{K}\boldsymbol{G}\boldsymbol{A}_l(\boldsymbol{D}\boldsymbol{F})'\boldsymbol{v}_l)$,

16. $(\boldsymbol{r}'\boldsymbol{K}\boldsymbol{G})^{\lambda}(\boldsymbol{D}\boldsymbol{F})^{\beta}_{\rho}[4\alpha_l\left(\boldsymbol{v}_l\right)^{\rho}\left(\boldsymbol{A}_l\boldsymbol{r}\right)_{\lambda}\left(\boldsymbol{A}_l\boldsymbol{r}\right)_{\beta}] = 4\alpha_l(\boldsymbol{r}'\boldsymbol{K}\boldsymbol{G}\boldsymbol{A}_l\boldsymbol{r})(\boldsymbol{v}_l'\boldsymbol{D}\boldsymbol{F}\boldsymbol{A}_l\boldsymbol{r})$,

17. $(\boldsymbol{r}'\boldsymbol{K}\boldsymbol{G})^{\lambda}(\boldsymbol{D}\boldsymbol{F})^{\beta}_{\rho}[-2\beta_l\alpha_l\left(\boldsymbol{v}_l\right)^{\rho}\left(\boldsymbol{A}_l\boldsymbol{r}\right)_{\lambda}\left(\boldsymbol{b}_l\right)_{\beta}] = -2\alpha_l\beta_l(\boldsymbol{r}'\boldsymbol{K}\boldsymbol{G}\boldsymbol{A}_l\boldsymbol{r})(\boldsymbol{v}_l\boldsymbol{D}\boldsymbol{F}\boldsymbol{b}_l)$,

18. $(\boldsymbol{r}'\boldsymbol{K}\boldsymbol{G})^{\lambda}(\boldsymbol{D}\boldsymbol{F})^{\beta}_{\rho}[-2\beta_l\alpha_l\left(\boldsymbol{v}_l\right)^{\rho}\left(\boldsymbol{b}_l\right)_{\lambda}\left(\boldsymbol{A}_l\boldsymbol{r}\right)_{\beta}] = -2\beta_l\alpha_l(\boldsymbol{r}'\boldsymbol{K}\boldsymbol{G}\boldsymbol{b}_l)(\boldsymbol{v}_l'\boldsymbol{D}\boldsymbol{F}\boldsymbol{A}_l\boldsymbol{r})$,

19. $(\boldsymbol{r}'\boldsymbol{K}\boldsymbol{G})^{\lambda}(\boldsymbol{D}\boldsymbol{F})^{\beta}_{\rho}[-2\beta_l\left(\boldsymbol{b}_l\right)^{\rho}\left(\boldsymbol{A}_l\right)_{\lambda\beta}] = -2\beta_l(\boldsymbol{r}'\boldsymbol{K}\boldsymbol{G}\boldsymbol{A}_l(\boldsymbol{D}\boldsymbol{F})'\boldsymbol{b}_l)$,

20. $(\boldsymbol{r}'\boldsymbol{K}\boldsymbol{G})^{\lambda}(\boldsymbol{D}\boldsymbol{F})^{\beta}_{\rho}[4\beta_l\left(\boldsymbol{b}_l\right)^{\rho}\left(\boldsymbol{A}_l\boldsymbol{r}\right)_{\lambda}\left(\boldsymbol{A}_l\boldsymbol{r}\right)_{\beta}] = 4\beta_l(\boldsymbol{r}'\boldsymbol{K}\boldsymbol{G}\boldsymbol{A}_l\boldsymbol{r})(\boldsymbol{b}_l'\boldsymbol{D}\boldsymbol{F}\boldsymbol{A}_l\boldsymbol{r})$,

21. $(\boldsymbol{r}'\boldsymbol{K}\boldsymbol{G})^{\lambda}(\boldsymbol{D}\boldsymbol{F})^{\beta}_{\rho}[-2\alpha_l\beta_l\left(\boldsymbol{b}_l\right)^{\rho}\left(\boldsymbol{A}_l\boldsymbol{r}\right)_{\lambda}\left(\boldsymbol{v}_l\right)_{\beta}] = -2\alpha_l\beta_l(\boldsymbol{r}'\boldsymbol{K}\boldsymbol{G}\boldsymbol{A}_l\boldsymbol{r})(\boldsymbol{b}_l\boldsymbol{D}\boldsymbol{F}\boldsymbol{v}_l)$,

22. $(\boldsymbol{r}'\boldsymbol{K}\boldsymbol{G})^{\lambda}(\boldsymbol{D}\boldsymbol{F})^{\beta}_{\rho}[-2\alpha_l\beta_l\left(\boldsymbol{b}_l\right)^{\rho}\left(\boldsymbol{v}_l\right)_{\lambda}\left(\boldsymbol{A}_l\boldsymbol{r}\right)_{\beta}] = -2\beta_l\alpha_l(\boldsymbol{r}'\boldsymbol{K}\boldsymbol{G}\boldsymbol{v}_l)(\boldsymbol{b}_l'\boldsymbol{D}\boldsymbol{F}\boldsymbol{A}_l\boldsymbol{r})$.

11 Code flowchart and basis set generation

11.1 Code flowchart

The process of generating highly accurate wave functions for quantum mechanical systems in the explicitly correlated Gaussian basis functions involves the application of the Rayleigh-Ritz variational method and minimizing the energy functional (13). The structure of the program that performs such large scale-quantum mechanical calculations is illustrated in Figure 1 and is designed for non-Born-Oppenheimer (non-BO) calculations. However, it is noteworthy that the same program framework can be adapted for BO calculations with minor adjustments in the input file (by changing the mass of the heaviest particle in the system of interest to infinity). The differences between BO and non-BO calculations are described in section 4.

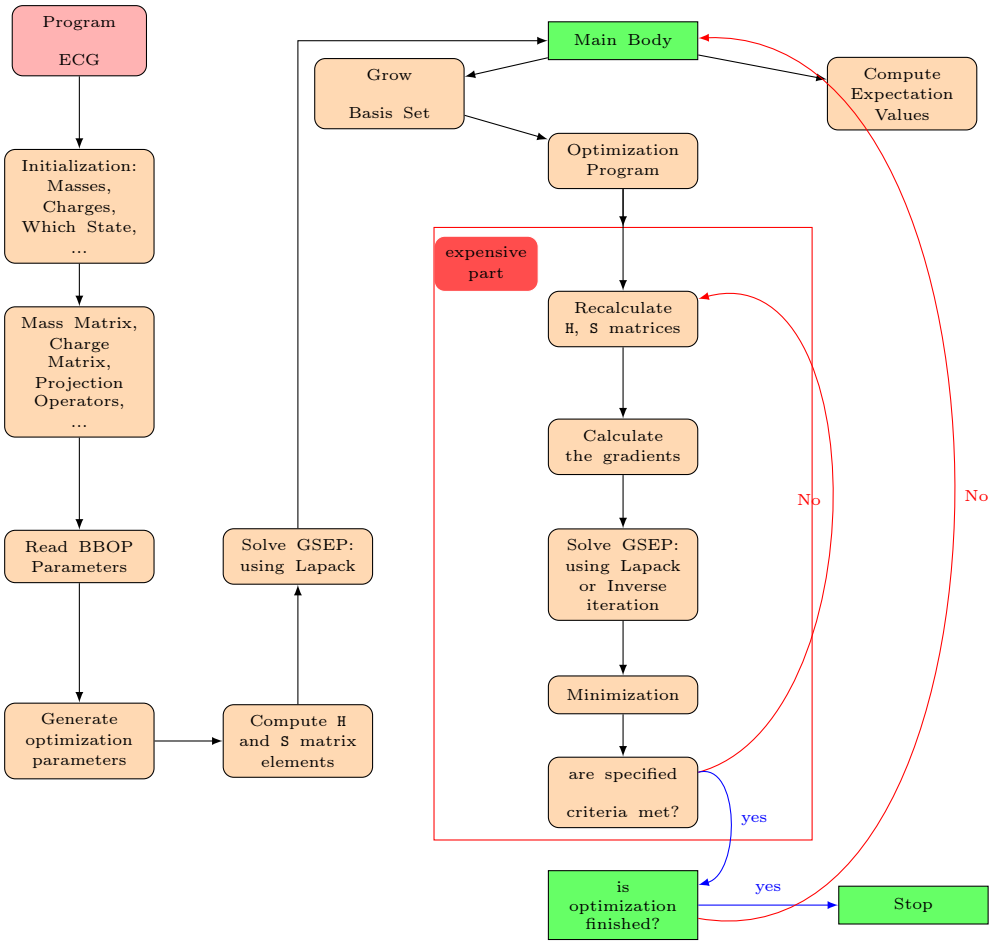

Figure 1: Code Flowchart

The program is called "ECG" and is written in FORTRAN 90 code. It begins by reading input parameters through a "root" process from an input file "inout.txt". These parameters may include masses, charges, symmetry as well as the state of the system ("Which Eigenvalue") under consideration. Subsequently, the program broadcasts these parameters (using "MPI BCAST") from the "root" process to all available "slave" processes, depending on the number of processors in the computer or cluster.

The program then proceeds to convert particle masses into the pseudoparticle reduced mass matrix (23) in the internal Hamiltonian (22), properly stores charges, and constructs permutation operators from the symmetry projector described in section 4. To account for potential restarts due to computer constraints or failures, the current trial wave function expansion (if available and provided in the input file) is saved in the input file.

This initialization process, described in above paragraphs alone, comprises up to 10,000 lines of code, highlighting the complexity of the program. By now it is evident that all expressions derived in this dissertation, including the matrix elements for the expectation values of orbit-orbit and mass velocity Hamiltonians, have been implemented in the parallelized FORTRAN 90. The parallelization of the code is achieved through the Message Passing Interface (MPI) library. It offers a straightforward yet highly effective approach for parallelizing calculations. Moreover, MPI software is accessible across all major hardware platforms, facilitating seamless migration of code from one computer system to another with minimal or no need for modification. Due to the large scope of the program, only a brief description is provided here, omitting the detailed steps that involve MPI commands.

After system initialization, the program reads the basis set, and Hamiltonian and overlap matrices are computed. Subsequently, the secular equation (13) is solved to derive linear expansion coefficients. Following the processing of all provided data in the input file, the main body of the program, called the Basis Building and Optimization Program (BBOP), initiates. BBOP, as its name suggests, is responsible for the process of constructing and optimizing the basis set, which demands considerable computational resources, as highlighted in red in the code flowchart, especially when dealing with large systems containing many particles and a substantial number of permutation operators in the Young symmetry projector (40). Despite its name, BBOP may also include directives for calculating single-point expectation values ("compute expectation values") and conducting several types of basis set optimization

11.2 Optimization of the Gaussian parameters

The "optimization program" constitutes the most time-consuming body of the program, providing users with the flexibility to choose from various optimization regimes, each presenting its own set of advantages and drawbacks. One optimization regime is known as the "full optimization", which proves highly effective when the analytical gradient of the energy with respect to the parameters is available. This method demonstrates efficiency, especially when optimizing relatively small basis sets. However, its cost tends to become prohibitively high as the number of basis functions exceeds a few hundred, particularly for

larger systems like boron and carbon atoms. Therefore, in practical terms, it is generally preferable to employ this option for optimizing basis sets that do not exceed a few hundred functions.

The commonly favored approach involves optimizing a single function at a time and executing multiple optimization cycles within a provided basis set. Generally, users can designate any subset of parameters for optimization. This time consuming optimization program involves the computation of Hamiltonian and overlap matrix elements, as well as the solution of the generalized eigenvalue problem (13). The former consumes a larger proportion of total time for systems with many particles, especially in scenarios involving identical particles (e.g. carbon atom). Conversely, the latter dominates computation time for smaller systems such as helium and lithium atoms. The solution of the eigenvalue problem takes also a large amount of total time for systems with large basis functions independent of weather we consider small or large systems. It is worth noting that both tasks require many times of repeated execution to achieve highly converged energy eigenvalues, particularly when employing large basis sets, which can use millions of iterations. The primary reason for this repetition lies in optimizing the nonlinear variational parameters of the basis functions, highlighting the importance of meticulous organizations of the codes for efficient calculations.

On the other hand, the computation of expectation values, although requiring computational resources, is typically less time-consuming compared to wave function generation, constituting a "single-point" calculation. Essentially, the computation of expectation values, such as interparticle distances (e.g., Tables 3 and 4), correlation functions, and relativistic corrections (e.g., Tables 6 and 5), occurs only once utilizing the highest-quality wave function provided as an input file. This case is applicable when the "Main Body" of the program directly calls the ("compute expectation values") option, as illustrated in the code flowchart. Usually, single-point expectation value calculations are repeated multiple times with different sizes of the wave functions if convergence patterns of the expectation values are required, as illustrated in Tables 4 through 5.

Now, we will discuss the optimization technique for the wave function generation in a bit more detail. The basis set optimization and basis set generation for all the systems considered in this dissertation follows a strategy used in previous research works

on ECGs, demonstrating its robustness. The process starts by randomly selecting the nonlinear parameters of one or a few Gaussians, represented by the elements of matrix L_k. Subsequently, optimization begins using an approach employing the analytic energy gradient. Additional basis functions are sequentially included, initially by randomly assigning their nonlinear parameters. The best-performing candidate, determined by the most substantial energy minimization, undergoes further optimization through the analytic energy gradient. During the random selection procedure, nonlinear parameters are sampled from a distribution based on those of existing ECGs in the basis. Typically, several hundred random basis function candidates are assessed before identifying the optimal one. After introducing a set number of new functions, a tuning cycle takes place, adjusting the parameters of all basis functions individually. Here, the optimal number of the set of new functions that needs to be added to the basis set typically ranges from 5 to 100. This is an input parameter that must be chosen through separate test calculations before initiating the BBOP program. The rough optimal value for this input parameter depends on the size of the system (i.e., the number of particles) and increases as the number of particles in the system increases.

One example of obtaining the optimal value for the number of basis function increment is illustrated in Figure 2, where the nonrelativistic energy versus calculation time for different basis size increments is plotted. To generate this figure, we performed several test calculations for the lowest doublet D state of the boron atom. As observed in the figure, the "rough" optimal value for the basis size increment falls within the range of 50 to 1500, as these basis increments minimize the energy with the fastest rate.

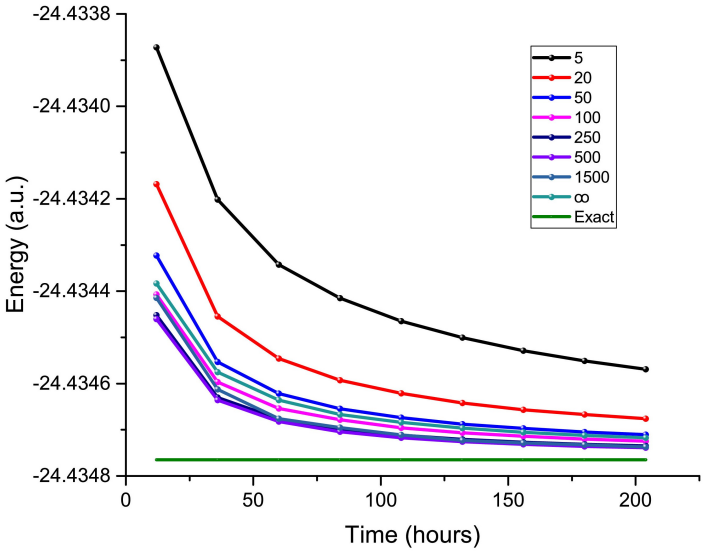

Figure 2: Nonrelaativistic energy vs calculation time for different basis increment for the lowest ^2D state of boron atom. The initial basis size is 1000 functions. The final basis size is in the range of [1300-7900].

Optimizing one function at a time results in significant computational savings, eliminating the need to recalculate all matrix elements and solve the generalized eigenvalue problem from scratch. Upon completing the optimization cycle, the process repeats, adding new set of functions and initiating a new optimization cycle. This controlled growth continues until the basis size reaches a predetermined value. Throughout this gradual expansion and optimization of the ECG basis, checks for potential linear dependencies among basis functions are performed to maintain numerical stability. If, at any point, it is identified that a new function candidate or modification of an existing basis function introduces significant linear dependencies (exceeding a predefined threshold), such additions or modifications are discarded. Work [23] provides a detailed description of the optimization of Gaussian nonlinear parameters.

It is worth noting that in addition to the L_k parameters, each Gaussian basis functions used in this dissertation (33) contains two integer parameters, i_k and j_k, which can undergo optimization. Although optimizing these parameters usually leads to only marginal improvements in energy minimization, such optimization remains crucial, particularly when aiming for highly accurate energy calculations. In the present work, we perform separate optimizations for each of these parameters, and this optimization process is carried out only once for each function after its selection in the basis set.

11.3 Comparison of two schemes

The validation process for the FORTRAN code for each matrix element derived in this dissertation, along with auxiliary functions and subroutines, involved a meticulous comparison against the numerical output produced by the MATHEMATICA symbolic algebra package. To validate the expressions for the matrix elements of the analytic gradient with respect to the Gaussian nonlinear parameters, we employed a five-point finite difference gradient. The correctness of the method was verified in our recent article [79]. Additionally, in this article we presented a table comparing the CPU timings spent on evaluating the matrix elements of the Hamiltonian and overlap with and without the gradient, using both new and old schemes. Below, in Table 1, we again include that table for the completeness of the dissertation.

Table 1: The calculation CPU time (in seconds) for evaluating matrix elements of the Hamiltonian+overlap (Gradient=no) and Hamiltonian+overlap+gradient (Gradient=yes) using two different schemes is provided. The number of iterations is 10^8.

		$L=1$			$L=2$		
System	Gradient	New	Old	Ratio	New	Old	Ratio
Li	yes	96.06	5202	54.15	97.02	8184	84.35
	no	11.39	511	44.86	16.25	820	50.46
Be	yes	305.20	15062	49.35	310.20	25781	83.11
	no	24.50	945	38.57	30.00	1462	48.73
B	yes	620.62	43610	70.27	628.75	65984	104.94
	no	41.36	1820	44.00	60.33	2524	41.83
C	yes	1062.60	120297	113.21	1081.70	154922	143.22
	no	71.94	3023	42.02	82.05	3733	45.50

As we can observe from the table, the new scheme explored in this dissertation yields an improvement of approximately two orders of magnitude compared to the previous scheme that represents basis functions as $\boldsymbol{r}'\boldsymbol{W}_k\boldsymbol{r}\exp\left[-\boldsymbol{r}'\boldsymbol{A}_k\boldsymbol{r}\right]$ [105]. It is noteworthy to mention that this speed-up of the matrix element calculation improves as the number of particles increases. For instance, for the D state ($L=2$) of the carbon atom, the ratio of the old and the new schemes is 143 when the analytic gradient matrix elements are included, while excluding the analytic energy gradient results in a 45-fold increase in

speed. On the other hand, these values for the case of the boron atom D state are 104.94 and 41.83, respectively. The higher ratio in gradient included cases can be attributed to the complexity of the expressions for the analytic gradient matrix element derived with basis functions in the form of $\boldsymbol{r}'\boldsymbol{W}_k\boldsymbol{r}\exp\left[-\boldsymbol{r}'\boldsymbol{A}_k\boldsymbol{r}\right]$.

12 Applications

12.1 Expectation values of operators

The expectation value of an operator corresponds to the average outcome obtained from measuring the particular observable on an ensemble of identically prepared quantum states. This concept is pivotal in bridging the abstract formalism of quantum theory with measurable and interpretable physical quantities, offering a crucial link between the theoretical framework and experimental observations. Therefore, expectation values serve as a key tool for predicting and interpreting the behavior of quantum systems, providing insights into the probabilistic nature inherent in the quantum systems.

As previously discussed in Section 11.2, calculating expectation values of the operators, which involve interparticle distances, correlation functions, and relativistic corrections, typically demands computational resources. However, it is relatively less time-consuming and involves a straightforward "single-poin" calculation. This process is carried out once using the highest-quality wave function provided as an input file. To check the correctness of the mathematical expressions derived for the matrix elements of the considered operators in this dissertation, we perform a convergence analysis of expectation values. This is achieved by conducting these single-point calculations multiple times, varying the basis function sizes, as demonstrated in Tables 4 through 5.

We initiated the numerical verification of the formulas for expectation values, focusing first on interparticle distances. To accomplish this, we generated up to 3000 basis functions for the ground ^2D state of a Li atom using the suitable basis function (30). This process is illustrated in Table 2, where we present the convergence of total nonrelativistic energies versus the basis size. We observe that almost 10 digits have converged, and the comparison with the benchmark result obtained with Hylleraas-type functions [106] further confirms the reliability of our basis generations.

After having well optimized basis functions, we can compute the expectation values of interparticle distances. Tables 3 and 4 presents the results, showcasing the convergence of these values.

As the basis size grows from 500 to 3235, the expectation values for $1/r_i$, $1/r_{ij}$, r_i, r_{ij}, $1/r_i^2$, $1/r_{ij}^2$, r_i^2, and r_{ij}^2 exhibit almost the same convergence trend as the total

Table 2: Convergence of the total nonrelativistic energies (in a.u.) of the lithium atom in the lowest ^2D state with the number of ECG basis functions.

	Basis size	$1s^2 3d\,(^2D)$
$^{\infty}$Li	1000	−7.335 523 501 56
	1500	−7.335 523 535 12
	2000	−7.335 523 540 22
	2500	−7.335 523 541 79
	3000	−7.335 523 542 61
^{7}Li	3000	−7.334 927 305 61
Hylleraas-type basis [106]		
$^{\infty}$Li	32 760	−7.335 523 543 524 685

Table 3: The expectation values of various interparticle distances for a fixed nucleus of Li atom in ^2D state

Basis size	$1/r_i$	$1/r_{ij}$	r_i	r_{ij}
500	1.8290327697	0.59674991880	3.876384976	7.28847046
1000	1.8290329704	0.59674993524	3.876409032	7.28852023
1500	1.8290329917	0.59674995170	3.876407843	7.28851815
2380	1.8290329918	0.59674994776	3.876408129	7.28851893
3235	1.8290329924	0.59674994789	3.876408129	7.28851895
907[107]	1.829033	0.596750	3.87641	7.28852

nonrelativistic energy. We observe that the number of converged digits for the expectation values falls within the range of 8-10 digits. Furthermore, the agreement between the values obtained for the largest basis size (3235) and the literature values from Strasburger et al. [107], who used Gaussian lobe functions, demonstrates the correctness of the formulas for the expectation values of interparticle distances (Equations 85, 87, and 89).

The matrix elements of these operators are derived from the matrix elements of the Dirac delta function (84, 86, 88). The good agreement of the interparticle distances with the literature values confirms the correctness of the expressions (84, 86, 88) for the Dirac delta function—a crucial quantity encountered in relativistic effect computations. However, since the Dirac delta function is a singular operator [15, 23]—localized in coordinate space—the convergence of its expectation values is approximately two times worse than nonsingular operators, such as total nonrelativistic energy and interparticle distances

Table 4: The expectation values of various interparticle distances for a fixed nucleus of Li atom in ^2D state

Basis size	$1/r_i^2$	$1/r_{ij}^2$	r_i^2	r_{ij}^2	$\mathcal{P}(1/r_{ij}^3)$
500	9.95647739	1.370656766	42.1761489	84.377990	0.04441
1000	9.95649201	1.370653008	42.1774696	84.380656	0.05611
1500	9.95649266	1.370652837	42.1774321	84.380590	0.05890
2380	9.95649278	1.370652799	42.1774436	84.380620	0.05972
3235	9.95649281	1.370652785	42.1774442	84.380621	0.06054
907[107]			42.177	84.3805	

reported above. This difference is illustrated in Tables 5 and 6, where we verify the correctness of the mathematical expressions derived for the matrix elements of operators encountered in leading relativistic corrections. In addition to the Dirac delta function, another singular term encountered in relativistic computations is the Mass-Velocity operator discussed in Section 9. The number of converged digits for its expectation values is also two times fewer than the nonrelativistic energy values (Table 6), which is, of course, an expected behavior.

Table 5: The expectation values of nonrelativistic energy and relativistic correction operators for fixed nucleus of Li atom in ^2D state

Basis size	E_{nr}	$\delta(\boldsymbol{r}_i)$	$\delta(\boldsymbol{r}_{ij})$	MV	OO
500	-7.335 522 7732	4.562953	0.1774807	-77.571760	-0.426939
1000	-7.335 523 5016	4.566500	0.1773350	-77.622550	-0.427653
1500	-7.335 523 5351	4.567150	0.1773061	-77.632002	-0.427753
2380	-7.335 523 5412	4.567357	0.1772982	-77.634936	-0.427470
3235	-7.335 523 5428	4.567438	0.1772910	-77.636605	-0.427122
6000[76]	-7.335 523 5430	4.567277	0.1769848	-77.635961	-0.427815
907[107]	-7.335 523 5250				

There are several techniques to improve the convergence of the expectation values of singular operators. These include the expectation value identity of Drachman [108], integral transform [109], the Hiller-Sucher-Feinberg (HSF) approach [110], and basis functions with linear prefactors [111] that can enhance the description of the cusp region. In our previous works [9, 15], for the simple Gaussian in Eq. (24) (function $\exp\left[-\boldsymbol{r}'\left(A_k \otimes \mathbf{I}\right)\boldsymbol{r}\right]$)

and for

$$z_{i_k} \exp\left[-\boldsymbol{r}'\left(A_k \otimes \mathbf{I}\right)\boldsymbol{r}\right], \tag{164}$$

we implemented Drachman's approach [108]. In this method, a singular operator can be replaced by a global non-singular operator, ensuring that its expectation value with the exact wave function matches that of the corresponding singular operator. In my master's thesis [112], we successfully implemented this approach for the basis function in (164) necessary for quantum systems with a single p electron and for angular momentum state $L = 1$. Extending this method to the basis functions considered in this dissertation requires significantly more work, as the functions in this thesis are more challenging to work with. Hence, this project is one of the future research directions.

As we can observe from Table 5, the number of converged digits for the Orbit-Orbit operator is the same as singular operators despite being the nonsingular operator. This means that there may be potential bugs in the codes for the analytical expressions derived for them in Section 10. As observed, there are hundreds of integrals and terms that need to be summed properly, requiring careful analysis. Therefore, rechecking all the lengthy and cumbersome analytical expressions for the expectation values of Orbit-Orbit operator needs to be performed multiple times, and the codes implemented for them need to be debugged to search for potential bugs. This is also one of the projects that need to be accomplished. A final remark regarding the relativistic operators that depend on the spin of particles, such as Spin-Orbit and Spin-Spin corrections, should be mentioned. Expectation values of these operators with the basis functions considered in this dissertation were recently accomplished with outstanding master student Pavel Rzhevskii at the Physics department. Specific applications regarding the fine structure splittings with spin-dependent relativistic operators will be published in scientific journals once well-optimized basis functions are available. It is worth noting that the project of spin-dependent relativistic operators with the functions (24) and (164) was accomplished by distinguished researcher and previous postdoctoral scholar at the Physics department, Dmitry Tumakov.

Table 6: The expectation values of nonrelativistic energy and some operators for ^{9}Be atom in ^2D state.

Basis	$E_{\rm nr}$	$\delta(\boldsymbol{r}_i)$	$\delta(\boldsymbol{r}_{ij})$	MV	$\mathcal{P}(1/r_{ij}^3)$
2000	-14.407 350 12	8.632429	0.255743	-263.5366	-1.16845
3000	-14.407 351 01	8.633125	0.255690	-263.5508	-1.16452
4000	-14.407 351 22	8.634206	0.255645	-263.5790	-1.16060
5000	-14.407 351 30	8.634697	0.255622	-263.5913	-1.15842
6000	-14.407 351 32	8.634783	0.255620	-263.5931	-1.15830
6900[75]	-14.407 351 34	8.634567	0.254950	-263.6024	
8192[77]	-14.407 351 38	8.636422	0.256903	-263.6262	-1.15303

12.2 Boron atom

The boron atom is composed of five electrons bound to nucleus containing five protons. In theoretical investigations of the boron atom, the majority of previous efforts have concentrated on the ground state (e.g. see [113–115]). Ruiz conducted preliminary Hylleraas-CI calculations [116], and highly precise nonrelativistic energies were computed using the explicitly correlated $\boldsymbol{r}_{12}$-MR-CI method [117], along with diffusion Monte Carlo (DMC) simulations [118]. Almora-Diaz and Bunge performed an extensive CI calculation [119], incorporating an orbital basis with functions corresponding to the l quantum number, reaching up to 20 (z-type orbitals). This approach yielded an energy only 31 μ-hartree above the variational limit, with a well-fitted extrapolation to the complete basis set missing this limit by 6 μ-hartree. The most accurate calculations were performed by explicitly correlated Gaussian functions (ECG) [120, 121], with the estimated error of the nonrelativistic energy for this state being less than 1 μ-hartree. Comparable precision was reached for the doublet S states [120], and transition energies between the ground state and S-symmetry states were reproduced within a fraction of cm^{-1}. These calculations took into consideration finite nuclear mass, relativistic effects (including fine and hyperfine structure for the ground-state term), and included leading radiative corrections.

Accurate wave functions and energies for the even parity quartet P and doublet D states, with comparable precision, are notably absent in the literature, as indicated by limited findings [122–126]. One of the applications of this dissertation is to address this gap by providing comprehensive results, thereby contributing to the resolution of discrepancies

related to the energy differences between the spin doublet and quartet terms of the boron atom. The future works will include reporting the use of well-optimized basis functions for these states and computing the relativistic effects, including both the spin-independent and dependent parts.

For preliminary results, in Table 7, we list the existing energy levels of the boron atom from the NIST atomic spectra database [127] and also report the current calculations using the functions in this work with estimated uncertainties.

In Tables 8, 9, and 10, we additionally report the nonrelativistic energies of the boron atom with an increasing number of basis functions. The energies are presented in atomic unities, and the considered levels include the lowest 10 doublet D states and the single existing quartet P state. All these calculations yield the lowest nonrelativistic energies ever obtained for these states. This can be speculated from Table 8, where for both ground ^2D and ^4P states, we have lower values than the benchmark energies recently obtained by Strasburger with Gaussian lobe functions [126].

Table 7: The existing energy levels of the boron atom with their configurations and term symbols. The calculated nonrelativistic (NR) energies in this dissertation are written in the third column in atomic units (a.u.)

Configuration	Term symbol	NR energy	Basis
$2s^2 2p$	$^2P^o$	-24.65386853[a]	16000
$2s2p^2$	^4P	-24.5220418(9)	10000
$2s^2 3s$	^2S	-24.47139364[a]	16000
$2s2p^2$	^2D	-24.4359815(8)	10000
$2s^2 3p$	$^2P^o$	-24.43234361[a]	16000
$2s^2 3d$	^2D	-24.4043112(8)	10000
$2s^2 4s$	^2S	-24.40318930[a]	16000
$2s^2 4p$	$^2P^o$	-24.39053870[a]	16000
$2s^2 4d$	^2D	-24.3804857(8)	10200
$2s^2 4f$	$^2F^o$		
$2s^2 5s$	^2S	-24.37979190[a]	16000
$2s^2 5p$	$^2P^o$	-24.37391548[a]	16000
$2s^2 6s$	^2S	-24.36916705[a]	16000
$2s^2 5d$	^2D	-24.3691271(8)	10000
$2s^2 5f$	$^2F^o$		
$2s^2 6p$	$^2P^o$	-24.36559000[a]	16000
$2s2p^2$	^2S	-24.36433000[a]	16000
$2s^2 6d$	^2D	-24.3629301(8)	10800
$2s^2 6f$	$^2F^o$		
$2s^2 7s$	^2S	-24.36156342[a]	16000
$2s^2 7p$	$^2P^o$	-24.36081896[a]	16000
$2s^2 7d$	^2D	-24.3591901(7)	10800
$2s^2 7f$	$^2F^o$		
$2s^2 8s$	^2S	-24.35861529[a]	16000
$2s^2 8p$	$^2P^o$	-24.35783220[a]	16000
$2s^2 8d$	^2D	-24.3567563(7)	10000
$2s^2 8f$	$^2F^o$		
$2s^2 9s$	^2S	-24.35640381[a]	16000
$2s^2 9p$	$^2P^o$	-24.35582553[a]	16000
$2s^2 9d$	^2D	-24.3550745(6)	10200
$2s^2 9f$	$^2F^o$	-24.35439767[a]	16000

[a] from manuscript of prof. Sergiy Bubin

Configuration	Term symbol	NR energy	Basis size
$2s^2 10s$	^2S	-24.35480808[a]	16000
$2s^2 10d$	^2D	-24.3538253(6)	9000
$2s^2 10f$	$^2F^o$		
$2s^2 11d$	^2D	-24.3527981(5)	7100
$2s^2 11f$	$^2F^o$		
$2s^2 12d$	^2D		
$2s^2 13d$	^2D		
...	...		
$2s^2 39d$	^2D		

Table 8: Nonrelativistic energies (NR energies) in atomic units (a.u.) of the boron atom in the lowest ten ^2D states and one ^4P state with the number of basis functions.

	Basis size	$2s2p^2\,(^4P)$	$2s2p^2\,(^2D)$	$2s^23d\,(^2D)$
^{11}B	4000	−24.520 826 431	−24.434 749 079	−24.403 058 043
	5000	−24.520 826 847	−24.434 756 493	−24.403 062 705
	6000	−24.520 827 047	−24.434 760 616	−24.403 064 628
	7000	−24.520 827 150	−24.434 762 907	−24.403 065 659
	8000	−24.520 827 211	−24.434 764 267	−24.403 066 230
	9000	−24.520 827 254	−24.434 765 121	−24.403 066 594
	10 000		−24.434 765 632	−24.403 066 814
$^{\infty}$B	9000	−24.522 041 775		
	10 000		−24.435 981 539	−24.404 311 199
		ECG lobe functions [126]		
$^{\infty}$B	4672	−24.522 041 430		
	8231		−24.435 981 009	

Table 9: Nonrelativistic energies (NR energies) in atomic units (a.u.) of the boron atom in the low lying ^2D states with the number of basis functions.

	Basis size	$2s^24d\,(^2D)$	$2s^25d\,(^2D)$	$2s^26d\,(^2D)$	$2s^27d\,(^2D)$
^{11}B	5000	−24.379 237 595	−24.367 879 014	−24.361 678 069	−24.357 929 174
	6000	−24.379 239 130	−24.367 880 803	−24.361 681 650	−24.357 937 371
	7000	−24.379 239 969	−24.367 881 775	−24.361 683 686	−24.357 941 469
	8000	−24.379 240 467	−24.367 882 365	−24.361 684 826	−24.357 943 702
	9000	−24.379 240 789	−24.367 882 749	−24.361 685 477	−24.357 945 032
	10 000	−24.379 241 002	−24.367 882 981	−24.361 685 894	−24.357 945 953
$^{\infty}$B	10 000	−24.380 485 678	−24.369 127 047	−24.362 929 984	−24.359 190 112

Table 10: Nonrelativistic energies (NR energies) in atomic units (a.u.) of the boron atom in the low lying ^2D states with the number of basis functions.

	Basis size	$2s^2 8d\,(^2D)$	$2s^2 9d\,(^2D)$	$2s^2 10d\,(^2D)$	$2s^2 11d\,(^2D)$
^{11}B	5000	−24.355 482 385	−24.353 765 598	−24.352 426 871	−24.351 096 727
	6000	−24.355 496 338	−24.353 794 514	−24.352 562 789	−24.351 562 748
	7000	−24.355 503 528	−24.353 810 093	−24.352 582 195	
	8000	−24.355 507 990	−24.353 819 198		
	9000	−24.355 510 842	−24.353 825 921		
	10 000	−24.355 512 868	−24.353 830 656		
$^{\infty}$B	10 000	−24.356 756 319	−24.355 074 492	−24.353 825 246	−24.352 798 061

12.3 Carbon atom

The carbon atom is composed of six electrons bound to nucleus containing six protons. In theoretical investigations of the carbon atom, as can be expected, the majority of previous efforts have concentrated on the ground state. This atom possess the most extensive chemistry among all elements, sees a prolific output of scientific articles each year, presenting diverse calculations on carbon compounds. However, accurately determining the properties of the carbon atom through theoretical means, with precision comparable to spectroscopic experiments, remains a challenge for computational chemistry. While this dissertation does not present a definitive solution to this challenge, one of the main applications of the present work is more modest—to showcase that an explicitly correlated wave function can achieve an energy accuracy of μ-hartree for a six-electron atom or for seven particle quantum systems. Historically, the best variational nonrelativistic energy for the carbon atom ground state was achieved in 1974 using the configuration interaction (CI) method [113], employing Slater orbitals with the angular momentum quantum number l up to 6 and up to quadruply excited configurations. A recent CI calculation, with configurations carefully selected but built from orbitals with l limited to 4, yielded slightly higher energy [128]. Comparing this work with studies on the boron atom and anion (discussed in the next section 12.4), which is isoelectronic with the carbon atom ground state [119], reveals that orbitals with much higher l are necessary to construct a many-electron basis capable of achieving an accuracy of about 1 m-hartree.

While CI variational energies have been surpassed by calculations using explicitly

correlated Gaussian (ECG) functions implemented in the form of $\boldsymbol{r}'\boldsymbol{W}_k\boldsymbol{r}\exp\left[-\boldsymbol{r}'\boldsymbol{A}_k\boldsymbol{r}\right]$ [23, 72], the reported results were only about 1.5 m-hartree above the estimate of the exact nonrelativistic energy [129]. Nonvariational methods such as coupled clusters with an exponential correlation factor (CC-F12) [130], diffusion quantum Monte Carlo simulations [118, 131], and "the free complement" method [125] have also approached this estimate. However, discrepancies among reported results persist, even by a few millihartree, and the standard deviations provided in some references [118, 125, 131] do not overlap.

The best literature values were reported in 2019 by Strasburger, employing Gaussian lobe functions [10]. In the article, he estimated new exact limits of the nonrelativistic energies for the ground state (^3P) and the odd-parity quintet S state ($^5S^o$). Furthermore, by incorporating finite nuclear masses and leading scalar relativistic corrections into the calculations, he reproduced the experimental excitation energy of the carbon atom with a precision of approximately 7 cm^{-1}. In this thesis, we enhanced the nonrelativistic energy calculation, extending it not only to ground state energies but also to those of excited states for various symmetries of the carbon atom. All the energies calculated in this dissertation, out of the existing carbon atom levels (refer to Table 15 from the NIST atomic spectra database [132]), are considered to be the lowest ever calculated. These values, along with the increasing number of basis functions, are reported in Tables 11 through 14. We also include the case of infinite mass energies for comparison with existing literature values, although only a few literature values for excited states are available, as mentioned before.

Table 11: Nonrelativistic energies (NR energies) in atomic units (a.u.) of the carbon atom in the lowest two ^3P and ^1P states with the number of basis functions.

	Basis size	$2s^22p^2\,(^3P)$	$2s^22p3p\,(^3P)$	$2s^22p^2\,(^1P)$	$2s^22p3p\,(^1P)$
^{12}C	1000	−37.842 598 0	−37.517 035 7	−37.528 964 4	−37.475 317 8
	2000	−37.843 024 8	−37.517 700 5	−37.529 314 1	−37.475 868 5
	3000	−37.843 110 2	−37.517 839 0	−37.529 370 1	−37.475 959 2
	4000	−37.843 139 8	−37.517 886 7	−37.529 400 8	−37.476 012 6
	5000	−37.843 157 6	−37.517 917 0	−37.529 416 5	−37.476 040 6
	6000	−37.843 168 2	−37.517 934 8		
	7000	−37.843 175 0	−37.517 946 1		
	8000	−37.843 179 3	−37.517 953 5		
	9000	−37.843 182 3	−37.517 956 8		
$^{\infty}$C	5000			−37.531 130 6	−37.477 753 5
	8000	−37.844 891 3	−37.519 667 5		
	9000	−37.844 894 3	−37.519 670 2		
		ECG lobe functions [10]			
$^{\infty}$C	5896	−37.844 889 402			
		Variational Monte Carlo [131]			
$^{\infty}$C			−37.496 97(5)		

Table 12: Nonrelativistic energies (NR energies) in atomic units (a.u.) of the carbon atom in the lowest two ^3D and ^1D states with the number of basis functions.

	Basis size	$2s^22p^2\,(^3D)$	$2s^22p3p\,(^3D)$	$2s^22p^2\,(^1D)$	$2s^22p3p\,(^1D)$
^{12}C	1000	−37.524 932 9	−37.474 086 8	−37.796 665 9	−37.511 477 5
	2000	−37.525 328 9	−37.474 701 7	−37.796 179 3	−37.512 074 4
	3000	−37.525 400 1	−37.474 806 2	−37.796 755 7	−37.512 193 2
	4000	−37.525 440 4	−37.474 867 2	−37.796 796 1	−37.512 249 2
	5000	−37.525 461 4	−37.474 899 8	−37.796 815 1	−37.512 265 2
	6000	−37.525 468 6	−37.474 916 8	−37.796 833 9	−37.512 302 6
$^{\infty}$C	6000	−37.527 188 1	−37.476 636 3	−37.798 543 3	−37.514 012 9

Table 13: Nonrelativistic energies (NR energies) in atomic units (a.u.) of the carbon atom in the lowest two $^3P^o$ and $^1P^o$ states with the number of basis functions.

	Basis size	$2s^2 2p^2\,(^3P^o)$	$2s^2 2p3p\,(^3P^o)$	$2s^2 2p^2\,(^1P^o)$	$2s^2 2p3p\,(^1P^o)$
^{12}C	1000	−37.567 355 8	−37.489 412 1	−37.560 140 0	−37.484 863 3
	2000	−37.567 844 8	−37.498 127 4	−37.560 553 5	−37.485 632 1
	3000	−37.567 937 0	−37.499 177 7	−37.560 627 6	−37.485 780 5
	4000	−37.567 990 1	−37.499 756 4	−37.560 671 4	−37.485 917 7
	5000	−37.568 018 6	−37.500 065 5	−37.560 694 8	−37.486 033 3
	5500	−37.568 028 1	−37.500 125 3	−37.560 705 7	−37.486 075 2
$^{\infty}$C	5500	−37.569 747 1	−37.501 850 8	−37.562 420 3	−37.488 012 9

Table 14: Nonrelativistic energies (NR energies) in atomic units (a.u.) of the carbon atom in the lowest two ^3S and ^1S states with the number of basis functions.

	Basis size	$2s^2 2p^2\,(^3S)$	$2s^2 2p3p\,(^3S)$	$2s^2 2p^2\,(^1S)$	$2s^2 2p3p\,(^1S)$
^{12}C	1000	−37.519 648 8	−37.471 512 5	−37.744 117 3	−37.504 573 7
	2000	−37.520 507 9	−37.472 988 6	−37.744 540 6	−37.505 648 8
	3000	−37.520 645 4	−37.473 224 2	−37.744 602 6	−37.505 693 6
	4000	−37.520 724 0	−37.473 372 6	−37.744 639 7	−37.505 917 7
	5000	−37.520 765 1	−37.473 460 9	−37.744 656 7	−37.506 533 3
$^{\infty}$C	5000	−37.522 485 0	−37.475 097 4	−37.746 366 1	−37.507 972 9

Table 15: The existing energy levels of the carbon atom with their configurations and term symbols. The calculated nonrelativistic (NR) energies in this dissertation are written in the third column in atomic units (a.u.)

Configuration	Term symbol	NR energy	Basis
$2s^2 2p^2$	^3P	-37.8448943(7)	9000
$2s^2 2p^2$	^1D	-37.7985433(6)	6000
$2s^2 2p^2$	^1S	-37.7463661(6)	5000
$2s2p^3$	$^5S^o$	-37.6917478[b]	4023
$2s^2 2p3s$	$^3P^o$	-37.5697471(6)	5500
$2s^2 2p3s$	$^1P^o$	-37.5624203(6)	5500
$2s2p^3$	$^3D^o$		
$2s^2 2p3p$	^1P	-37.5311306(6)	5000
$2s^2 2p3p$	^3D	-37.5271881(7)	6000
$2s^2 2p3p$	^3S	-37.5224850(6)	5000
$2s^2 2p3p$	^3P	-37.5196702(6)	9000
$2s^2 2p3p$	^1D	-37.5140129(5)	6000
$2s^2 2p3p$	^1S	-37.5079729(4)	3000
$2s2p^3$	$^3P^o$	-37.5018508(6)	5500
$2s^2 2p3d$	$^1D^o$		
$2s2p4s$	$^3P^o$		
$2s^2 2p3d$	$^3F^o$		
$2s^2 2p3d$	$^3D^o$		
$2s^2 2p4s$	$^1P^o$	-37.4880129(6)	5500
$2s^2 2p3d$	$^1F^o$		
$2s^2 2p3d$	$^1P^o$		
$2s^2 2p3d$	$^3P^o$		
$2s^2 2p4p$	^1P	-37.4777535(6)	5000
$2s^2 2p4p$	^3D	-37.4766363(6)	6000
$2s^2 2p4p$	^3S	-37.4750974(5)	5000
$2s^2 2p4p$	^3P	-37.4741856(4)	4200
$2s^2 2p4p$	^1D		
$2s^2 2p4p$	^1S		
$2s^2 2p4d$	$^1D^o$		
$2s2p5s$	$^3P^o$		
$2s^2 2p4d$	$^3F^o$		
$2s^2 2p4d$	$^3D^o$		

[b] K. Strasburger, Phys. Rev. A 99, 52512 (2019) [10]

Configuration	Term symbol	NR energy	Basis
$2s^2 2p5s$	$^1P^o$		
$2s^2 2p4d$	$^1F^o$		
$2s^2 2p4d$	$^1P^o$		
$2s^2 2p4d$	$^3P^o$		
$2s^2 2p5p$	^1P		
$2s^2 2p5p$	^3D		
$2s^2 2p5p$	^3P	-37.4564025(4)	3200
$2s^2 2p5p$	^1D		
$2s^2 2p5p$	^1S		
$2s^2 2p5d$	$^1D^o$		
$2s^2 2p5d$	$^3F^o$		
$2s^2 2p6s$	$^3P^o$		
$2s^2 2p5d$	$^3D^o$		
$2s^2 2p6s$	$^1P^o$		
$2s^2 2p5d$	$^1F^o$		
$2s^2 2p5d$	$^1P^o$		
$2s^2 2p5d$	$^3P^o$		
$2s^2 2p6p$	^1P		
$2s^2 2p6p$	^3D		
$2s^2 2p6p$	^3P	-37.4563817(4)	3100
$2s^2 2p6p$	^1D		
$2s^2 2p6p$	^1S		
$2s^2 2p6d$	$^1D^o$		
$2s^2 2p6d$	$^3F^o$		
$2s^2 2p7s$	$^3P^o$		
$2s^2 2p6d$	$^3D^o$		
$2s^2 2p7s$	$^1P^o$		
$2s^2 2p6d$	$^1F^o$		
$2s^2 2p6d$	$^1P^o$		
$2s^2 2p6d$	$^3P^o$		
$2s^2 2p7p$	^1P		
$2s^2 2p7p$	^3D		
$2s^2 2p7p$	^3P	-37.4295133(3)	2000
$2s^2 2p7p$	^1D		
$2s^2 2p7p$	^1S		
...	...		

12.4 Boron anion

The boron anion, denoted as B^-, is characterized as the least stable among weakly bound anions. In contrast, H^-, C^-, O^-, and F^- exhibit stability, while Li^- is weakly bound, and He^- and Be^- are considered metastable [133–135]. The less stability of B^- is attributed to accommodating the odd electron in the outermost orbital and the nuclear charge being screened by doubly occupied inner shells. Atomic anions typically possess low binding energy and share approximately the same amount of energy as correlation energy. Despite the smaller nuclear charge (Z) compared to the number of electrons, this difference does not pose significant computational challenges. However, the diffuse nature of the single occupied orbital presents challenges in standard one-electron basis sets. Consequently, achieving good agreement with experimental data often requires highly correlated wave functions [135]. Various strategies share a common approach of initiating with robust methods like Multiconfigurational Hartree-Fock (MCHF) [136], Coupled Cluster (CC) theory [137], or Configuration Interaction (CI) [133, 138] to capture a substantial portion of the correlation energy. Further refinements involve adding relativistic corrections or those related to the Born-Oppenheimer approximation.

In this dissertation, we perform nonrelativistic calculations using the same input file as for the Carbon atom ^3P state, with small adjustments. The adjustment involves simply reducing the charge of the nucleus by 1 and performing a similar basis building and optimization program. In Table 16, we present the nonrelativistic energies calculated with an increasing number of basis functions for the ground ^3P state of the boron anion. We also include the best literature value obtained by Configuration Interaction method [119] for comparison with our results. It is evident that all the calculations performed in this dissertation represent new lower bound energies, demonstrating the robustness of the method described herein.

Table 16: Nonrelativistic energy calculation of the ground ^3P state of the boron anion with the number of basis functions

	Basis	NR energy
^{11}B	1000	-24.662021
	2000	-24.662632
	3000	-24.662803
	4000	-24.662872
	4500	-24.662887
$^{\infty}$B	4500	-24.664125
Configuration interation (CI) [119]		
$^{\infty}$B	STO($l = 24$)	-24.66401395

13 Conclusion

In conclusion, this dissertation explored the products of Explicitly Correlated Gaussians (ECGs) and bipolar harmonics within the Rayleigh-Ritz variational method, presenting an efficient approach to accurately describe arbitrary quantum systems in the S, P, and D states of even parity. The considered functions are suitable for configurations where two particles possess orbital angular momenta $l_i = 1$ (coupling to $L = 0, 1, 2$) or a single particle with $l_i = 2; (L = 2)$, while other particles carry zero angular momentum ($l_i = 0$). The developed scheme, employing the form $[\boldsymbol{v}'_k\boldsymbol{r}][\boldsymbol{w}'_k\boldsymbol{r}]\exp[-\boldsymbol{r}'\boldsymbol{A}_k\boldsymbol{r}]$, represents a significant improvement over previously used forms, resulting in a substantial increase in computational efficiency, ranging from 1 to 2 orders of magnitude.

This advancement is crucial not only for enhancing the precision of numerical calculations but also for opening new avenues in high-precision computations of few-particle quantum systems, including atoms, molecules, and positronic complexes, with spectroscopic accuracy. The dissertation provided detailed derivations and compact expressions for matrix elements of various operators (e.g, Dirac delta function, mass-velocity) necessary for high-accuracy calculations, facilitating their straightforward implementation into a computer program.

Furthermore, the dissertation discussed and presented benchmark results from various calculations of nonrelativistic energies for the low-lying levels of carbon and boron atoms. For these calculations, computer codes based on the formulas developed in this dissertation

were utilized. In addition to the new scheme for deriving matrix elements, it is noteworthy that the implemented algorithm includes an independent optimization routine for integer indices labeling the particles. This optimization method enhances the overall robustness of the development introduced in this dissertation, facilitating calculations on systems with more than one nucleus.

Looking ahead, it is essential to underscore that the test calculations presented herein were primarily conducted to validate the new algorithm for computing matrix elements, encompassing various operators encountered in leading relativistic corrections. In future research works, the focus will shift to specific applications, particularly those targeting bound states of atoms, ions (e.g. the boron anion in 12.4), and systems with exotic particles such as positrons, once a sufficient number of basis functions are available. Given the concentration on 6-7 particle systems, obtaining high-quality basis functions necessary for achieving spectroscopic accuracy requires several months of calculations on computer clusters. Therefore, the majority of applications stemming from the developments in this dissertation, along with more comprehensive numerical data and detailed analyses, will be presented in future publications in scientific journals.

Bibliography

[1] W. Kołos and L. Wolniewicz, "Nonadiabatic Theory for Diatomic Molecules and Its Application to the Hydrogen Molecule," Rev. Mod. Phys. **35**, 473 (1963).

[2] G. W. F. Drake, "Second Bound State for the Hydrogen Negative Ion," Phys. Rev. Lett. **24**, 126 (1970).

[3] G. W. F. Drake and R. A. Swainson, "Quantum defects and the 1/n dependence of Rydberg energies: Second-order polarization effects," Phys. Rev. A **44**, 5448 (1991).

[4] Z.-C. Yan and G. W. F. Drake, "Computational methods for three-electron atomic systems in Hylleraas coordinates," Journal of Physics B: Atomic, Molecular and Optical Physics **30**, 4723 (1997).

[5] V. I. Korobov, "Coulomb three-body bound-state problem: Variational calculations of nonrelativistic energies," Phys. Rev. A **61**, 064503 (2000).

[6] H. Nakatsuji, H. Nakashima, Y. Kurokawa, and A. Ishikawa, "Solving the Schrödinger Equation of Atoms and Molecules without Analytical Integration Based on the Free Iterative-Complement-Interaction Wave Function," Phys. Rev. Lett. **99**, 240402 (2007).

[7] G. G. Ryzhikh and J. Mitroy, "Positronic Lithium, an Electronically Stable Li-e^+ Ground State," Phys. Rev. Lett. **79**, 4124 (1997).

[8] S. Bubin and O. V. Prezhdo, "Excited States of Positronic Lithium and Beryllium," Phys. Rev. Lett. **111**, 193401 (2013).

[9] S. Bubin and L. Adamowicz, "Lowest ^2S Electronic Excitations of the Boron Atom," Phys. Rev. Lett. **118**, 043001 (2017).

[10] K. Strasburger, "Explicitly correlated wave functions of the ground state and the lowest quintuplet state of the carbon atom," Phys. Rev. A **99**, 052512 (2019).

[11] C. D. Lin, "Properties of doubly-excited states of Li- and Be: the study of electron correlations in hyperspherical coordinates," Journal of Physics B: Atomic and Molecular Physics **16**, 723 (1983).

[12] W. Cencek and W. Kutzelnigg, "Accurate relativistic energies of one- and two-electron systems using Gaussian wave functions," The Journal of Chemical Physics **105**, 5878 (1996).

[13] W. Cencek, J. Rychlewski, R. Jaquet, and W. Kutzelnigg, "Sub-microhartree accuracy potential energy surface for H_3^+ including adiabatic and relativistic effects. I. Calculation of the potential points," J. Chem. Phys. **108**, 2831 (1998).

[14] S. Bubin and K. Varga, "Ground-state energy and relativistic corrections for positronium hydride," Phys. Rev. A **84**, 012509 (2011).

[15] S. Nasiri, T. Shomenov, S. Bubin, and L. Adamowicz, "High-accuracy calculations of the lowest eleven Rydberg ^{2}P states of Li atom," J. Phys. B **54**, 085003 (2021).

[16] J.-M. Richard, "Stability of the hydrogen and hydrogenlike molecules," Phys. Rev. A **49**, 3573 (1994).

[17] K. Strasburger, "Binding energy, structure, and annihilation properties of the positron-LiH molecule complex, studied with explicitly correlated Gaussian functions," The Journal of Chemical Physics **111**, 10555 (1999).

[18] W. Cencek and J. Rychlewski, "Benchmark calculations for He_2^+ and LiH molecules using explicitly correlated Gaussian functions," Chem. Phys. Lett. **320**, 549 (2000).

[19] M. Stanke, D. Kędziera, S. Bubin, M. Molski, and L. Adamowicz, "Lowest vibrational states of $^4He^3He^+$: Non-Born-Oppenheimer calculations," Phys. Rev. A **76**, 052506 (2007).

[20] S. Bubin, M. Stanke, D. Kędziera, and L. Adamowicz, "Improved calculations of the lowest vibrational transitions in HeH^+," Phys. Rev. A **76**, 022512 (2007).

[21] K. Pachucki and J. Komasa, "Nonadiabatic corrections to rovibrational levels of H_2," J. Chem. Phys. **130**, 164113 (2009).

[22] J. Mitroy, S. Bubin, W. Horiuchi, Y. Suzuki, L. Adamowicz, W. Cencek, K. Szalewicz, J. Komasa, D. Blume, and K. Varga, "Theory and application of explicitly correlated Gaussians," Rev. Mod. Phys. **85**, 693 (2013).

[23] S. Bubin, M. Pavanello, W.-C. Tung, K. L. Sharkey, and L. Adamowicz, "Born–Oppenheimer and Non-Born–Oppenheimer, Atomic and Molecular Calculations with Explicitly Correlated Gaussians," Chem. Rev. **113**, 36 (2013).

[24] J. P. Karr, F. Bielsa, T. Valenzuela, A. Douillet, L. Hilico, and V. I. Korobov, "High-accuracy calculations in the H_2^+ molecular ion: towards a measurement of m_p/m_e," Can. J. Phys. **85**, 497 (2007).

[25] Z.-C. Yan, W. Nörtershäuser, and G. W. F. Drake, "High Precision Atomic Theory for Li and Be^+: QED Shifts and Isotope Shifts," Phys. Rev. Lett. **100**, 243002 (2008).

[26] D. C. Morton, Q. Wu, and G. W. F. Drake, "Nuclear charge radius for ^{3}He," Phys. Rev. A **73**, 034502 (2006).

[27] G. Drake and Z.-C. Yan, "Studies of light halo nuclei by the isotope shift method," Hyperfine Interact. **172**, 141 (2006).

[28] G. W. F. Drake and Z.-C. Yan, "Properties of halo nuclei from atomic isotope shifts," Nucl. Phys. A **790**, 151c (2007).

[29] K. Pachucki and A. M. Moro, "Nuclear polarizability of helium isotopes in atomic transitions," Phys. Rev. A **75**, 032521 (2007).

[30] M. Stanke, D. Kędziera, M. Molski, S. Bubin, M. Barysz, and L. Adamowicz, "Convergence of Experiment and Theory on the Pure Vibrational Spectrum of HeH^+," Phys. Rev. Lett. **96**, 233002 (2006).

[31] M. Stanke, D. Kędziera, S. Bubin, and L. Adamowicz, "Lowest Excitation Energy of ^{9}Be," Phys. Rev. Lett. **99**, 043001 (2007).

[32] M. Stanke, J. Komasa, S. Bubin, and L. Adamowicz, "Five lowest ^1S states of the Be atom calculated with a finite-nuclear-mass approach and with relativistic and QED corrections," Phys. Rev. A **80**, 022514 (2009).

[33] S. Bubin, M. Stanke, and L. Adamowicz, "Vibrational transitions of the ^{7}LiH$^+$ ion calculated without the Born–Oppenheimer approximation and with leading relativistic corrections," J. Chem. Phys. **134**, 024103 (2011).

[34] B. A. Bushaw, W. Nörtershäuser, G. W. F. Drake, and H.-J. Kluge, "Ionization energy of ^{6,7}Li determined by triple-resonance laser spectroscopy," Phys. Rev. A **75**, 052503 (2007).

[35] V. I. Korobov, "Bethe logarithm for the helium atom," Phys. Rev. A **69**, 054501 (2004).

[36] K. Pachucki, "Helium energy levels including $m\alpha^6$ corrections," Phys. Rev. A **74**, 062510 (2006).

[37] K. Pachucki, "Improved Theory of Helium Fine Structure," Phys. Rev. Lett. **97**, 013002 (2006).

[38] M. Puchalski, D. Kędziera, and K. Pachucki, "Ionization potential for excited S states of the lithium atom," Phys. Rev. A **82**, 062509 (2010).

[39] G. D. Dickenson, M. L. Niu, E. J. Salumbides, J. Komasa, K. S. E. Eikema, K. Pachucki, and W. Ubachs, "Fundamental Vibration of Molecular Hydrogen," Phys. Rev. Lett. **110**, 193601 (2013).

[40] D. Ceperley and B. Alder, "Quantum Monte Carlo," Science **231**, 555 (1986).

[41] B. L. Hammond, W. A. Lester, and P. J. Reynolds, *Monte Carlo Methods in Ab Initio Quantum Chemistry* (WORLD SCIENTIFIC, 1994).

[42] C. D. Sherrill and H. F. Schaefer III, "The configuration interaction method: Advances in highly correlated approaches," in *Advances in quantum chemistry*, Vol. 34 (Elsevier, 1999) pp. 143–269.

[43] R. J. Bartlett and G. D. Purvis, "Many-body perturbation theory, coupled-pair many-electron theory, and the importance of quadruple excitations for the correlation problem," Int. J. Quantum Chem. **14**, 561 (1978).

[44] R. Krivec, "Hyperspherical-Harmonics Methods for Few-Body Problems," Few-Body Syst. **25**, 199 (1998).

[45] C. Møller and M. S. Plesset, "Note on an Approximation Treatment for Many-Electron Systems," Phys. Rev. **46**, 618 (1934).

[46] R. J. Bartlett and G. D. Purvis, "Molecular Applications of Coupled Cluster and Many-Body Perturbation Methods," Phys. Scr. **21**, 255 (1980).

[47] C. F. Fischer and P. Jönsson, "MCHF calculations for atomic properties," Computer Physics Communications **84**, 37 (1994).

[48] J. Toulouse, R. Assaraf, and C. J. Umrigar, "Introduction to the variational and diffusion Monte Carlo methods," in *Advances in Quantum Chemistry*, Vol. 73 (Elsevier, 2016) pp. 285–314.

[49] B. Jeziorski and H. J. Monkhorst, "Coupled-cluster method for multideterminantal reference states," Physical Review A **24**, 1668 (1981).

[50] K. Sneskov and O. Christiansen, "Excited state coupled cluster methods," Wiley Interdisciplinary Reviews: Computational Molecular Science **2**, 566 (2012).

[51] P. Piecuch, S. A. Kucharski, and R. J. Bartlett, "Coupled-cluster methods with internal and semi-internal triply and quadruply excited clusters: CCSDt and CCSDtq approaches," The Journal of chemical physics **110**, 6103 (1999).

[52] H. J. Monkhorst, "Calculation of properties with the coupled-cluster method," International Journal of Quantum Chemistry **12**, 421 (1977).

[53] P. G. Szalay, M. Nooijen, and R. J. Bartlett, "Alternative ansätze in single reference coupled-cluster theory. III. A critical analysis of different methods," The Journal of Chemical Physics **103**, 281 (1995).

[54] C. Schwartz, "Further Computations of the He Atom Ground State," arXiv (2006), math-ph/0605018 .

[55] C. Schwartz, "Experiment and theory in computations of the He atom ground state," Int. J. Mod. Phys. E **15**, 877 (2006).

[56] S. F. Boys, "The Integral Formulae for the Variational Solution of the Molecular Many-Electron Wave Equations in Terms of Gaussian Functions with Direct Electronic Correlation," Proc. R. Soc. London, Ser. A **258**, 402 (1960).

[57] K. Singer, "The Use of Gaussian (Exponential Quadratic) Wave Functions in Molecular Problems. I. General Formulae for the Evaluation of Integrals," Proc. R. Soc. London, Ser. A **258**, 412 (1960).

[58] E. A. Hylleraas, "Über den grundzustand des heliumatoms," Zeitschrift für Physik **48**, 469 (1928).

[59] E. A. Hylleraas, "Neue Berechnung der Energie des Heliums im Grundzustande, sowie des tiefsten Terms von Ortho-Helium," Z. Phys. **54**, 347 (1929).

[60] Z.-C. Yan and G. W. F. Drake, "Eigenvalues and expectation values for the $1s^2 2s\ ^2S$, $1s^2 2p\ ^2P$, and $1s^2 3d\ ^2D$ states of lithium," Phys. Rev. A **52**, 3711 (1995).

[61] F. W. King, D. Quicker, and J. Langer, "Compact wave functions for the beryllium isoelectronic series, Li^- to Ne^{6+}: A standard Hylleraas approach," J. Chem. Phys. **134**, 124114 (2011).

[62] T. Kato, "On the eigenfunctions of many-particle systems in quantum mechanics," Commun. Pure Appl. Math. **10**, 151 (1957).

[63] V. I. Kukulin and V. M. Krasnopol'sky, "A stochastic variational method for few-body systems," J. Phys. G **3**, 795 (1977).

[64] K. Varga and Y. Suzuki, "Precise solution of few-body problems with the stochastic variational method on a correlated Gaussian basis," Phys. Rev. C **52**, 2885 (1995).

[65] Y. Suzuki and K. Varga, *Stochastic Variational Approach to Quantum-Mechanical Few-Body Problems*, Lecture Notes in Physics (Springer, Berlin, 1998).

[66] J. Rychlewski, *Explicitly Correlated Wave Functions in Chemistry and Physics: Theory and Applications*, Progress in Theoretical Chemistry and Physics (Kluwer, Dordrecht, 2003).

[67] S. Bubin and L. Adamowicz, "Matrix elements of N-particle explicitly correlated Gaussian basis functions with complex exponential parameters," J. Chem. Phys. **124**, 224317 (2006).

[68] S. Bubin and L. Adamowicz, "Energy and energy gradient matrix elements with N-particle explicitly correlated complex Gaussian basis functions with $L = 1$," J. Chem. Phys. **128**, 114107 (2008).

[69] K. L. Sharkey, M. Pavanello, S. Bubin, and L. Adamowicz, "Algorithm for quantum-mechanical finite-nuclear-mass variational calculations of atoms with two p electrons using all-electron explicitly correlated Gaussian basis functions," Phys. Rev. A **80**, 062510 (2009).

[70] K. L. Sharkey, N. Kirnosov, and L. Adamowicz, "An algorithm for quantum mechanical finite-nuclear-mass variational calculations of atoms with $L = 3$ using all-electron explicitly correlated Gaussian basis functions," J. Chem. Phys. **138**, 104107 (2013).

[71] J. Komasa, "Dipole and quadrupole polarizabilities and shielding factors of beryllium from exponentially correlated Gaussian functions," Phys. Rev. A **65**, 012506 (2001).

[72] K. L. Sharkey, S. Bubin, and L. Adamowicz, "Analytical energy gradient in variational calculations of the two lowest ^3P states of the carbon atom with explicitly correlated Gaussian basis functions," J. Chem. Phys. **132**, 184106 (2010).

[73] K. L. Sharkey, S. Bubin, and L. Adamowicz, "Refinement of the experimental energy levels of higher ^2D Rydberg states of the lithium atom with very accurate quantum mechanical calculations," J. Chem. Phys. **134**, 194114 (2011).

[74] K. L. Sharkey, S. Bubin, and L. Adamowicz, "Singlet–triplet energy splitting between ^1D and ^3D ($1s^2 2snd$) n=3,4,5, and 6, Rydberg states of the beryllium atom (^{9}Be) calculated with all-electron explicitly correlated Gaussian functions," Chem. Phys. Lett. **616-617**, 254 (2014).

[75] M. Stanke, E. Palikot, K. L. Sharkey, and L. Adamowicz, "Benchmark calculations of the ^1D Rydberg spectrum of beryllium," Chem. Phys. Lett. **779**, 138823 (2021).

[76] M. Stanke, E. Palikot, K. L. Sharkey, and L. Adamowicz, "Benchmark calculations of the ^2D Rydberg spectrum of lithium," Mol. Phys. **119**, e1925765 (2021).

[77] M. Puchalski, J. Komasa, and K. Pachucki, "Fine and hyperfine splitting of the low-lying states of ^{9}Be," Phys. Rev. A **104**, 022824 (2021).

[78] J. R. Magnus and H. Neudecker, *Matrix-Differential Calculus with Applications in Statistics and Econometrics* (Wiley, Chichester, 1988).

[79] T. Shomenov and S. Bubin, "Explicitly correlated Gaussians for high-precision variational calculations of S^e, P^e, and D^e states of quantum systems: An efficient algorithm," Phys. Rev. E **108**, 065308 (2023).

[80] D. J. Griffiths and D. F. Schroeter, *Introduction to quantum mechanics* (Cambridge university press, 2018).

[81] Y. Suzuki and K. Varga, *Stochastic variational approach to quantum-mechanical few-body problems*, Vol. 54 (Springer Science & Business Media, 1998).

[82] K. Varga, Y. Suzuki, and J. Usukura, "Global-Vector Representation of the Angular Motion of Few-Particle Systems," Few-Body Syst. **24**, 81 (1998).

[83] M. Hamermesh, *Group Theory and Its Application to Physical Problems* (Addison-Wesley, Reading, MA, 1962).

[84] R. Pauncz, *Spin Eigenfunctions* (Plenum, New York, 1979).

[85] R. Pauncz, *The Symmetric Group in Quantum Chemistry* (CRC Press, Boca Raton, 1995).

[86] D. C. Morton, Q. X. Wu, and G. W. F. Drake, "Energy levels for the stable isotopes of atomic helium(^{4}He I and ^{3}He I)," Can. J. Phys. **84**, 83 (2006).

[87] W. Kołos and L. Wolniewicz, "Potential-Energy Curve for the $B^1\Sigma_u^+$ State of the Hydrogen Molecule," J. Chem. Phys. **45**, 509 (1966).

[88] W. Kołos and L. Wolniewicz, "Polarizability of the Hydrogen Molecule," J. Chem. Phys. **46**, 1426 (1967).

[89] W. Kolos and L. Wolniewicz, "A complete non-relativistic treatment of the H_2 molecule," Phys. Lett. **2**, 222 (1962).

[90] W. E. Caswell and G. P. Lepage, "Effective lagrangians for bound state problems in QED, QCD, and other field theories," Phys. Lett. B **167**, 437 (1986).

[91] T. Kinoshita and M. Nio, "Radiative corrections to the muonium hyperfine structure: The $\alpha^2(Z\alpha)$ correction," Phys. Rev. D **53**, 4909 (1996).

[92] H. A. Bethe and E. E. Salpeter, *Quantum Mechanics of One- and Two-Electron Atoms* (Plenum, New York, 1977).

[93] M. Stanke, J. Komasa, D. Kędziera, S. Bubin, and L. Adamowicz, "Three lowest S states of $^9Be^+$ calculated with including nuclear motion and relativistic and QED corrections," Phys. Rev. A **77**, 062509 (2008).

[94] M. Stanke, J. Komasa, D. Kędziera, S. Bubin, and L. Adamowicz, "Accuracy limits on the description of the lowest S excitation in the Li atom using explicitly correlated Gaussian basis functions," Phys. Rev. A **78**, 052507 (2008).

[95] M. Stanke, D. Kędziera, S. Bubin, M. Molski, and L. Adamowicz, "Orbit-orbit relativistic corrections to the pure vibrational non-Born-Oppenheimer energies of H_2," J. Chem. Phys. **128**, 114313 (2008).

[96] A. I. Akhiezer and V. B. Berestetskii, *Quantum Electrodynamics* (John Wiley & Sons, New York, 1965).

[97] H. Araki, "Quantum-Electrodynamical Corrections to Energy-Levels of Helium," Prog. Theor. Phys. **17**, 619 (1957).

[98] J. Sucher, "Energy Levels of the Two-Electron Atom to Order α^3 ry; Ionization Energy of Helium," Phys. Rev. **109**, 1010 (1958).

[99] P. K. Kabir and E. E. Salpeter, "Radiative Corrections to the Ground-State Energy of the Helium Atom," Phys. Rev. **108**, 1256 (1957).

[100] K. Pachucki, "Simple derivation of helium Lamb shift," J. Phys. B **31**, 5123 (1998).

[101] Z.-C. Yan and G. W. F. Drake, "Relativistic and QED Energies in Lithium," Phys. Rev. Lett. **81**, 774 (1998).

[102] K. Pachucki and J. Komasa, "Relativistic and QED Corrections for the Beryllium Atom," Phys. Rev. Lett. **92**, 213001 (2004).

[103] K. Pachucki, "$\alpha^4 R$ corrections to singlet states of helium," Phys. Rev. A **74**, 022512 (2006).

[104] M. Stanke, A. Bralin, S. Bubin, and L. Adamowicz, "Leading relativistic corrections for atomic P states calculated with a finite-nuclear-mass approach and all-electron explicitly correlated Gaussian functions," Phys. Rev. A **97**, 012513 (2018).

[105] K. L. Sharkey, S. Bubin, and L. Adamowicz, "An algorithm for calculating atomic D states with explicitly correlated Gaussian functions," J. Chem. Phys. **134**, 044120 (2011).

[106] L. M. Wang, Z.-C. Yan, H. X. Qiao, and G. W. F. Drake, "Variational energies and the Fermi contact term for the low-lying states of lithium: Basis-set completeness," Phys. Rev. A **85**, 052513 (2012).

[107] K. Strasburger, "High angular momentum states of lithium atom, studied with symmetry-projected explicitly correlated Gaussian lobe functions," J. Chem. Phys. **141**, 044104 (2014).

[108] R. J. Drachman, "A new global operator for two-particle delta functions," J. Phys. B **14**, 2733 (1981).

[109] K. Pachucki, W. Cencek, and J. Komasa, "On the acceleration of the convergence of singular operators in Gaussian basis sets," J. Chem. Phys. **122**, 184101 (2005).

[110] J. Hiller, J. Sucher, and G. Feinberg, "New techniques for evaluating parity-conserving and parity-violating contact interactions," Phys. Rev. A **18**, 2399 (1978).

[111] K. Pachucki and J. Komasa, "Gaussian basis sets with the cusp condition," Chem. Phys. Lett. **389**, 209 (2004).

[112] T. Shomenov, "Expectation Values of Singular Operators in Variational Calculations of Atomic P-States," (2020).

[113] F. Sasaki and M. Yoshimine, "Configuration-interaction study of atoms. I. Correlation energies of B, C, N, O, F, and Ne," Phys. Rev. A **9**, 17 (1974).

[114] D. Feller and E. R. Davidson, "A multireference CI determination of the isotropic hyperfine constants for first row atoms B–F," The Journal of Chemical Physics **88**, 7580 (1988).

[115] H. Meyer, T. Müller, and A. Schweig, "Accurate inelastic scattering factors for lithium to argon calculated from MR-SDCI wavefunctions," Chemical Physics **191**, 213 (1995).

[116] P. E. Hoggan, M. B. Ruiz, and T. Özdogan, "Molecular integrals over slater-type orbitals. From pioneers to recent developments," Quantum Frontiers ofAtoms and Molecules , 64 (2011).

[117] R. J. Gdanitz, "Accurately solving the electronic Schrödinger equation of atoms and molecules using explicitly correlated (r12-)MR-CI. II. Ground-state energies of first-row atoms and positive atomic ions," The Journal of Chemical Physics **109**, 9795 (1998).

[118] P. Seth, P. L. Ríos, and R. J. Needs, "Quantum Monte Carlo study of the first-row atoms and ions," J. Chem. Phys. **134**, 084105 (2011).

[119] C. X. Almora-Díaz and C. F. Bunge, "Nonrelativistic CI calculations for B^+, B, and B^- ground states," Int. J. Quantum Chem. **110**, 2982 (2010).

[120] S. Bubin and L. Adamowicz, "Correlated-Gaussian calculations of the ground and low-lying excited states of the boron atom," Phys. Rev. A **83**, 022505 (2011).

[121] M. Puchalski, J. Komasa, and K. Pachucki, "Explicitly correlated wave function for a boron atom," Phys. Rev. A **92**, 062501 (2015).

[122] P. Jönsson and C. Froese Fischer, "Large-scale multiconfiguration Hartree-Fock and configuration-interaction calculations of isotope shifts and hyperfine structures in boron," Phys. Rev. A **50**, 3080 (1994).

[123] F. J. Gálvez, E. Buendía, and A. Sarsa, "Excited states of boron isoelectronic series from explicitly correlated wave functions," The Journal of Chemical Physics **122**, 154307 (2005).

[124] F. C. Fischer, S. Verdebout, M. Godefroid, P. Rynkun, P. Jönsson, and G. Gaigalas, "Doublet-quartet energy separation in boron: A partitioned-correlation-function-interaction method," Phys. Rev. A **88**, 062506 (2013).

[125] H. Nakatsuji, H. Nakashima, and Y. I. Kurokawa, "Solving the Schrödinger equation of atoms and molecules with the free-complement chemical-formula theory: First-row atoms and small molecules," The Journal of Chemical Physics **149**, 114106 (2018).

[126] K. Strasburger, "Energy difference between the lowest doublet and quartet states of the boron atom," Phys. Rev. A **102**, 052806 (2020).

[127] A. E. Kramida, Y. Ralchenko, J. Reader, and NIST ASD Team, *NIST Atomic Spectra Database (ver. 5.9) [Online]* (2021), available at http://physics.nist.gov/asd.

[128] M. B. Ruiz and R. Tröger, "Chapter Twelve - Configuration Interaction Study of the 3P Ground State of the Carbon Atom," in *Novel Electronic Structure Theory: General Innovations and Strongly Correlated Systems*, Advances in Quantum Chemistry, Vol. 76, edited by P. E. Hoggan (Academic Press, 2018) pp. 223–238.

[129] S. J. Chakravorty, S. R. Gwaltney, E. R. Davidson, F. A. Parpia, and C. Froese Fischer, "Ground-state correlation energies for atomic ions with 3 to 18 electrons," Phys. Rev. A **47**, 3649 (1993).

[130] J. Noga, S. Kedžuch, J. Šimunek, and S. Ten-no, "Explicitly correlated coupled cluster F12 theory with single and double excitations," The Journal of Chemical Physics **128**, 174103 (2008).

[131] P. Maldonado, A. Sarsa, E. Buendía, and F. J. Gálvez, "Jastrow correlated and quantum Monte Carlo calculations for the low-lying states of the carbon atom," J. Chem. Phys. **134**, 134102 (2011).

[132] A. E. Kramida, Yu. Ralchenko, J. Reader, and NIST ASD Team, *NIST Atomic Spectra Database, ver. 5.1 [Online]* (2013), available at http://physics.nist.gov/asd.

[133] R. A. Kendall, T. H. Dunning Jr., and R. J. Harrison, "Electron affinities of the first-row atoms revisited. Systematic basis sets and wave functions," The Journal of Chemical Physics **96**, 6796 – 6806 (1992), cited by: 13303.

[134] J. S. Sims, "Hylleraas-configuration interaction study of the ^1S ground state of the negative Li ion," Journal of Physics B: Atomic, Molecular and Optical Physics **50**, 245003 (2017).

[135] M. B. Ruiz, "Chapter Six - Configuration interaction study of the 3P ground and low-lying states of the boron anion. The boron electron affinity," in *State of The Art of Molecular Electronic Structure Computations: Correlation Methods, Basis Sets and More*, Advances in Quantum Chemistry, Vol. 79, edited by L. U. Ancarani and P. E. Hoggan (Academic Press, 2019) pp. 135–153.

[136] C. Froese Fischer, A. Ynnerman, and G. Gaigalas, "Multiconfiguration-Hartree-Fock calculations for the electron affinity of boron," Physical Review A **51**, 4611 – 4616 (1995), cited by: 35.

[137] D. Feller, "Application of a convergent, composite coupled cluster approach to bound state, adiabatic electron affinities in atoms and small molecules," J. Chem. Phys. **144**, 014105 (2016).

[138] H. F. Schaefer and F. E. Harris, "Calculation of the electron affinity of boron," Physical Review **170**, 108 – 115 (1968), cited by: 14.